NASA TN D-1105

# TECHNICAL NOTE

## D-1105

SPACE DEBRIS HAZARD EVALUATION

By Elmer H. Davison and Paul C. Winslow, Jr.

Lewis Research Center
Cleveland, Ohio

NATIONAL AERONAUTICS AND SPACE ADMINISTRATION
WASHINGTON

December 1961

NATIONAL AERONAUTICS AND SPACE ADMINISTRATION

TECHNICAL NOTE D-1105

# SPACE DEBRIS HAZARD EVALUATION

By Elmer H. Davison and Paul C. Winslow, Jr.

## SUMMARY

The hazard to space vehicles from natural space debris has been explored. A survey of the available information pertinent to this problem is presented. The hope is that this presentation gives a coherent picture of the knowledge to date in terms of the topic covered. The conclusion reached is that a definite hazard exists but that it can only be poorly assessed on the basis of present information. The need for direct measurement of this hazard is obvious, and some of the problems involved in making these direct measurements have been explored.

## INTRODUCTION

The advent of vehicles into space has brought into sharp focus some of the problems to be surmounted. One among these many problems is space debris and the hazard it presents to space vehicles. The main emphasis is on the near-Earth hazard and the proposed direct methods of evaluating this hazard.

Truly definitive measurements of this hazard have yet to be made, but there is a wealth of information from other fields that is pertinent to estimating the character and magnitude of this hazard. Three broad fields of inquiry provide the only information presently available on this subject. Astronomy, the foremost source of information, has recently been supplemented by a second source of information, namely, satellite and space probe research. The third source of information comes from laboratory hypervelocity impact studies. All three fields of research endeavor are large and expanding rapidly, thus making it difficult to obtain a comprehensive picture of any one. Further, they all bear on the subject matter of this report, and it is therefore doubly difficult to weld this information into a coherent and cohesive picture of the hazard presented to space vehicles by space debris. It has nevertheless been attempted.

The scope of each field also does not permit a complete discussion of each. Therefore, the authors, for the sake of brevity, selected

information to give a picture of the knowledge to date in terms of the topic covered. This information was then combined to estimate the magnitude and character of the hazard of space debris. This information was further used to investigate the problems associated with vehicle design and space experiments for gathering direct information on the hazard. (Note: An attempt has been made to reference the most appropriate material supporting the discussion. However, the scope of the subject matter covered is very broad, and some of the subjects covered are quite extensive. It is very likely, therefore, that more appropriate references could have been selected in some instances.)



## SPACE DEBRIS

There is in our solar system a great number of bodies orbiting the Sun. These include, of course, the most familiar bodies such as the planets, asteroids, and comets. However, in addition to the large familiar objects, there is a vast number of smaller bodies orbiting the Sun. These bodies range down in size to a micron or two in diameter.

Particles smaller than approximately 1 micron experience repulsive forces greater than those due to gravitational attraction and consequently are swept from the solar system as quickly as they are generated. Light pressure alone is sufficient because, for a given particle density, the area-to-mass ratio varies inversely with particle radius, and therefore a size is reached at which the force of the light pressure on the area becomes greater than gravity forces and drives the particle away from the Sun. (This phenomenon is described in ref. 1. Several updated discussions of light pressure and other forces of consequence on small bodies in space are given in refs. 2 and 3.)

The space debris in the solar system has, in the opinion of most astronomers, only two origins. These two sources are comets and asteroids. They further believe that interstellar debris, if any, constitutes less than 1 percent of the material encountered. It might be well therefore to describe briefly the main characteristics of comets, asteroids, and the other material.

### Asteroids

Asteroids are irregularly shaped solid bodies with a density between approximately 3 and 9 grams per cubic centimeter (ref. 4). The most probable density is around 3.5 grams per cubic centimeter. Their size may range up to 500 miles in diameter. Their orbits are, in general, inclined to the plane of the ecliptic (mean inclination to the ecliptic, approx. $10^{\circ}$, ref. 4); and, in general, their orbits keep them between the orbits of Mars and Jupiter. They have the same

CONTENTS

direction of motion around the Sun as the planets (direct orbits) but follow, in general, more eccentric paths. Some are known to pass between the Sun and the Earth's orbit, and some rather large ones are known to pass between the orbits of Earth and Mars. A group of asteroids of particular interest is known as the Trojans. The Trojans follow the same orbit as Jupiter but either trail or lead Jupiter by 60°. These orbits are in agreement with the three-body equilibrium conditions predicted from theoretical considerations (ref. 5). Many astronomers believe that the asteroids are the remains of a planet that once had an orbit between Mars and Jupiter.



## Comets

Comets are probably the least understood of all the major bodies orbiting the Sun. It is not known for certain that they all do orbit the Sun. It is also incorrect to describe them as a body because they are thought to be, in general, a collection of particles following the same orbit. The known comets have highly eccentric orbits which may be inclined at any angle to the plane of the ecliptic and may be following either retrograde or direct orbits. They can only be observed when they approach the Sun; therefore, only those having highly eccentric orbits are observed. Because only those comets with highly eccentric orbits that bring them close to the Sun are observed (approximately 1 A.U. or closer), there may be vast numbers of other aggregates orbiting the Sun unobserved.

When a comet approaches the Sun, it produces a long luminous tail and bright head. The processes by which the luminous tail and head are produced are not well understood. The fact that stars can be seen through the tail or head with no reduction in brightness indicates that the particles in the aggregate are small in size and widely dispersed. This must be tempered, of course, by the understanding that these particles are at great distances from Earth; and therefore a description of their size as small is a relative one.

In general, the orbits or periods of the comets are not known although there is a group (about 70) of short-period (less than 100 yr) comets that have been cataloged. Most of these short-period comets have direct orbits, and it is thought that they may have been perturbed into their present orbits by Jupiter at one time as a result of passage near Jupiter. About 40 other comets of known period (periods of 100 to 1000 yr) are observed, but these apparently have no relation to Jupiter. A list of some of the short-period comets and associated meteor streams is given in reference 4 (see also refs. 6 and 7).

The composition of comet particles is open to question. There have been a number of theories advanced to explain comets' behaviors in terms

of their composition and apparent association with meteor displays. Whipple of the Harvard College Observatory has proposed an icy-comet model to explain some of the comets' behavior as well as meteor phenomena that result when these particles enter the Earth's atmosphere (ref. 8). His proposal in brief is that the comet particles are a frozen conglomerate away from the Sun; and, as the comet approaches the Sun, the more volatile portions are driven off, leaving a porous fragile structure. Another leading astronomer, Öpik, is also a proponent of the fragile structure school of thought. His concept differs slightly from Whipple's in that he believes the cometary particles that enter the Earth's atmosphere and produce meteors are dust balls composed of a great number of individual grains (see, e.g., refs. 9 and 10).



The present authors would like to propose that boiling in a so-called zero-g field might also explain some of the phenomena noted.

## Zodiacal Dust

Other evidence of space debris is furnished by the zodiacal light observed in the night sky. This light, which forms a tapered band stretching up from the horizon into the sky, is attributed to sunlight reflecting from vast numbers of small particles in space. (For a good general discussion of the zodiacal light phenomenon by one of the authorities in the field, see ref. 11.) The dust's origin is thought to be cometary (ref. 2), although the asteroids are also considered a possible source. (There are also other less accepted theories as to the dust origin.) These particles are thought to be removed from the space environment by spiraling into the Sun and by other means. They therefore necessitate a mechanism of replacement in order to satisfy the present presence of the zodiacal cloud of particles. The comets are credited, as mentioned, with the ability to act as a source for the zodiacal particles (ref. 2). Other theories are available.

The zodiacal dust particles are thought to be more highly concentrated in the plane of the ecliptic. They have two components of drift as they orbit the Sun, one toward the plane of the ecliptic and one toward the Sun (ref. 1). The drift toward the plane of the ecliptic results from the attraction of the planets. The drift or spiraling in toward the Sun is a result of a component of the light pressure that tends to slow the particles down (referred to in the literature as the Poynting-Robertson effect, e.g., see refs. 6 and 12). Other evidence of the concentration in the plane of the ecliptic results from the shape of the Sun's Fraunhofer corona (refs. 11 and 13). Basically, the Fraunhofer corona is shaped by the absorbing medium through which the sunlight passes. The medium through which it passes, in this case, is a zodiacal dust cloud that results in the so-called F-corona for the Sun. (Other mediums through which the sunlight passes acccunt for other components of the corona, see ref. 11.)

The range of particle size most often quoted for these particles is from 1 to 300 microns (see, e.g., refs. 3, 11, 14, and 15). The lower limit has been discussed previously. As the particle size increases, the contribution to the zodiacal light decreases rather rapidly with no significant contribution attributable to particles greater than approximately 300 microns. (A note of caution should probably be introduced at this point because the estimates of the range of particle size vary considerably. As a result, the estimates of the contribution to the zodiacal light of the different size particles also vary considerably.)

Beard (ref. 3) gives the following estimates of the concentrations of these particles:

(1) At Earth's orbit, $10^{-14}$ to $10^{-15}$ particle per cubic centimeter

(2) At Earth's surface due to gravitational attraction, $10^{-10}$ to $10^{-11}$ particle per cubic centimeter

Beard in reference 3 has compared his estimates to the satellite data from 1958 Alpha (Explorer I) with very close agreement being noted.

Based on Beard's estimates it would appear that the material density of these particles must be equal to or less than 0.3 gram per cubic centimeter. However, it should be pointed out that other estimates do not lead to such low material densities. Other estimates lead to densities of 3 to 9 grams per cubic centimeter and consequently a lower minimum size particle.

Another phenomenon that occurs in the night sky, the Gegenschein, is attributed by some astronomers to sunlight reflecting from a concentration of zodiacal dust at one of the unstable-equilibrium points of the Earth-Sun system (ref. 5). These points occur along a radial line from the Sun through the Earth. Particles at these points would tend to remain there unless perturbed by some outside force.

Thus far only those space debris phenomena which are viewed from great distances in our solar system have been discussed. However, there is also a considerable amount of information on this material as it enters the Earth's atmosphere, strikes the Earth's surface, or drifts to the Earth's surface through the atmosphere. The most recent data have been acquired by satellites and space probes measuring the particle flux rates in space.

## Meteors and Meteorites

Telescopic surveys. - Perhaps the greatest amount of information gathered has been based on meteor studies. Meteors are the light trails

with a geometry assumption (e.g., spherical particles) the density of the particles can be calculated. Calculations of this type have been made by Harvard astronomers, and Whipple in reference 17 states that the density of some meteor particles may be as low as 0.05 gram per cubic centimeter. (Öpik, in ref. 10, discusses some of the possible errors in this approach and the assumptions involved.) Whipple also cites other evidence which he believes supports the contention that the particle density may be such a low value. However, Whipple also accepts that the density may vary widely between particles, and, of course, even less evidence is available as to the density of particles smaller than meteor particles.



Determining the material density of meteoroid particles prior to entering the Earth's atmosphere is one of the most critical problems associated with establishing the hazard presented by this debris. An indirect approach to this problem has been reported by McCrosky in reference 23. The approach consisted of using simulated meteors to estimate the luminous efficiency of the process. Although the experiment was not conclusive in many respects, it indicated that the extreme lower limit estimated for luminous efficiency was higher by a factor of 3 than that used by Cook and Whipple (see ref. 7). McCrosky also states that a value as much as 100 times as large was not precluded by the experiment. An increase of 100 in the efficiency would have two ramifications. It would decrease the mass associated with a particular meteor sighting by a factor of 100 and increase the particle density for spherical particles by a factor of 10. These values are cited here not because they are particularly significant but only to illustrate that there is considerable uncertainty in this area of research.

The variation of number of particles with mass is fairly well agreed on. The variation of number with mass most commonly used (first credited, to the authors' knowledge, to Watson) is given by the following equation:

$$dN = \frac{-K_1 dm}{m^S} \tag{2}$$

Integration of this equation gives

$$N_1 - N_2 = \frac{K_1}{S - 1}\left(\frac{1}{m_1^{S-1}} - \frac{1}{m_2^{S-1}}\right) \tag{3}$$

If, as one limit, the mass $m$ is taken as that at which the number of meteor particles is negligible and if, in addition, the mass of interest is, say, an order of magnitude less than the mass for which $N$ is negligible, the following approximate equation may be used:

$$N = \frac{K_1}{(S - 1)m^{S-1}} \tag{4}$$

An acceptable value for S is approximately 2 (see ref. 18) for meteors between magnitude 0 and +10. (Meteor particles smaller than +5 magnitude particles are surveyed by radio echo techniques which will be discussed subsequently.) This is also the value used by Whipple in reference 17. For S = 2, equation (4) reduces to

$$N = \frac{K_2}{m} \tag{5}$$

Using Whipple's meteor influx numbers from reference 17 (for an up-dated version of this reference, see ref. 24) to evaluate the constant $K_2$ of equation (5) leads to the following equation for flux rate:

$$N = \frac{5.81 \times 10^7}{m} \frac{\text{Number entering Earth's atmosphere}}{\text{Day}} \tag{6}$$

where m is in grams and N is the number of particles of mass m or greater.

Equation (6) has been used to estimate the flux values for particles much smaller than those responsible for meteor displays. Attempts have been made to check the integrated mass flux onto the Earth's surface based on equation (6) with values estimated by other means. There is purported to be some agreement. One method has been to analyze the nickel content in ocean sediment and thereby estimate the Earth's accumulation rate of meteoritic material (ref. 25). Another approach has been to correlate zodiacal light calculations with meteor studies. Most recently satellite measurements have become available as a means of checking the extrapolated values. This will be discussed subsequently.

Other approaches to measuring the total influx of meteoritic material onto Earth have been the attempts to collect some of the meteoritic material as it drifts down through the atmosphere. Mountain-top collection stations (ref. 25) and high-flying aircraft (ref. 26) have been used for this purpose.

When particles are small enough, their area-to-mass ratios permit them to be decelerated by the atmosphere without burning up. This feature, in conjunction with the fact that some of this material is metallic (mainly iron with a fair amount of nickel), permits the investigators to separate out the magnetic metal spherules and estimate the total influx.

The aircraft work reported in reference 26 is in a very early stage of investigation. The particles collected have been in the range of 7 to 20 microns. They are nominally solid bodies with some central bubbles. The exact mechanism for their introduction into the atmosphere is not known with certainty. They may, for example, be introduced as individual particles or by the breakup of meteor particles. Other mechanisms or combinations are, of course, not ruled out.

It is interesting to note that the estimate of total influx rate given in reference 25 gives about an order of magnitude greater value than is obtained on the basis of equation (6). Although this is not conclusive evidence, it might be assumed with reservations that equation (6) gives a low estimate of the number of particles entering the atmosphere per day.

Equation (6) is also admittedly only a crude estimate of the number-mass variation of particles. Other authors have used equations similar to (6) with m to some power slightly greater than 1.0. Others have used even more complex number-mass relations in an attempt to introduce fine structure into the distribution. This is primarily to get better mating of satellite and meteor data or to introduce the concept of a dust belt around the Earth. These correlations seem somewhat premature to the authors and therefore have not been pursued too extensively herein. It must be recognized that considerable uncertainty must be associated with any estimate or even measurement of the number density or flux of particles. For the purposes of this report equation (6) serves quite well, although it appears to give low estimates for the number of smaller particles near Earth.

Meteorite studies. - Several other aspects of meteors are also worth noting. On the basis of the trajectories these particles have and other evidence it is believed that almost all meteors (90 percent or more) are of cometary origin (ref. 27). Almost all these particles are burned up before reaching Earth's surface, but some of the brighter meteors will penetrate to Earth's surface. These particles and, in particular, the remains picked up on the Earth's surface are known as meteorites.

Meteorites, in contrast to most of the particles that cause meteors, are thought to be of asteroidal origin (ref. 27). The evidence for this is again their trajectories and also their composition. Meteorites are classified into three groups: irons, stony irons, and stones. They are all solid bodies with the irons including other minerals, notably nickel (up to 20 percent). The stones may also have small spherical inclusions of metal throughout. The stony irons, of course, are another arbitrary class between the stones and irons.

Meteorites are also classified as either falls or finds. Those seen falling are in the first class, and for this class the stones predominate (about 80 to 90 percent of the total, e.g., see refs. 4, 7, and 28). Finds constitute those meteorites stumbled upon randomly and recognized as meteorites. Because the iron variety are more easily recognized, they predominate in this class. Although bodies large enough to survive passage through the atmosphere such as meteorites are some of the most deadly debris one could encounter in space, they are fortunately so infrequent that they do not represent a great hazard. It is estimated that about five per day strike the entire Earth's surface, although

occasionally swarms of particles are encountered (refs. 4 and 28). It should be pointed out also that these particles will be more frequent in the vicinity of Mars, because they are thought to be of asteroidal origins, and this problem will eventually need evaluation.

Radio echo surveys. - Many of the particles entering the Earth's atmosphere do not possess enough kinetic energy to cause meteor displays. However, some do have enough kinetic energy to ionize the air during passage, and thus leave ionization trails. These trails are detectable by radio echo or radar techniques, and a considerable amount of information has been obtained in this manner. These radio echo surveys have a great advantage over meteor studies in that they may be conducted during the daylight hours as well as at night. In addition they allow the investigator potentially to obtain information up to a magnitude of about +12. (Note: Particle size decreases as magnitude increases.) Magnitude ratings above +5 are fictitious ratings because luminous displays no longer prevail. Magnitude, however, is still the accepted method of rating the particle size, and the relation of particle mass to magnitude developed for meteors is used.



Because 24-hour surveys can be made, the influx pattern into the Earth's atmosphere can be mapped. One such pattern in the plane of the ecliptic taken from reference 29, by Hawkins, is shown in figure 3. This polar diagram for an Earth-centered system represents the influx pattern an Earthbound observer would see. For example, the vector shown in figure 3 gives the direction of the incoming particles, while the vector length is a measure of the number of particles from that direction.

With the measured distribution of figure 3, Hawkins has constructed the heliocentric direction distribution of these particles at a point on Earth's orbit. This was done in the following way: To the observed velocity relative to Earth, the Earth's heliocentric velocity of 30 kilometers per second was added; the particles were all assumed to have a heliocentric velocity of 40 kilometers per second when intercepted by Earth. The resulting distribution is shown in figure 4. The pattern shown in figure 4 is based on assumptions as to particle velocity, and so forth, and is therefore more of a model than the actual pattern that prevails. If a lower heliocentric velocity had been assumed for the particles, an even greater elongation in the direction of the antapex would have resulted.

This survey also showed a concentration of particle orbits near the ecliptic with direct orbits predominating. The concentration toward the plane of the ecliptic is not demonstrated by either figure 3 or 4. However, if planes at increasing inclination to the ecliptic were used to construct figures corresponding to figure 3, the pattern shown would progressively shrink toward the origin as the inclination increased.

The survey in reference 29 was conducted in the northern hemisphere. A similar survey was conducted in the southern hemisphere and is reported in reference 30. This survey agreed in general with that of reference 29 with one notable exception. In the northern hemisphere survey (ref. 29), the yearly variation showed about a fourfold increase in meteor activity between February and May and then a plateau of this high-level activity until approximately August. In the southern hemisphere survey (ref. 30) the yearly variation shows an activity peak or plateau during the interval of approximately August to January, which was about 50 percent higher than the minimum activity. No definite explanation for this difference in peak activity is available according to Weiss's knowledge (ref. 30). However, Weiss states that it is possible that this disagreement is due to the dominating influence of the sporadic activity associated with the summer daytime showers.



The northern survey (ref. 29) had a very interesting correlation. The yearly variation in this survey was compared to the cometary index for the year with very good correlation, giving further evidence that meteors are of cometary origin. It might also be pointed out at this point that it is often difficult to distinguish the weaker showers from the sporadic background. This accounts in part for the difficulty in determining if time variations exist in the sporadic background rates.

Some values for the concentration of these orbits to the plane of the ecliptic are given in reference 18. It is estimated that approximately 50 percent of the sporadic meteors are concentrated within $15^{\circ}$ of the ecliptic. Another group of about 15 percent moves in rather circular orbits with inclinations grouped around $60^{\circ}$ and $120^{\circ}$. No cosmological reason for this latter type of distribution is presently available according to Lovell (ref. 18).

In the radio echo field of astronomy as in other branches of astronomy, agreement is not easily come by. In reference 31 Bain, using data of Vogan and Campbell (ref. 32), found substantial agreement between the data and a model postulated on Hawkins' measured three-lobed distributions. However, in references 33 and 34 the existence of a three-lobed pattern as measured by Hawkins is disputed. In any event there is agreement that an Earthbound observer sees many more radio and visual meteors on the morning side of Earth. It is also accepted by most that the majority of this material encountered by Earth is following direct orbits with orbit planes more concentrated near the ecliptic plane.

Visual surveys. - The oldest method employed in making meteor surveys is simply that of an observer viewing a given portion of the sky and recording the meteors sighted. Perhaps the most extensive compilation of such sightings is given by Olivier in reference 35, which covers a period of some 58 years.

One assumption made in assessing the danger of space debris to a space vehicle is that the sporadic flux can be characterized by some average rate of impact and a frequency distribution about this average rate. The frequency distributions for the data of reference 35 are shown in figure 5. Each figure is a plot of the frequency of sighting of various rates for a particular astronomical time, which means that all observers would be observing the same portion of the pattern shown in figure 3. The ordinate gives the number of times a particular count occurs, while the abscissa is the counting rate observed.

The interesting features of figure 5 are as follows: On a yearly basis the sporadic visual meteor sightings appear to have a single peaked frequency distribution. This implies that the material can be described using single-population parameters. In some instances the point could be stretched to say there are separate peaks, but the data taken as a whole do not seem to warrant such a possibility. In any event the possibility is not considered herein. In addition, whenever particle populations are dealt with herein, it is implied, unless otherwise stated, that particles of a given size or larger are being considered.

The data of reference 35 are, however, biased, because many of the counting rates reported are averages for a number of observers. In addition, counts which Olivier thought represented showers or unreasonably high values were eliminated. Olivier has been kind enough to furnish the authors with the original data (ref. 36) of individual sightings. These data have been corrected for rate reductions due to cloud cover, and so forth, but this should not affect the frequency distributions to any extent. Examinations of these data also showed the characteristic single peaked distributions of figure 5. It might also be noted that the authors felt justified in plotting the data on a yearly basis because the variations noted from year to year in the sporadic rates are fairly minor (ref. 30).

The hourly averages obtained from figure 5 are shown in figure 6 as a polar diagram similar to figure 3. The figures are not directly comparable because figure 6 does not contain the directionality data used in figure 3 (fig. 6 also gives only the hourly visual meteor rates for the various longitudes shown without corrections for rate reductions in the early evening or late morning sightings). The data in the figure, however, do show the same characteristic increase in rate toward the morning side of Earth noted for radio echo and telescopic surveys.

Satellite and space probe surveys. - Recently satellites and space probes have become available to make direct measurements of cosmic debris phenomena, in particular, the rate of impact of the very small particles called micrometeoroids.

Some of the micrometeoroid data have been reported in references 37 to 41. This material has also been published in other publications. With the exception of the 1958 Gamma satellite these data were obtained using piezoelectric crystals to sensitize the satellite surfaces in a microphone fashion. The manner in which the piezoelectric crystals are attached to the skin surfaces to pick up the vibrations due to impacting micrometeoroids is detailed in reference 42. There is, at present, one major point of controversy about these measurements that arises because the instruments have not been calibrated for the range of impact velocity corresponding to micrometeoroid particles.



The most extensive calibration of these devices is described in reference 43, which reports a linear variation of pulse voltage with impacting momentum. This relation held over a momentum range of four orders of magnitude. However, the maximum impact velocity was approximately 6 kilometers per second, which is low in comparison with micrometeoroid velocities. The linear relation of pulse and momentum of reference 43 is used in reducing almost if not all the U.S. satellite data.

Some investigators, in particular the Russians, feel that the pulse voltage is a function of the energy of impact at the higher velocities or at least velocity to some power between 1 and 2 (ref. 44). (For other discussions of the Russian data, see refs. 45 and 46.)

Regardless of whether the microphones measure a momentum, energy, or some hybrid value, they do measure only this and the rate of impact of particles above the particular sensitivity level of the microphone being used. If the momentum is assumed measured, an estimate of particle mass is obtained by assuming a velocity of impact. By also assuming a particle density the particle size can be estimated.

Another device employed on satellites that has supplied micrometeoroid data is the wire-wound cards. Rupture of the wire by an impacting micrometeoroid destroys the electrical continuity of the wire. This is sensed by the satellite data measuring system and transmitted to the ground by telemetry. These devices were also evaluated (ref. 43) to determine the particle size required to rupture the wire. Sensors of this type were used on the 1958 Gamma satellite (ref. 37) as well as some more recent satellites for which data have not been published to date. Other micrometeoroid sensing devices have been used on satellites, but no data have been published as of the writing of this report.

The satellite data from references 37 to 41 have been plotted in figure 7 along with the predicted values obtained by extrapolation with equation (6). Because the satellite data reported are not always as detailed as one might desire, it is difficult to compare all the results on exactly the same basis. Where no statement was made as to viewing loss due to a near-Earth orbit, a value of 0.33 was assumed. (Viewing

loss used in this case was simply the solid angle subtended by Earth when viewed from the satellite's altitude.) Similarly an impact velocity of 30 kilometers per second and a particle density of 2.7 grams per cubic centimeter were assumed. (The velocity, density, and viewing loss values were essentially the same as those used in the other data for which no corrections were needed. The assumed velocity of 30 km/sec appears high to the authors, but fortunately it does not affect the resulting mass calculations seriously.)



Notwithstanding the difficulty of comparing the various data, there is remarkable agreement both between the measured values and the extrapolated equation. The notable exceptions are several readings reported for Sputnik III. However, it should be pointed out that the three readings reported for Sputnik III were for three different time periods. If a time average were taken (as was done with the other data), much closer agreement with the extrapolated value would exist. All the data shown with the exception of 1958 Gamma were obtained with the microphone-type instrumentation.

None of the data from early vertical sounding rocket work has been included herein, the reason being that the area-time product of exposure is insignificant in comparison to the satellite data.

Some of the satellite data and, in particular, the space probe data have been interpreted as indicating a concentration or blanket of micrometeoroid material near Earth. (This was theoretically predicted in ref. 3.) Substantial experimental verification of this blanket hypothesis is not yet available and is therefore only briefly mentioned here. (For discussions of the subject, see refs. 24, 47, and 48.)

## HYPERVELOCITY IMPACT

There are two major fields of endeavor that bear on the problem of vehicle hazard due to space debris. The first field, the nature of space debris, has already been discussed. It should be apparent that perhaps the outstanding questions to be answered in this field are: What is the material density of this space debris? What are the flux rates? The second field, the damage associated with hypervelocity impact, will be explored in this section.

The study of hypervelocity impact has to date suffered from a serious deficiency. This deficiency is the inability of experimenters to obtain velocities in the range of interest (36,000 to 235,000 ft/sec) with particles of known mass and dimensions.

Another problem with these studies is the inability of experimenters to agree on the damage to be expected even in the velocity region now under investigation (up to 20,000 ft/sec).

## General Description of Phenomena

The nature of the damage inflicted by an impacting particle is affected significantly by the velocity of the particle. A very good description of the effect of velocity on the character of impact damage is given by Summers in reference 49. This dependence is illustrated in figure 8, which was taken from reference 49. The three regions delineated for tungsten-carbide spheres impacting lead targets are the undeformed projectile region, the transition region, and the fluid impact region. It is interesting to note that Atkins (ref. 50) observed that the same three regions of impact exist and obtained essentially the same curve shown in figure 8 for copper targets impacted by tungsten-carbide spheres. For other projectile and target materials these regions of impact are not always well delineated, if they exist at all. Fortunately (perhaps unfortunately) the two low-velocity regions of impact are of minor importance to the space vehicle designer. However, they do serve to explain the total impact phenomena picture and point out the danger of extrapolating low-velocity data to higher velocities.



The fluid impact region is of the greatest interest and therefore will be discussed most fully. In the following discussion of the fluid impact region it should be remembered that experimenters have only recently been able to obtain data in this region for many materials of interest. In addition, they have only invaded the very lower fringes of this area, and generalization or extrapolation of these results is rather risky. This will be more apparent when a comparison of results is discussed subsequently. With the exception of a few materials, notably lead, the true fluid impact region is not reached for many materials until velocities around 20,000 feet per second are attained. Velocities in the low 20,000-foot-per-second range for particles of known mass and geometry have been obtained with light gas guns (refs. 51, 52, and 53). Higher velocities in the neighborhood of 30,000 feet per second have been obtained with plastic slugs, but the data have not yet been published (information received from Thomas Canning of Ames Research Center). A technique for accelerating particles to approximately 30,000 feet per second by drag forces generated by a dense high-velocity gas has been developed and is reported in reference 54. Unfortunately it is difficult to establish the condition of the projectiles prior to impact with this technique, and only a very modest amount of data has been obtained with this device to date. The shaped charge has also been used to obtain particle velocities around 30,000 feet per second (refs. 43 and 55). A multitude of particles is fired, however, and it is difficult to associate individual craters and particles. Individual particles have also been fired by shaped charges but never at the higher velocities (refs. 56 and 57). J. W. Gehring, Jr. of the Ballistic Research Laboratory has recently achieved velocities of approximately 45,000 feet per second for microparticles using the techniques reported in reference 58. He has also accelerated 0.1 to 0.2 gram of material

in an undetermined state (i.e., solid or molten particles, or jets) to approximately 70,000 feet per second (private communication from Gehring).

In the fluid impact region it is generally agreed that the craters formed in the target material are hemispherical. The exceptions to this general observation are the plastics and some brittle metals or metal alloys. However, there is evidence to indicate that the craters of at least the brittle metals if not the plastics approach hemispheric proportions as the speed increases. The ratio of crater depth to diameter in general approaches a limiting value of approximately 0.5 as velocity increases and true fluid impact is obtained (see, e.g., ref. 56). Even the brittle metals or alloys appear to agree with this general observation if the velocity is high enough (see ref. 54).

Another fluid impact phenomenon generally agreed upon is that the crater volume varies linearly with the kinetic energy of the impacting particle (e.g., see refs. 49, 52, and 58). This behavior, in conjunction with the observation that the ratio of crater depth to diameter approaches a limiting value of 0.5, would indicate that the depth of penetration should vary as the velocity of impact to the two-thirds power. This latter observation has indeed been borne out by experimental data reported in references 49 and 52. However, there are some notable disagreements with these observations.

Collins and Kinard (ref. 58) found that the depth of penetration correlated with the momentum per unit frontal area of the impacting particle. This, of course, means that the depth of penetration is a linear function of velocity as they indicate. However, it was also found that the volume of the crater varied linearly with kinetic energy of the impacting pellet. These two correlations may possibly be explained by the fact that the velocity of impact upon which the data were based did not exceed 13,200 feet per second. Fluid impact was apparently not achieved for all materials tested, in particular for aluminum targets which had irregularly or conically shaped craters. It was also noted that lead targets did not correlate in the same manner as other target material, and it could well be that this result is due to the fact that lead was probably the only material in which true fluid impact was achieved. However, Collins, Kinard, and Hopko have published data to approximately 20,000 feet per second (refs. 59 and 60) for nylon impacting aluminum that still indicate a linear relation of crater depth and particle velocity.

Another notable exception to the two-thirds velocity variation arose in a theoretical investigation by Bjork, reported in references 61 and 62. In reference 61 Bjork analyzed the impact phenomenon on the basis of a hydrodynamic model. This analysis is considered by many in the field to be the best theoretical approach to the problem to

date, but it should be pointed out that it has had essentially no experimental verification. By the authors' own stipulation it also does not apply except for the purely fluid impact situation. In any event, reference 62 indicates that the depth of penetration should vary as the momentum of the impacting particle to the one-third power.

For the sake of completing the picture it should be noted that other experimenters (ref. 63) found that the depth of penetration varied with velocity to the 1.4 power. It was noted also by Atkins (ref. 50) that this variation described fairly well the region of impact in figure 8 called the undeformed projectile region. Atkins used a velocity variation to the four-thirds power, which is slightly different from 1.4 but not enough to be of any great consequence.



It appears to the writers that a fairly decent picture of the impact phenomena is emerging from the welter of data being reported. This picture can be described as follows:

(1) Undeformed projectile region. In this range of velocity the depth of penetration varies as velocity to approximately the four-thirds power. The craters formed are not hemispherical but deep wells with depth-to-diameter ratios in excess of 1.0.

(2) Transition region. In this region it is impossible to obtain any meaningful correlation of depth of penetration with velocity or any other parameter. The craters are not true hemispheres as in the fluid impact region, but the similarity is becoming more pronounced.

(3) Fluid impact region. This region is probably best characterized by the hemispherical craters formed with depth-to-diameter ratios of 0.5. The depth of penetration appears to vary with velocity to the two-thirds power. In terms of crater volume this means that the crater volume varies directly with the kinetic energy of the impacting particles.

(4) Micrometeoroid impact region. The character of the crater phenomenon in this region is perhaps hinted at by Bjork's analysis. In this region the craters still have the appearance of hemispheres, but the depth of penetration varies with velocity to some power less than two-thirds and perhaps, as Bjork suggests, velocity to the one-third power.

The cratering phenomenon, while heavily dependent on velocity of impact, is also influenced by other parameters. In the low-velocity regions the cratering appears to be dependent on the mechanical properties of the target and pellet material as well as the density of the two materials. A popular correlation employed is that of plotting depth of penetration against the ratio of impact velocity to velocity of sound in the target material. Some early experiments were conducted (ref. 64) to show that a transition in the depth of penetration occurred when the

velocity ratio reached 1.0. It is fairly well accepted at present, however, that there is no marked transition in the depth of penetration with velocity at a velocity ratio of 1.0. It is probably a fair summary to state that the physical phenomenon of cratering and its dependence on material properties are not well understood at present. There are, however, some other damage phenomena that are worth noting.



## Target Thickness

A number of investigations have been made into the effect of target thickness on the cratering phenomenon. The most notable effect is that the depth of penetration is increased as the depth of penetration approaches the target thickness. Kinard, et al. found (ref. 65) for the same pellet (same velocity, mass, etc.) that thin targets suffered approximately a 50 percent greater depth of penetration than semi-infinite targets. The greatest increase (50 percent) occurred when the target was (effectively) just penetrated.

Bjork has used a theoretical approach to this problem similar to that in reference 61. These results have not been published to date. However, Bjork in reference 62 states that, based on his theoretical studies, it appears that a 50 percent greater depth of penetration can be obtained in a thin target as compared to a semi-infinite target. The two studies, one theoretical and the other experimental, tend to substantiate one another although they were carried out for different velocity ranges.

## Spalling

With incomplete penetration of a target spalling sometimes occurs. A brief description of this phenomenon is as follows: At impact a compression wave is generated and travels to the rear face of the target. If the wave is strong enough, an interaction occurs at the rear face which stresses the target material to the point of rupture. Typically a thin circular layer of material is thrown off the rear face of the target. The region between the spalled surface and bottom of the crater is normally cracked or damaged, but not always. The conditions for spalling are only partially known, and several investigations are under way (e.g., see ref. 66) in an attempt to understand this phenomenon better.

## Target Temperature

Both the depth of penetration and crater volume would probably be expected to increase with target temperature. This was verified experimentally in reference 67 for the conditions of steel projectiles impacting Pb, Zn, Cd, and Cu targets. It was found, for example, that the

increase in crater volume with temperature for Pb was a smooth function. The crater volume for Pb increased by a factor of approximately four when the temperature was increased from -200° C to approximately the melting temperature. The increase in crater volume with temperature for the other materials did not show the smooth increase of Pb as a result of the change in the crystalline structure of the material with temperature. The only other material besides Pb taken to near the melting point was Zn, which showed an increase in crater volume of about four over that at room temperature. It should be noted that these data were obtained at a velocity of 5 kilometers per second, and therefore the details of the phenomenon might be different at a higher velocity. However, the general characteristic of increasing volume with temperature would in all likelihood prevail.



## Oblique Impact

It has been observed that at low speeds the craters formed at oblique angles of impact up to 30° or 40° from the vertical are not measurably different than if the particle impacts vertically (ref. 49, see also refs. 56 and 68). At angles less than approximately 30° the depth of penetration correlates with the normal component of velocity in the same manner noted for vertical impacts (ref. 49).

The authors of reference 49 also noted that the oblique angle at which circular craters were formed increased with increased impact velocity. They speculate, as have others, that at very high velocity the craters formed will all be circular with exception perhaps of extremely oblique or glancing impacts. The evidence cited for this theory is the circular Moon craters and those formed in the Earth's surface by meteorites. Most astronomers attribute Moon craters to meteoroid impact and even theorize that some of the material spewed from these craters reaches the surface of Earth (ref. 69). However, other crater theories have been presented (e.g., see ref. 70).

This evidence of circular craters at very oblique angles of impact has led some people to propose an explosive model of cratering at very high velocities. (I.e., the impact is equivalent to detonating an explosive charge at the face of the target.) The validity of these theories, like many others, awaits experimental verification.

## Comparison of Penetration Models

The parameter of greatest importance to space vehicle designers is depth of penetration. Unfortunately the disagreements among experiments and between experiment and theory are quite large in the meteoroid velocity range.

Comparisons of some of the results reported are shown in figure 9. The correlation equations are given in appendix B. The experimental references were selected because they are based on extensive collections of data obtained by experienced observers. The theoretical prediction by Bjork is considered one of the best by many in the field. Unfortunately it is difficult to find data obtained under apparently identical conditions but gathered by independent experimenters. For example, in figure 9(a) only the data of Atkins (ref. 52) and Collins and Kinard (ref. 58) are directly comparable. The curve based on Summers data (ref. 49) was derived using an empirical equation developed from data for projectiles with a wide range of densities impacting lead and copper targets.

From figure 9(a) it can be seen that Summers and Atkins agree quite closely. Both have developed empirical relations that indicate the depth of penetration varies with impact velocity to the two-thirds power. Collins and Kinard have developed an empirical relation that indicates the depth of penetration varies linearly with velocity. From figure 9(a) it is apparent that this linear velocity relation results in much greater depths of penetration at the high velocities. A possible explanation of this difference in estimates was given previously.

Perhaps one of the most disturbing features of figure 9(a) is the difference between the depths of penetration measured by Collins and Kinard, and Atkins for supposedly identical conditions in the velocity range at which the experimental data were obtained.

Bjork's analysis leads to a more conservative estimate of the depth of penetration than any of the experimental extrapolations indicate (except at low velocities where Bjork stipulates his equation does not apply). It might, in fact, be safely said that Bjork's analysis leads to more conservative depths of penetration than any expected from experimental data. It may well be that at the higher velocities the depth of penetration will vary as velocity to the one-third power as Bjork predicts, but it would appear in any case that the general level of his curve is low.

Figure 9(b) is an additional comparison of Collins and Kinard, and Summers data. The discrepancy at the high velocities is obvious. In the range of velocity for which experimental data were obtained it is seen that at very low velocities the results agree. However, as velocity increases, a marked discrepancy evolves. This discrepancy arises even though the data were obtained under supposedly identical conditions.

## SIGNIFICANCE OF PROBLEM FOR SPACE VEHICLES

### Near-Earth Vehicles and Sporadic Meteoroids

Perhaps the best method of determining the significance of space debris on space vehicle design is to consider the case of a spherical surface or a randomly tumbling flat surface as it orbits Earth. The chief concern of the following discussion is the rate at which such a surface in a near-Earth orbit will be punctured by sporadic micrometeoroids.



Considerations in predicting rates. - The important considerations in calculating the puncture rates expected are listed as follows. Assumptions made for each of these considerations are also enumerated.

(1) Impingement rate. The rates shown in figure 7 were divided by the spherical area of Earth to obtain the rate per unit area on a surface near Earth.

(2) Angle and velocity of impact. A velocity of impact of 15 kilometers per second directed perpendicular to the surface in question was assumed. The assumed value of 15 kilometers per second is in line with the observation discussed previously that the velocities of meteoroids relative to Earth decrease with decreasing particle size.

(3) Density and shape of impacting particles. A density of 2.7 grams per cubic centimeter (approximately that of stone) was assumed for the particles. This does not appear to be too unreasonable for zodiacal particles (up to 300 microns) but might be too high for the larger particles (meteors). All impacting particles were assumed to be spherical.

(4) Penetration criteria. The empirical equation of Summers with one modification (see (5)) was used. This equation was developed for impact velocities less than those of interest herein but was assumed to give reasonable estimates at the velocities considered (see discussion in HYPERVELOCITY IMPACT section).

(5) Effect of target thickness. The equation of Summers was developed for semi-infinite targets. The depths of penetration so calculated were multiplied by a factor of 1.5 to account for the depth of penetration equaling or exceeding the thickness of the target (see discussion in HYPERVELOCITY IMPACT section).

(6) Viewing loss. No correction of the rates due to Earth blockage was applied.

The authors believe this set of assumptions should give reasonable, although somewhat low, estimates of the rates of penetration to be

expected for thin surfaces exposed near Earth. However, the effects of particle density, particle velocity, and other penetration criteria are also briefly discussed.

Predicted rates. - The rates of penetration that surfaces would sustain in the near-Earth region for five materials are shown in figure 10. Shown also are the mass and diameter of the impacting micrometeoroid.

Based on the previous assumptions, the rate at which penetrations are sustained varies with skin thickness h in the following manner:

$$r = \frac{K}{h^3} \qquad \frac{\text{Number of penetrations}}{\text{sq ft-hr}} \tag{7}$$

This penetration rate variation with skin thickness holds equally well (with minor exceptions) for all the penetration criteria now in vogue. (See appendix B. The exceptions to equation (7) are the Collins and Kinard penetration criteria for steel and aluminum when the impacting micrometeoroids are very small.) The values of K used for figure 10 are as follows:

| | Aluminum | Beryllium or titanium | Copper | Stainless steel |
|---|---|---|---|---|
| K | $6.72\times10^{-9}$ | $2.29\times10^{-9}$ | $1.23\times10^{-9}$ | $0.77\times10^{-9}$ |

For a given material thickness (h, in.) the rates of penetration for the five materials vary as the values of the constant K given above.

The value of the constant in equation (7) does vary with the different criteria employed. Thus the numerical value of the penetration rate or the level of the curves given in figure 10 may be erroneous, but the rate variation with thickness should hold. The factor most likely to alter the rate variation described in equation (7) would be a puffball type of micrometeoroid rather than the solid variety assumed. However, penetration criteria for low-density, high-velocity material have not been developed. If an explosive model of penetration applied, for example, less dense particles would probably not radically alter the penetration rates of figure 10. This follows because there is fair agreement on the number against mass variation shown in figure 7 and on meteoroid velocities. However, the effect of particle density on penetration rate for the penetration criteria employed is shown in figure 11 for stainless steel. All assumptions are the same as for figure 10(a) except that particle density is varied. The density values shown range from the lowest estimate to date (0.05 g/cc by Whipple) to the maximum expected (7.9 g/cc for an iron meteorite). The value of 2.7 grams per cubic centimeter represents a stony material, while 0.30 gram per cubic centimeter corresponds to the estimate of Beard. The obvious inference to be drawn from

figure 11 is that the particle density assumption may alter the rates of penetration to be expected by several orders of magnitude.

The effect of impact velocity on penetration rate is shown in figure 12 for stainless steel. All assumptions are the same as for figure 10(a) except that particle velocity is varied. The range of impact velocities actually experienced will probably be greater than the 15 to 75 kilometers per second range shown but not radically different (i.e., the velocity of the satellite relative to Earth will be roughly 8 km/sec). It is apparent that rather large variations in the rate of impact can occur from one velocity extreme to the other. However, comparison of figures 11 and 12 shows that the uncertainty in particle density is more critical than the possible variations in impact velocity. It should be kept in mind, however, that this comparison is being made with an equation based on relatively low velocity data.



The variation of penetration rate with penetration criteria for aluminum is shown in figure 13. (Aluminum was selected because it is the only material for which all criteria can be readily compared.) All assumptions are the same as for figure 10(b) except the penetration criteria varied. Some assumptions must be made in applying these criteria to the problem at hand. These are detailed in appendix B.

Perhaps the most noteworthy fact illustrated by figure 13 is that the spread in the predicted depth of penetration results in a much greater spread in the predicted rate of penetration. (For example, at 50,000 ft/sec, fig. 9(a) shows a spread in penetration depth of approximately 2.6, while fig. 13, which was constructed for an assumed velocity of 15 km/sec or 50,000 ft/sec, shows a spread in rate of penetration of an order of magnitude in some instances.) Figure 13 then demonstrates quite well the necessity of developing reliable penetration criteria in the micrometeoroid range of velocity.

The deviation of the Collins and Kinard curve from the others for small thicknesses is a result of their requirement that the impacting particle must attain a certain minimum momentum before any penetration takes place. The equations for aluminum impacting aluminum (see appendix B) give, for example, the following results: At 49,000 feet per second (approximately 15 km/sec) the impacting particle must have a dimension of at least 9 mils before any penetration is achieved. This does not appear to be a reasonable hypothesis to these authors. (An earlier penetration criterion developed by Kinard, et al. (ref. 65) did not lead to this apparently unreasonable result.) Once again, however, it should be noted that this is a gross extrapolation from the data for which the equations were developed.

The rates shown in figures 10 to 13 will be reduced by the shielding effect of Earth. The viewing loss due to the presence of Earth is

shown in figure 14. For a spherical body, or one randomly tumbling, the rate of penetration could be reduced by the appropriate viewing loss factor corresponding to the height of the body above Earth. The equation upon which figure 14 is based is given in appendix B. The equation was developed on the simple basis that, viewed from a given height, Earth blocks a certain portion of the $4\pi$ steradians seen from a point in space. The percent of the $4\pi$ steradians view blocked out by Earth is called the viewing loss, and it is assumed that the rate of penetration will be reduced accordingly.

Hole size. - An estimate of the minimum diameter of the hole expected in the various skin thicknesses when penetrated is shown in figure 15. This figure was constructed on the basis of two rather gross simplifying assumptions. The first is that the ratio of hole depth to diameter of craters in semi-infinite targets is 0.5. The second is that the depth of penetration in thin sheets is 1.5 times that in semi-infinite targets when the depth of penetration is equivalent to the sheet thickness. These two assumptions lead to the rather simple result that

$$d_{cm} = \frac{4}{3} h \tag{8}$$

Equation (8) gives only the minimum size hole to be expected because, for particles with mass or velocity greater than that required to just penetrate the surface, the hole size is greater. This can be seen from the following equation which was obtained from the Summers penetration criteria and the assumption that $D/d_c = 0.5$:

$$d_c = 2(2.28)\left(\frac{\rho_p}{\rho_t}\right)^{2/3}\left(\frac{V}{V_s}\right)^{2/3} d \tag{9}$$

Thus, if either the micrometeoroid velocity or mass (reflected as $d$ in eq. (9)) increases, the crater diameter $d_c$, and consequently the hole size in thin sheets, increases.

The minimum hole diameter $d_{cm}$ is, of course, only an approximation but it appears to be reasonable. It also applies only for those situations which for lack of a better definition are called complete penetration as distinguished from those impacts where the hole diameter is smaller. The cratering phenomenon is affected by the thickness of the target, but at the beginning of the process it is the same as for a semi-infinite target. Subsequently, however, if the penetration is complete or nearly so as shown in the microphotograph of figure 16 for the low-impact-velocity situation, a plug will be punched out with a diameter slightly less than the diameter of the crater at the face of the sheet. (Fig. 16 was obtained by impacting a 15-mil stainless-steel ball into an 18-mil 302 stainless-steel target at approximately 6000 ft/sec.)

Figure 16(a) shows the cross section prior to etching with the pellet material at the bottom of the crater still very much in evidence. However, because of preferential etching effects the pellet material does not appear in the etched photograph (fig. 16(b)). The shear-plug mentioned shows quite well in figure 16(b) along with the change in crystalline structure of the material surrounding the hole.

Significance of predicted rates. - The rates of penetration shown in figure 10 are quite low, but in terms of space vehicles rate r is only one of the three parameters of importance. The other two parameters, of course, are the area of the exposed surface a and the time of exposure t. The fact that should not be lost sight of when evaluating the meaning of figure 10 is that the product rat is the important consideration for space vehicles.

For skin thicknesses most commonly considered the probability of receiving a penetration can be obtained if it is assumed that an average or mean rate of penetration can be defined. For an average or mean rate of penetration the survival probabilities can be calculated using Poisson's relations. By assuming then that the rate of penetration has a frequency distribution corresponding to a Poisson distribution, the probability of not receiving a penetration $p_0$ is as follows:

$$p_0 = e^{-\lambda at} \tag{10}$$

where $\lambda$ is the mean rate for a Poisson distribution. The probability of receiving at least one penetration p is

$$p = 1 - p_0 = 1 - e^{-\lambda at} \tag{11}$$

(where the product $\lambda at$ is nondimensional and assumed to be the same as rat). Further if the product $\lambda at$ is small (i.e., $\lambda at \ll 1.0$), the probability of penetration p can be approximated as follows:

$$p = rat \tag{12}$$

Thus from equation (11) and figure 10(a) it is apparent that, for a reasonable thickness of, say, 30 mils of stainless steel (corresponds to a penetration rate r of $3 \times 10^{-5}$ number/(sq ft-hr)), either a very large area or an extended exposure time can result in a substantial probability of penetration. (A note of caution in regard to fig. 10 would perhaps be well taken at this point. Fig. 10 may become increasingly less reliable for micrometeoroids with diameters greater than 300 microns because the density of the impacting particles may be decreasing to those predicted for meteor particles.)

The previous discussion of the importance of the product of rate, area, and time rat might be better illustrated by figure 17. In figure 17 the area required for a 0.9 probability of at least one penetration in a time interval of 1 year has been plotted against skin thickness for various target materials. These probability calculations are, of course, no better than the estimated mean rate upon which they are based. In addition, one should be cautious in assuming that Poisson statistics apply. However, the assumption of Poisson statistics is useful in developing a feeling for the problems involved.

For the majority of satellites and probes that have been launched to date with exposed vulnerable areas of only a few square feet, rather thick skins, and life expectancies of months or less, the probability of sustaining a penetration is rather small. However, if large areas of relatively thin skin are exposed in space for extended periods of time in the form of thermal radiators, fuel tanks, or living quarters, the probability of sustaining a penetration becomes very real and cannot be ignored (see fig. 17). It should be noted that the particle masses presently being measured by satellites are of the order of $10^{-9}$ to $10^{-8}$ gram and, as can be seen from figure 10, correspond to sizes of particles that would penetrate very thin surfaces. Thus, although the rates are relatively high, the particles do not have any appreciable penetrating capability.

Figure 17 illustrates very well the point that the skin thicknesses dictated by most structural or containment requirements are very likely to be penetrated. Thus, a governing factor in the design of space vehicle skins will be a consideration of the micrometeoroid hazard.

Near-Earth summary. - In summary of the previous sections it is felt that figure 10 represents a reasonable estimate of the average rate of penetration to be expected in thin surfaces of a single thickness exposed in space near Earth. The average rates shown are based on the sporadic meteoroid flux and randomly oriented surfaces in space. Reduction of these rates and protection against penetration will be discussed subsequently. Figure 15 represents the approximate minimum hole size to be expected from penetrations in a single sheet.

## Other Considerations

As one departs from the vicinity of Earth or vehicles other than spheres or randomly tumbling surfaces are employed, the penetration rates discussed in the previous sections could change drastically.

Regions away from Earth. - As an example, the concentration of the very small particles (those responsible for the zodiacal light phenomena) may decrease by as much as a factor of $10^3$ (ref. 3) in regions removed from Earth. However, if the vehicle's path takes it nearer the

Sun, the concentration of the very small particles will increase. Reference 3 estimates the concentration to vary as $R^{-1.5}$ where R is the distance from the Sun. A note of caution should be added here because, although it is generally agreed that these trends exist, the numerical values estimated vary greatly. It might also be pointed out at this point that Jupiter has a much greater concentrating effect on space debris than Earth.

In addition to these trends, there are concentrations of space debris which it would be well for space vehicles to avoid. These are, for example, the Gegenschein region and Trojan asteroid region that were discussed previously. It might also be assumed that space journeys in the vicinity of Mars and Jupiter will be relatively hazardous because asteroidal material is more likely to be encountered. This of course means that the probability of encountering relatively large solid bodies is increased.



Orientation and relative velocity. - Most of the space debris encountered in space as noted previously is following direct orbits around the Sun. These orbits also have in general small inclinations to the plane of the ecliptic. The latter characteristic could be used to good advantage in the case of the flat surfaces by orienting them parallel to the plane of the ecliptic. Flat surfaces oriented perpendicular to the plane of the ecliptic could also be employed as protective devices for many kinds of structures.

It was noted in figures 3 and 4 that the relative velocity effect between Earth and space debris makes it appear that almost all the material strikes Earth from the forward $180^{\circ}$. This results because an increase in the apparent or relative velocity increases the rate of interception of particles. This characteristic could also be gainfully used by orienting the major axis of a surface parallel to the apex of Earth's way and by concentrating any protective devices in this direction. This would be particularly true of probes leaving Earth in the direction of the Earth's apex.

It could be concluded, therefore, that the preferred orientation of a surface is parallel to the plane of the ecliptic with the major axis parallel to the apex of the Earth's way. In addition, any protective surface would be most effective when it is perpendicular to the plane of the ecliptic and at the forward end of the vehicle when the direction of motion is toward the Earth's apex.

Showers. - In discussing rates of penetration the average flux rate was considered. Although the sporadic flux for meteors represents 70 to 80 percent of the total flux measured, the rates during showers can on occasion be many times that of the average rate. It is conceivable, therefore, that on some flights punctures could be received at a greatly

increased rate. However, there is no conclusive evidence at present that the increased rates observed during meteor showers extend to the smaller particles. It is also entirely possible therefore that the rates of penetration which depend on the small particles will not change radically during showers. This follows because the meteor particles are relatively large and rare by comparison with micrometeoroids and may be of different composition. An increase in the number of meteor size particles with no attending increase in micrometeoroids would alter the penetration rates shown in figure 10 for thicknesses of perhaps 50 to 100 mils or greater.

Unfortunately very little is known about this situation, and some experiments are obviously required. It is known that shower meteors are on the average brighter than sporadic meteors, indicating perhaps that particles of larger mass are involved. Further, a number of satellites have survived showers, although there has been some conjecture about one being put out of commission during a known shower by meteoroid impact (1958 Gamma). Present information, however, neither supports nor refutes the contention that meteor showers will not change the penetration rates drastically. This aspect of the space debris hazard most certainly needs direct experimental investigation.

The possibility of greatly increased rates of penetration during showers makes it very desirable to measure the time of an event in the direct measurement investigations. In addition, the experiment should be designed to prevent swamping of the equipment if greatly increased rates of penetration are encountered. The experimental approach to obtain direct measurements of the hazard is explored more fully in the subsequent EXPERIMENT DESIGN CONSIDERATIONS AND DATA INTERPRETATION section.

Other time variations. - The showers will probably be the time variation of most concern for exposed space structures. However, other variations on an hourly to yearly basis should be investigated. Some clues as to the magnitude of these variations can be obtained from the studies discussed in the SPACE DEBRIS section of this report.

Excluding the occasional intense shower, no great variation should be expected from year to year. However, the average monthly rate may vary by as much as an order of magnitude, although this is rather uncertain at present. There is little dispute, on the other hand, that the rates on a daily and hourly basis may vary from the average by orders of magnitude. This problem is also explored more fully in the subsequent EXPERIMENT DESIGN CONSIDERATIONS AND DATA INTERPRETATION section.

Protective measures. - In addition to distributing the protective devices or vehicle surfaces involved to take advantage of the directional characteristics of space debris, there are other devices or schemes that may be useful.

A technique of segmentation of a containment vessel or radiator can be employed not only to permit taking out of the system those segments suffering a penetration but to reduce the weight required of the component for sufficient protection against micrometeoroids. An example of this is shown in figure 18, which illustrates the effect of segmentation on the weight of a thermal space radiator. (Fig. 18 was taken from ref. 71.) Figure 18 shows the obvious result that increasing the number of segments decreases the weight function or weight. This can be carried on indefinitely until an infinite number of segments is employed, and, therefore, the area loss due to puncture is essentially zero. This is dependent of course on assuming that the number of particles passing through a given area is finite. The less obvious result shown in figure 18 is that for a given number of segments there is an optimum ratio of the number of surviving segments to the initial number. This means that there is some trade off between total initial area and required thickness for a given survival probability. The overall weight savings of such a scheme is not clear-cut since the weight function shown in figure 18 does not include the weight required for additional valving, manifolding, and so forth. In any event, however, segmentation can be used to some advantage.



Another protective device that might be employed is a bumper guard first proposed by Whipple. This device employs a thin outer surface to break up the impacting meteoroid and spread the broken fragments over a larger area of the sub or working surface. A number of investigators are presently conducting experiments on the effect of bumper thickness, spacing, and so forth, to determine the effectiveness of the bumper concept. It is too early at this stage to evaluate the results fairly, and, in addition, the concept of what constitutes damage varies.

Figure 19, which illustrates this rather well, shows the result of firing 75-mil glass balls at two 10-mil stainless-steel sheets spaced 0.5 inch apart. The velocity of impact was approximately 7500 feet per second. Although the glass beads were shattered or dissipated in the process of penetrating the first sheet, they generated a metal slug similar to that shown being formed in figure 16. This slug perforated the second sheet and formed a hole that was larger than that generated by the glass ball in the first sheet. It must be kept in mind, however, that the phenomena with meteoroid particles and velocities will probably be quite different. Reference 72 presents the results of another bumper investigation at low velocities.

In reference 52 aluminum pellets fired at aluminum targets at much higher velocities (17,500 ft/sec) resulted in the same type of damage to subsequent sheets noted previously for glass beads. (This should not be taken to imply that the phenomena were exactly the same.) In reference 52 it was found that the combined depth of penetration was reduced when the target thickness was divided among a number of sheets. Although the depth of penetration was reduced, the hole diameter in subsequent layers increased. These two effects then could vary in importance

depending upon the application. It is rather obvious from this brief description of results that considerably more work is required to evaluate properly the effectiveness of bumpers.

In addition to bumpers and segmentation there are many other schemes for meteoroid protection. It would be impossible, however, to discuss them all, and many are for very specialized application only (e.g., see ref. 73).

## EXPERIMENT DESIGN CONSIDERATIONS AND DATA INTERPRETATION

The subjects of experiment design and data interpretation are very broad and complex. It is necessary, therefore, to limit the objectives to be discussed in this section. The specific set of conditions to be explored in this section is:

(1) Experimental observation of rates of penetration in surfaces near Earth

(2) The likelihood that the probability of puncture will not be uniform in time

(3) The considerations involved in determining the variation of the average rate of penetration with surface thickness

In exploring this set of conditions the authors are concerned with whether average rates of penetration on some gross time basis can be established for a sphere orbiting Earth with given skin thicknesses. They are further concerned with determining when excursions (expected to be due mainly to showers) from an established frequency distribution occur. The previous set of conditions is explored using simple statistical and probability relations. The object is to bring out the problems involved in making direct experimental investigation of the meteoroid hazard. The statistical applications are, therefore, not necessarily those a statistician would employ either in analyzing data or designing an experiment.

Experiments to determine, for example, hourly, daily, or monthly variations are not discussed. Neither are such variations as might be expected with oriented surfaces, and so forth, considered. The general philosophy discussed, however, could be extended to such experiments. It should also not be construed that because such experiments are not discussed they are only minor variations of the general problem and of little consequence.

The section has been broken into two main subsections entitled (1) Interpretation of Data and (2) Design Considerations. These subsections are not entirely independent, and therefore the division of

material is rather arbitrary. In both subsections two experimental approaches with auxiliary conditions are considered. They are as follows:

Case I. - The exposed surface is capable of recording every puncture received. The surface area exposed is effectively constant for the duration of the experiment.

(a) Only the total time of the experiment is known.

(b) The time to each event or puncture is known.

Case II. - The exposed surface is segmented, and each segment, upon receiving a puncture, is removed from the system (i.e., cannot be used for recording additional punctures). Loss of a segment is always recorded.

(a) Only the total time of the experiment is known.

(b) The time to each event or loss of a segment is known.

## Interpretation of Data

The information desired from an experiment is considered to be the following:

(1) Can a mean rate of puncture be determined?

(2) Can an appropriate statistical model be found that fits the data?

(3) What are the magnitudes of the excursion from the background rate and how might these be determined? This, of course, would presume that a background rate could be established.

(4) How might the data be used to develop a model of the variation of average rate of puncture with material thickness?

There are, of course, other questions that could be considered. Consideration of all the problems would be impractical, however, and no attempt is made to look at all the facets of the problem. Even the scope of these questions is so broad that the authors have limited the discussion to a rather brief general consideration of the problem.

Case I(a). - Since definitive experimental data are lacking, the assumption made initially for this situation is that Poisson statistics apply. (Poisson's distribution describes the frequency distribution of random events which have a probability of occurring in time dt proportional to dt and which are independent.) This initial assumption

appears to fit reasonably well the physical situation and, in addition, simplifies the calculation. However, it is important to note that the actual situation may differ, and this is discussed under Case I(b).

The probability $p_x$ of observing a specific number of events $x$ if the mean rate $\lambda$ is known can be obtained from the following equation (see any standard text, e.g., ref. 74):

$$p_x = \frac{(\lambda at)^x}{x!} e^{-\lambda at} \tag{13}$$

If, as an estimate of $\lambda$, we take

$$\lambda = \frac{N}{at} \tag{14}$$

(where $N$ is the total number of events or punctures recorded), equation (13) becomes

$$p_x = \frac{N^x}{x!} e^{-N} \tag{15}$$

Estimating the rate with equation (14) would then permit an estimate using equation (15) of the probability of observing any given number of events $x$. By summing the probabilities for $x$ the probability of receiving more than or less than $x$ punctures could also be estimated.

If, on the other hand, $x$ is taken equal to $N$, equation (13) becomes

$$p_N = \frac{(\lambda at)^N}{N!} e^{-\lambda at} \tag{16}$$

and with $at$ and $N$ known, then

$$p_N = f(\lambda) \tag{17}$$

Equation (16) could be used to estimate the likely variation in rate based on observing $N$ events. This might be done with an equation of the following form:

$$\frac{\int_{\lambda_1}^{\lambda_2} p_N \, d\lambda}{\int_0^{\infty} p_N \, d\lambda} = K \qquad K < 1.0 \tag{18}$$

where the choice of the value of $K$ is up to the experimenter. The likely variation in rate $\lambda$ would, however, probably be more quickly apparent simply from a graphical plot of $p_N$ against $\lambda$.

Case I(b). - The case just discussed gives the experimenter only a limited amount of information. It further has one serious drawback in that for it to be useful the experimenter must assume that equation (14) is a good estimate of the average rate to be expected. Far more information can be obtained if the time to each event is also known. This situation is discussed next. The equations and concepts used are taken from reference 75, which includes a very good presentation on applied statistics. In the discussion of interval distributions for Poisson statistics in reference 75 it is shown that the expected number of events $x$ with time intervals between events longer than $t_1$ is as follows:

$$x = Ne^{-\lambda a t_1} \tag{19}$$

(Note: The nomenclature has been changed slightly from ref. 75.) A plot of this expected interval distribution is shown in figure 20(a). The histogram of the actual data could be plotted in conjunction with this curve. A histogram of the data as they might occur is also shown in figure 20(a). In comparing the theoretical distribution to the actual data the initial estimate of $\lambda$ is given by the total number of punctures divided by the exposed area and total time of the experiment.

Comparison of the data with the theoretical distribution could give the following information:

(1) The first situation would be agreement between the two distributions. In this situation it would be possible to state that Poisson statistics apply and to calculate a meaningful average rate of penetration.

(2) If the histogram has some smooth distributions but differs from the theoretical, the logical course would be to look at other distributions (normal, etc.) that might fit the data. If one could be found, the applicable statistics would be known and probability values for various events could be calculated.

(3) There may be definable excursions from the statistical distributions to be investigated. For purposes of estimating a mean background rate, the excursions could then be eliminated from the data. The data of the excursions would, of course, be very valuable in themselves because they would give a measure of the rate increases expected during a shower. In this respect the data might be made much more valuable if, concurrent with the satellite experiment, ground survey experiments were

conducted. It might, for example, be possible to correlate the satellite data with radio echo data.

(4) It may be that none of the previous situations apply. In this event it would not be meaningful to look for an average rate on the basis of the elapsed time of the experiment and the other conditions of the experiment that prevailed. It might, for example, become necessary to examine the rate on the basis of elongation, time of the year, surface orientation in space, or some combination of these and other factors.



Case II(a). - It appears to the authors that the binomial probability distribution is the most appropriate distribution to use in a segmented approach. Use of the binomial distribution implies that each segment of the surface is equally likely to be penetrated, which certainly appears to be a reasonable assumption. For a binomial distribution the probability $p_x$ of having exactly $x$ segments lost of a total of $z$ segments is given by the following equation:

$$p_x = \frac{z!}{x!(z - x)!} p^x(1 - p)^{z-x} \tag{20}$$

where $p$ is the probability that an individual segment will be lost. (Eq. (20) is given in any standard textbook, e.g., see ref. 74.)

Equation (20) has been plotted in figure 21 with $p_x$ as the ordinate and $p$ as the abscissa. In figure 21(a), for example, $z$ was held constant and curves of constant $x$ are plotted (the data for these figures were taken from ref. 76). For the moment it is assumed that the experiment has been designed and has been exposed to punctures for some time $t$.

The significance of figure 21 can be illustrated by the following example: Suppose at the end of the experiment there have been 500 of 1000 segments destroyed. Figure 21(c) then shows that the maximum probability $p_x$ of observing 500 events with 1000 segments is 0.025. This probability corresponds to a 0.50 probability of each segment being penetrated and the condition that each segment was equally likely or probable of being penetrated. Figure 21(c) also shows that, if the probability of penetrating each segment is less than approximately 0.45 or greater than approximately 0.55, the probability $p_x$ of observing 500 events with 1000 segments is for all practical purposes zero. The conclusion to be drawn from this example then is that, if 500 events are observed by exposing 1000 segments, the probability of losing an individual segment lies for all practical purposes between 0.45 and 0.55. If one wished to assume Poisson statistics applied, an average rate of puncture could be calculated using the measured probability $p$ because

$$p = 1 - e^{-\lambda at} \tag{21}$$

However, the end purpose really of determining an average rate is to permit the probability of receiving penetrations to be calculated. If this can be determined directly, there is really no need to go through the intervening step of determining an average rate.

Case II(b). - The previous case (Case II(a)) parallels Case I(a) in that only a limited amount of information is obtained. It would be desirable to be able to determine that the probability of losing a segment was not dependent upon the total time interval for which the experiment was conducted. (This corresponds for the assumption of Poisson statistics to a constant average rate.) If the time to each event is known, the validity of the assumption that the probability of losing a segment is the same for all time intervals can be checked. This can be done as follows:



(1) Let $p_t$ = probability of losing a segment in time $t$.

(2) Then $1 - p_t$ = probability of not losing a segment in time $t$,

(3) And $(1 - p_t)^n$ = probability of not losing a segment in time $nt$,

(4) Where $n \geq 1$.

The probability of losing a segment by the time the experiment is concluded $p$ is then

$$p = 1 - (1 - p_t)^n \tag{22}$$

where $n$ = (Time of experiment)/$t$. Solving equation (22) for $p_t$ gives

$$p_t = 1 - (1 - p)^{1/n} \tag{23}$$

The number of events expected by any time $t$ is then

$$zp_t = z\left[1 - (1 - p)^{1/n}\right] \tag{24}$$

A typical plot of equation (24) is shown in figure 20(b) along with a histogram of data as they might occur.

Comparison of the data with the theoretical distribution parallels Case I(b).

Rate variation with thickness. - The variation of the mean penetration rate with thickness proposed in equation (7) could be generalized

(by taking the log of both sides; $\ln r = \ln K - 3 \ln h$) into the following form:

$$y = \alpha + \beta x \tag{25}$$

where $y = \ln r$, $x = \ln h$, and the coefficients $\alpha$ and $\beta$ are to be determined from the experimental data.



It would be desirable to use the data obtained on the measured mean rates as discussed in Case I and Case II to evaluate the coefficients $\alpha$ and $\beta$ of equation (25) if the proposed model is appropriate. The most common procedure is to apply a least-squares technique to determine the coefficients of $\alpha$ and $\beta$. An example of this technique for a physical problem described by equation (25) is worked out on pages 206 to 209 of reference 74. Unfortunately the usual simplifying assumptions are made in the reference in order to make the problem tractable. The assumptions are:

(1) For a given value of $x$ the variation of the estimated or measured means about the true mean is normal.

(2) The standard deviation or variance of these normal distributions is constant for all values of $x$. (However, the more general case of a variation in the variance with the independent variable $x$ is discussed in ref. 74.)

In the situation considered herein some knowledge of the statistical nature of the penetration rate will be known if time to penetration is recorded per Case I(b) or Case II(b). However, it is unlikely that enough data will be obtained to permit determination of the statistical fluctuations of the measured or estimated mean values about the true mean of the population. (This will be discussed more fully in the subsequent section.) If the meteoroid population is such that in obtaining an estimated mean it appears that a Poisson, normal, or binomial distribution applies to the data, it can be reasonably assumed that the measured means will have a normal distribution about the true mean of the population (see ch. 8, ref. 77). This would then satisfy assumption (1), but not assumption (2). It should be pointed out that assumption (2) is only of consequence in setting confidence levels on the estimated $\alpha$ and $\beta$. This sophistication is often ignored in practice by using weighted averages and the least-squares technique to obtain the best estimate of $\alpha$ and $\beta$.

There are two other facets of this problem that should probably be mentioned. The first concerns the weighting of data. In the subsequent section it will be seen that when a selected set of material thicknesses is exposed more events will be recorded for the smaller thicknesses even with less area exposed. In this situation rate estimates at these thicknesses should be given more weight during the curve-fitting process.

This can be done by treating the data at each thickness selected as multiple estimates of the rate with each rate estimate based on the same number of events. The thickness with the minimum number of events (presumably the maximum thickness exposed) will have a weight of unity and will serve as the unit or basic measurement for determining the weight given the data at other thicknesses.

The second facet concerns the extrapolation of the estimated rates of punctures to thicknesses of material which are impractical to expose. There are a number of extrapolation procedures that can be employed (e.g., see ref. 78) to estimate the rates of puncture at thicknesses greater than those exposed and to estimate the expected dispersion in these rates. These techniques are beyond the scope of this report.



## Design Considerations

This section is not intended to develop equations whereby an optimum experiment could be obtained. Rather, the intent is to explore some of the general problems associated with obtaining direct experimental measurements of puncture rates.

In this section only the influence of four parameters on the problem of obtaining direct measurement of puncture rates is investigated. The parameters of concern are surface area, material thickness, time, and, in the case of a segmented approach, the number of segments. A discussion of the general considerations involving area, time, and material thickness follows.

General considerations. - The problem posed is as follows: If a space vehicle must be designed for a given survival probability, what must the area of an experiment be to obtain the required engineering data upon which a design may be based. The problem will be explored using a specific example. In addition, in order to simplify the presentation to follow it will be assumed that Poisson statistics are applicable. However, the conclusions drawn are quite general and are not restricted by these initial assumptions.

The probability of receiving no punctures will be taken as the survival probability. For Poisson statistics then, the probability of receiving no punctures in a given area $a$ in time $t$ is

$$p_0 = e^{-\lambda at} \tag{26}$$

and it will be deemed necessary to predict the survival probability $p_0$. It is then desirable to obtain experimentally the mean rate of puncture $\lambda$ so that the survival probability can be calculated.

The precision of the resulting measurement of a statistical process is, as is well known, a function of the number of events recorded. For Poisson statistics, if a large number of events are measured (N), there is to a close approximation a 0.95 probability that N will be within the interval $N_m \pm 2\sqrt{N_m}$ where $N_m$ is the expected mean or theoretical expected average number of events. The precision (or fractional dispersion about the true mean) expected from the data could then be expected to vary as $2\sqrt{N}/N$. Making this ratio $2\sqrt{N}/N$ smaller increases the precision with which an average rate of puncture can be estimated. For purposes of this example it will be assumed that a precise estimate of the average rate is not required. The ratio of $2\sqrt{N}/N$ assumed, therefore, is 0.5:

$$\frac{2\sqrt{N_1}}{N_1} = 0.5 \tag{27}$$

The average value of $N_1$ will be

$$N_1 = \lambda a_1 t_1 \tag{28}$$

(It should be noted that there is no certainty of observing exactly $N_1$ events. There is, for example, a 50 percent chance of observing at least $N_1$ or more events, and therefore eq. (28) is only an approximation of the number of events expected.)

Let it be deemed desirable that the survival probability of the space vehicle be 0.99. (Selection of the values 0.5 and 0.99 is not critical for the point this discussion illustrates.) Then

$$0.99 = e^{-\lambda a_2 t_2} \tag{29}$$

Further let the space experiment (area $a_1$) be exposed for the same length of time as the vehicle (i.e., $t_1 = t_2$). Then combining equations (27), (28), and (29) yields the following result:

$$a_1 \simeq 1600\, a_2 \tag{30}$$

It is quite obvious from this example that, if the space vehicle area $a_2$ is of any reasonable size, it becomes impractical to make direct experimental measurements of the rates of penetration to be expected. There is one other aspect of the area problem that is not brought out by this treatment. This involves the thickness of the surface exposed. As the thickness is increased, it becomes increasingly more impractical to expect anything approaching even the precision of experimental results called for by equation (27). However, it should also be mentioned that it is also not always necessary to obtain precise rate estimates in order to obtain useful information. In fact, the case of no events is useful information if the experimenter has confidence

that his results are correct and not due to a malfunction of the experiment. In addition, the experimenter is at liberty to vary the time of exposure of his experiment and thus reduce the area required. Some of these aspects are considered in the following discussions.

Figure 22 shows a plot of the average number of events expected as a function of skin thickness for various area-time products. The figure was constructed for stainless steel and is based on figure 10(a). Figure 22 is perhaps most meaningful if a specific example is considered. If it is desired to obtain the same precision as in equation (27) (i.e., $N_1$ = 16 events) for an exposed thickness of 170 mils, then the area-time product required is $10^8$ square foot-hours. This number means that an area of $1.142 \times 10^4$ square feet would have to be exposed for a period of 1 year to record on the average 16 events. In terms of area and weight (a minimum weight of perhaps 50 tons would be required) this requirement is obviously impractical. If the rates predicted in figure 10(a) are substantially correct, experimenters from a practical standpoint will be forced to settle for rather poor precision when thicknesses of even 50 mils are exposed. In addition, the capability of defining average rates of puncture for many thicknesses of interest (100 to 250 mils or greater) by direct measurement does not appear to exist. This then requires that results from thin surfaces be extrapolated to obtain estimated rates at greater thicknesses. Another alternative is to infer what these rates might be from other data, perhaps from astronomical and hypervelocity impact data as was done early in this report.



Segmentation. - The previous area considerations apply whether a segmented or unsegmented area approach is used for the experiment. However, the segmented approach places another restriction upon the design that will be explored here.

Segmentation (as denoted herein) does not permit the total number of punctures in a surface to be measured. The increased range of the confidence interval can be obtained from the following equation derived in appendix C:

$$\frac{\Delta N}{N} = \frac{z}{N}\left\{\ln\left[e^{-\frac{N}{z}} + 2\sqrt{\frac{e^{-\frac{N}{z}}\left(1 - e^{-\frac{N}{z}}\right)}{z}}\right] - \ln\left[e^{-\frac{N}{z}} - 2\sqrt{\frac{e^{-\frac{N}{z}}\left(1 - e^{-\frac{N}{z}}\right)}{z}}\right]\right\} \quad \text{(C11)}$$

This equation predicts the 95 percent confidence interval $\Delta N$ as a function of the average number of events $N$ and number of segments $z$ and is plotted in figure 23. The confidence interval $\Delta N$ is not symmetrical about $N$, but to a close approximation the range is $N \pm \frac{\Delta N}{2}$. Three pertinent facts can be noted from this figure:

(1) The number of segments required that will give essentially the same results as for an unsegmented approach and the minimum

number of segments needed to interpret the data in terms of an average rate of penetrations. An unsegmented approach means that every penetration in the total surface is recorded.

(2) The effect of the number of events measured on the accuracy of the measurement.

(3) A practical indication of the number of segments to use in an experiment.

The dashed lines in figure 23 show the normalized confidence interval for an infinite number of segments (unsegmented approach) corresponding to various values of the average number of events expected N. It will be noted in all cases that, if the number of segments is 100 times the number of events, the results are essentially identical to an unsegmented approach. For a large number of events, such as 500 or 1000, a ratio of $z/N = 10$ is practically the same as for infinite segmentation.

The normalized confidence interval $\Delta N/N$ is very strongly affected by the number of events N and cannot be reduced below the values indicated for $z/N = \infty$. This indicates the value of measuring a large number of events (also mentioned previously). It will also be noted that the confidence interval $\Delta N$ approaches the minimum (infinite number of segments) very rapidly, and therefore no practical purpose is served by using an excessive number of segments (i.e., more than 1000 segments). This indicates that with a reasonable number of segments a segmented approach does not require acceptance of gross inaccuracies over and above those inherent in the statistical nature of the phenomena.

The distance of the intersection of lines for constant z and constant N above the dashed lines for $z/N = \infty$ shows the increase in the confidence interval due to segmentation. If the number of events, which is limited by the amount of area that can be exposed, is small (say 10 to 20), the number of segments should probably be at least two to five times the average number of events expected. If, however, the number of events to be measured is large, in excess of 200, it is probably unnecessary to have more segments than the average number of events expected. This indicates also that, if an experiment is designed for the eventuality of rates much greater than the average (i.e., showers) or expected rate, upwards of 200 segments should be used.

The reader should be reminded that figure 23 is a curve for choosing the number of segments in designing an experiment. Curves similar to figure 21 are required to determine the confidence interval for the actual experimental data.

One other point should also be noted from figure 23. If too few segments are used, it is impossible to predict with any accuracy the average number of punctures (i.e., average rate) because too few

segments would result in z/N values to the left of the knee of the curve in figure 23. This is somewhat misleading because time has not been used as a variable in the treatment. Suppose upon executing an experiment it was found that the data put one to the left of the knee. This would simply mean that the experiment did not last as long as anticipated (the result of a penetration rate higher than expected), and the results would have to be investigated on the basis of a shorter exposure time. This simply lends more support to the need for time of event in an experiment of this nature.



One final point is also worth noting. The decision as to what constitutes an acceptable prediction error or confidence interval varies with the intended use of the data. More importantly, it is also a matter of personal choice depending on the individual making the decisions. There has, therefore, been no attempt made to define points as optimum on either figure 21 or 23.

Establishing a model. - It would be highly desirable to be able to obtain a model that would describe the variation of average rate of penetration with material thickness. Up to this point only the problem of establishing an average rate for an individual thickness has been discussed. To investigate, for example, the model of figure 10(a) with an experiment requires certain considerations or compromises not considered up to this point. The following is a discussion of some of these considerations.

In order to simplify the discussion a specific example is used, and an unsegmented approach is considered. It will be assumed that 1000 square feet of area can be exposed near Earth for a period of 1 year. It is desired that this area be used to give a good definition of the variation of rate of puncture with material thickness. The problem faced by the experimenter in its simplest aspect is to decide how to divide the total area between various material thicknesses.

It is rather obvious that the best definition of the model will be obtained when the difference between the maximum and minimum thicknesses employed is as large as practical. The governing parameter on these limits is, of course, the decision of the experimenter as to the acceptable dispersion expected about the predicted mean rate. Selection of the minimum thickness does not present a difficult problem because with a given assigned area (e.g., 50 sq ft of the total of 1000 sq ft to be exposed) the number of events expected can be made acceptably high simply by going to thinner material. There is a minor restriction in this regard in that the minimum useful thickness is equal to or greater than that penetrated by approximately 1-micron-size particles. The maximum thickness presents a different problem because, even if the total area of 1000 square feet is employed, the dispersion expected about the predicted mean rate becomes rapidly less acceptable as the thickness is increased. This fact, however, permits the experimenter to determine

the maximum thickness feasible by assigning the major portion of the area to this thickness and stipulating an acceptable dispersion. For example, let 700 square feet of the total be assigned to the maximum thickness and the dispersion assumed such that

$$\frac{2\sqrt{N}}{N} = 0.5 \tag{31}$$

where $N$ is the number of events expected. The rapid decrease of rate of puncture with thickness of material makes it obvious that the value of the ratio $2\sqrt{N}/N$ must decrease as thicker material is exposed. The selection of 0.5 for the ratio of $2\sqrt{N}/N$ is arbitrary and was made only to illustrate the problems involved.



Equation (31) is satisfied for a value of $N = 16$. Thus for 700 square feet of area and an exposure of 1 year this corresponds to a puncture rate of $2.6\times10^{-6}$ penetration per square foot per hour because

$$r = \frac{N}{at} = \frac{16}{700 \times 8760} = 2.6\times10^{-6} \text{ penetration/sq ft-hr} \tag{32}$$

From figure 10(a) this rate corresponds to a rate of penetration for a material thickness of approximately 66 mils. It is obvious that utilization of the total area of 1000 square feet for the maximum thickness would not permit much of an increase over the 66 mils (approx. 75 mils).

For the variation in $N$ of $\pm2\sqrt{N}$, a corresponding variation in $r$ of the following is obtained:

$$1.31\times10^{-6} < r < 3.92\times10^{-6} \tag{33}$$

This range in $r$ has been shown as a vertical line in figure 10(a) and may be thought of as a tolerance limit. It represents the interval in which actual data would be expected to fall if the true mean were the value shown by the curve.

The tolerance limit for the minimum thickness is shown in figure 10(a) for the following assumptions. The area employed is 50 square feet and the dispersion is such that $2\sqrt{N}/N = 0.1$. Also shown in figure 10(a) is the tolerance limit if the remaining area (250 sq ft) is allotted to a thickness midway between the maximum and minimum thicknesses.

In the situation where a segmented approach is used, it would be necessary to select the number of segments to be used with each thickness on the basis of considerations already discussed. There would, of course, be some practical considerations involved, such as the number of segments it might be possible to interrogate with present telemetry techniques, and so forth.

The example presented illustrates the point that direct experimental determination of a model of rate of puncture variation with material thickness will be confined to a range of thickness less than that which might be desired. As greater thicknesses are exposed, it will also be necessary to accept less precision in the results. As a consequence of this, less information will be obtained as to the statistical fluctuations to be expected.

It is obvious that the selection of the numerical values for the previous example was arbitrary. More involved methods of choosing thicknesses and corresponding areas will probably be required in order to determine an optimum distribution. The cost of conducting space experiments is so great that the most refined statistical design procedures that are consistent with the existing estimates of the environment should be utilized in the experiment design. These procedures should aim at getting the maximum possible information from the experiment, within area and weight limitations, in order to obtain the best possible description of the penetration rate as a function of material thickness. This description should cover the range of thicknesses where data can be readily obtained, and it should provide the most reasonable extrapolation of data to greater thicknesses. It appears at this time that the statistical design procedure required is not in the available literature. The development and description of such a procedure could be another report in itself and is beyond the scope intended for this report.



## CONCLUDING REMARKS

The hazard to space vehicles of meteoroid material in space is at present of great concern. An attempt to assess the extent of this hazard on the basis of present information has been made herein. The obvious conclusion reached is that a hazard exists, but only very crude estimates of this hazard can be made at present. The uncertainty in these estimates, which may be in error by orders of magnitude, results from a lack of information in two general areas. The first area falls most nearly into the realm of meteor astronomy and some closely allied subjects. The second area, which is relatively new to science, is that of hypervelocity impact.

Both of these areas of knowledge are expanding rapidly, but it is unlikely that they will provide all the information needed on the hazard of meteoroids. In addition, considerable time will be needed to accumulate enough information in these two fields to permit a wedding of the information to yield a comprehensive picture of the meteoroid hazard. For this reason, it is imperative to make direct measurements of meteoroid damage by space experiments. Some aspects of this experimental approach have been explored herein, and the pertinent conclusions are as follows:

1. The design of experiments at present is largely a matter of intelligent guesswork. This leads then to the obvious need for some early experiments to crudely determine the rate of penetration for some thicknesses of skin material so that more intelligently planned future experiments can be conducted.

2. It is also obvious that no one experiment can be devised that will answer all the design questions. Because many experiments are needed, it is doubtful, in view of the cost and other requirements, that all the data desired will ever be gathered directly. It thus behooves the experimenters to give very careful consideration to the experiments conducted and to build one experiment upon another.

3. The most urgently needed information at present for space vehicle designers is a knowledge of the rate of penetration to be expected. In looking at the design requirements of such experiments it becomes apparent that very large areas must be exposed for extended periods of time in space. It is further highly desirable to be able to know the time of event so that the statistical characteristics of the puncture rates can be investigated.

4. Only the problem of defining an average rate is explored in detail, but the results are general enough that they can be applied to the problem of determining when showers occur and the rates during showers. Although also not explored in detail herein, the design of experiments to investigate the effect of orientation relative to the plane of the ecliptic, Earth concentrating effects, and so forth, will be very important considerations in the design of space vehicles, and direct experimental investigations of these effects should be made.

5. The problem of establishing a model for the variation of average rate with material thickness was also explored. It was obvious that a definitive model obtained by direct measurement would be limited in range. This introduces the problem of selecting experimental points to give the best definition of rate with thickness, and this was briefly explored in the text.

6. Direct measurement of the penetration rates through thick materials seems to be impractical at present. The recourse, if this is the situation, will be to extrapolate from direct measurements at smaller thicknesses or to infer what these rates will be from other measurements, such as radio echo surveys, hypervelocity impact studies, and so forth.

Lewis Research Center
National Aeronautics and Space Administration
Cleveland, Ohio, August 28, 1961

# APPENDIX A

## SYMBOLS

| | |
|---|---|
| $A_d$ | area subject to aerodynamic drag |
| a | area exposed to puncture |
| C | quantity of momentum necessary to produce penetration |
| $C_D$ | aerodynamic drag coefficient |
| D | depth of penetration |
| d | diameter of impacting particle |
| $d_c$ | crater diameter |
| $d_{cm}$ | minimum hole diameter |
| H | height or altitude above Earth's surface |
| h | surface thickness |
| $K_a$ | impact constant, ratio of striking energy to crater volume for specific target-particle combinations |
| $K_p$ | functional constant for impacting particle material |
| $K_t$ | functional constant for target material |
| $K, K_1, \ldots$ | arbitrary constants |
| L | characteristic particle dimension |
| M | meteor magnitude |
| m | particle mass |
| N | number of events |
| p | probability of an event |
| R | radial distance from Sun |
| $R_e$ | radial distance from center of Earth |

| | |
|---|---|
| r | average rate of penetration |
| S | constant determining variation in number of particles with mass |
| t | time |
| V | particle velocity |
| $V_s$ | velocity of sound in target material |
| V.L. | viewing loss due to presence of Earth |
| x, y, z | variables whose specific meanings are given in text |
| $\alpha$ | regression coefficient defining intercept of a straight line |
| $\beta$ | regression coefficient defining slope of a straight line |
| $\lambda$ | mean rate for a Poisson distribution (this is, in general, taken to be equal to r) |
| $\rho_a$ | atmospheric density |
| $\rho_p$ | particle density |
| $\rho_t$ | target density |

# APPENDIX B

## RATE OF PENETRATION

The number of meteoroids of mass m or greater entering Earth's atmosphere per day was given in the text as follows:

$$N = \frac{5.81 \times 10^7}{m} \frac{\text{Number entering Earth's atmosphere}}{\text{Day}} \tag{6}$$



For spherical particles of constant density this can be written as

$$N = \frac{\text{const.}}{d^3} \tag{B1}$$

### Ames Penetration Criteria

Most penetration criteria assume that the depth of penetration D varies linearly with some dimensions of the impacting particle, usually the diameter d. Thus, for example, the Ames penetration criteria give

$$D = 2.28 \left(\frac{\rho_p}{\rho_t}\right)^{2/3} \left(\frac{V}{V_s}\right)^{2/3} d \tag{B2}$$

If further it is assumed that the target thickness h just equals the depth of penetration (see assumptions in text; for thin targets the depth is 1.5 times that of infinite targets), then

$$h = 1.5\ D = 3.42 \left(\frac{\rho_p}{\rho_t}\right)^{2/3} \left(\frac{V}{V_s}\right)^{2/3} d \tag{B3}$$

and the skin thickness just penetrated also varies linearly with particle diameter.

Combining equations (B1) and (B3) leads to the conclusion that the rate of penetration r varies as follows:

$$r = \frac{\text{const.}}{h^3} \tag{B4}$$

where

$$r = \frac{N}{\text{Earth's surface area}} \tag{B5}$$

The constant in equation (B4) can be evaluated for a given set of conditions, for example, as follows: Select the target material $\rho_t$ and $V_s$, a particle $\rho_p$ and d, and velocity of impact V. Calculate the target thickness that will be penetrated for these conditions using equation (B3). Calculate the particle mass and from equation (B5) the rate r. The constant in equation (B4) for this set of conditions is given as the product of the calculated r and $h^3$. This constant can be employed in equation (B4) to calculate the rate of penetration expected for any other thickness. Figure 10 was constructed on this basis.

## Langley Penetration Criteria

The Langley penetration criteria are as follows:

$$D = K_p K_t(\rho_p VL - C) \tag{B6}$$

For aluminum impacting aluminum the value of the constants $K_p$, $K_t$, and C gives

$$D = 0.054(\rho_p VL - 1.3) \tag{B7}$$

(Eq. (B7) was not developed for the case of stone pellets impacting aluminum targets but is used as such herein.)

With the penetration criteria of equation (B7), equation (B4) has the following form:

$$r = \frac{\text{const.}}{(h + \text{const.})^3} \tag{B8}$$

Equation (B7) leads to the rather unlikely situation discussed in the text that particles must be of a certain size before any penetration is obtained. This results in a leveling out of the penetration rate with decreasing thickness as would be expected from inspection of equation (B8). This effect is also apparent upon inspection of figure 13.

## Atkins and Bjork Penetration Criteria

Both the Bjork and Atkins penetration criteria result in a rate of penetration equation like equation (B4). The constant, of course, differs in each case. Neither equation was developed for the conditions peculiar to the calculations herein and thus each necessitates some assumptions.

Atkins penetration criteria which follow

$$D = \left(\frac{3}{4\pi K_a}\right)^{1/3} m^{1/3} V^{2/3} \tag{B9}$$

require an assumption as to the value of the constant $K_a$, which is the ratio of striking energy to crater volume. The value of this constant varies with the different combinations of pellets and targets. A range of $4\times10^9$ to $2\times10^{10}$ joules per cubic centimeter was assumed likely to cover the situation herein. The rates of penetration in figure 13 are therefore shown as a band for Atkins.



Bjork's penetration criteria which follow

$$D = 1.09(mV)^{1/3} \tag{B10}$$

were developed for aluminum impacting aluminum. It was assumed to hold for the case of stone (having the same density as aluminum) impacting aluminum.

As noted in the text all the penetration criteria cited were developed for semi-infinite targets, and the depths of penetration so obtained were multiplied by 1.5 to obtain the sheet thickness that will be penetrated.

## Viewing Loss

The viewing loss from a point above the Earth's surface due to the presence of Earth is given by the following equation:

$$V.L. = \frac{1 - \cos\theta}{2} \tag{B11}$$

where

$$\sin\theta = \frac{R_e}{R_e + H} \tag{B12}$$

# APPENDIX C

## OPTIMUM NUMBER OF SEGMENTS

The possible error in estimating the mean number of punctures in a segmented surface can be estimated by approximating the binomial distribution with a normal distribution. A new random variable $y$ can be defined for a binomial distribution as follows:

$$y = \frac{x - \mu_x}{\sigma_x} \tag{C1}$$

where for a binomial distribution

$\mu_x$ mean or expected number of events

$x$ variable describing variations or distribution of the number of events about the mean $\mu_x$

$\sigma_x$ standard deviation of $x$ about mean $\mu_x$

For a binomial distribution it can also be shown (see ref. 74) that

$$\mu_x = zp \tag{C2}$$

$$\sigma_x = \sqrt{zpq} \tag{C3}$$

where

$$q = 1 - p \tag{C4}$$

$z$ number of trials (i.e., number of segments)

$p$ probability of the event in question occurring (i.e., a segment will be punctured)

$q$ probability of the event in question not occurring

The random variable $y$ can be approximated quite precisely for large $z$ ($z > 10$) by a normal distribution with a mean of zero and a standard deviation $\sigma = 1.0$. This fact can be used as follows:

For a confidence level such that there is a 0.95 probability of $x$ within $x \pm \Delta x$, $y$ has a range $-2 \leq y \leq 2$. The value of $\Delta x$, therefore, from equations (C1) to (C4) is

$$\Delta x = 2\sqrt{zp(1 - p)} \tag{C5}$$

If it is assumed that Poisson statistics apply to the penetration rate, then

$$p = 1 - e^{-\lambda at} = 1 - e^{-\lambda At/z} = 1 - e^{-N/z} \tag{C6}$$

where

a area of a segment

t time of exposure

$\lambda$ mean rate of puncture

A total area exposed

N average number of punctures for total area

Substitution of equation (C6) in (C5) gives

$$\Delta x = 2\sqrt{ze^{-N/z}\left(1 - e^{-N/z}\right)} \tag{C7}$$

From (C6) it can also be seen that

$$\Delta N = z \ln\left(\frac{1 - p_1}{1 - p_2}\right) \tag{C8}$$

where

$$p_1 = p - \Delta p = p - \frac{\Delta x}{z} \tag{C9}$$

$$p_2 = p + \Delta p = p + \frac{\Delta x}{z} \tag{C10}$$

Substituting (C7), (C9), and (C10) into (C8) and dividing both sides by N give

$$\frac{\Delta N}{N} = \frac{z}{N} \ln\left[\frac{e^{-N/z} + 2\sqrt{\frac{e^{-N/z}\left(1 - e^{-N/z}\right)}{z}}}{e^{-N/z} - 2\sqrt{\frac{e^{-N/z}\left(1 - e^{-N/z}\right)}{z}}}\right] \tag{C11}$$

It can be seen from equation (C11) that the total possible error represented by the normalized confidence interval $\Delta N/N$ in estimating the average number of punctures N for the total surface is only a function of the number of segments z and the ratio z/N. (It should

be noted that time was not taken into account as a variable in this treatment. See the text for a discussion of the influence of time.)

This measure of error $\Delta N/N$ reaches a minimum for $N = \infty$. This can be seen more easily by investigating the variations in probability value $p$. Thus,

$$\sigma_{\bar{p}} = \sqrt{\frac{pq}{z}} \tag{C12}$$

where $\sigma_{\bar{p}}$ is the standard deviation for the estimated probability. The parameter to minimize, however, is $\sigma_{\bar{p}}/p$. Thus,

$$\frac{\sigma_{\bar{p}}}{p} = \sqrt{\frac{q}{zp}} \tag{C13}$$

$$\ln \left(\frac{\sigma_{\bar{p}}}{p}\right)^2 = \ln q - \ln z - \ln p \tag{C14}$$

$$\frac{d \ln \left(\frac{\sigma_{\bar{p}}}{p}\right)^2}{dz} = \frac{1}{q}\frac{dq}{dz} - \frac{1}{z} - \frac{1}{p}\frac{dp}{dz} \tag{C15}$$

If $q = 1 - p = e^{-N/z}$ it can be easily shown that

$$\lim_{z \to \infty} \left[\frac{d \ln \left(\frac{\sigma_{\bar{p}}}{p}\right)^2}{dz}\right] = 0 \tag{C16}$$

and, therefore, the error in the estimated probability $\bar{p}$ and, hence, the error $\Delta N/N$ are a minimum when $z \to \infty$.

A plot of $\Delta N/N$ for various values of $z/N$ and $N$ has been shown in figure 23. For a discussion of the figure see the text.

## REFERENCES


1. Robertson, H. P.: Dynamical Effects of Radiation in the Solar System. Roy. Astronautical Soc. Monthly Notices, vol. 97, Apr. 1937, pp. 423-438.

2. Whipple, F. L.: A Comet Model. III - The Zodiacal Light. Astrophys. Jour., vol. 121, no. 3, May 1955, pp. 750-770.

3. Beard, David B.: Interplanetary Dust Distribution. The Astrophys. Jour., vol. 129, no. 2, Mar. 1959, pp. 496-506.

4. Allen, C. W.: Astrophysical Quantities. The Athlone Press (Univ. London), 1955.

5. Moulton, Forest Ray: An Introduction to Celestial Mechanics. The Macmillan Co., Second revised ed., 1958.

6. Lovell, A. C. B.: Meteor Astronomy. Clarendon Press (Oxford), 1954.

7. Whipple, Fred L., and Hawkins, Gerald S.: Meteors. Encyclopedia of Phys., S. Flügge, ed., vol. LII - Astrophysics. III: The Solar System. Springer-Verlag, 1959.

8. Whipple, F. L.: A Comet Model. I - The Acceleration of Comet Encke. Astrophys. Jour., vol. 111, Mar. 1950, p. 375.

9. Öpik, E. J.: The Masses and Structure of Meteors. Meteors, T. R. Kaiser, ed., Pergamon Press, Ltd., 1955, pp. 33-35.

10. Öpik, E. J.: Problems in the Physics of Meteors. Am. Jour. Phys., vol. 26, no. 2, Feb. 1958, pp. 70-80.

11. Blackwell, D. E.: The Zodiacal Light and Its Interpretation. Endeavour, vol. 19, no. 73, Jan. 1960, pp. 14-19.

12. Wyatt, Stanley P., Jr., and Whipple, Fred L.: The Poynting-Robertson Effect on Meteor Orbits. The Astrophys. Jour., vol. 111, no. 1, 1950, p. 134.

13. Chapman, Sydney: The Earth in the Sun's Atmosphere. Sci. Am., vol. 201, no. 4, Oct. 1959, pp. 64-71.

14. Siedentopf, H.: Diffuse Matter in the Solar System. Meteors, T. R. Kaiser, ed., Pergamon Press, Ltd., 1955, pp. 145-148.

15. Van De Hulst, H. C.: Zodiacal Light in the Solar Corona. Astrophys. Jour., vol. 105, May 1947, pp. 471-488.

16. Hawkins, Gerald S., and Southworth, Richard B.: The Statistics of Meteors in the Earth's Atmosphere. Smithsonian Contributions to Astrophys., vol. 2, no. 11, 1958, pp. 349-364.

17. Whipple, Fred L.: The Meteoritic Risk to Space Vehicles. Paper 499-57, Am. Rocket Soc., Inc., 1957.

18. Lovell, A. C. B.: Geophysical Aspects of Meteors. Encyclopedia of Phys., S. Flügge, ed., vol. XLVIII - Geophysics II. Springer-Verlag, 1957, pp. 427-454.

19. Schley, Dewey R.: Meteor Correlation Study. TR 60-160, Rome Air Dev. Center, Aug. 1960.

20. Struve, Otto: Visual Observations of Meteors. Sky and Telescope, vol. XIX, no. 4, Feb. 1960, pp. 200-204.

21. Harris, I., and Jastrow, R.: An Interim Atmosphere Derived from Rocket and Satellite Data. Planetary Space Sci., vol. 1. Pergamon Press, 1959, pp. 20-26.

22. Emmons, Howard W., ed.: Fundamentals of Gas Dynamics. Vol. III - High Speed Aerodynamics and Jet Propulsion. Princeton Univ. Press, 1958.

23. McCrosky, Richard E.: Observations of Simulated Meteors. Smithsonian Contributions to Astrophys., vol. 5, no. 4, 1961, pp. 29-37.

24. Whipple, Fred L., P. Campbell, ed.: Particulate Contents of Space. (To be publ. in Medical and Biological Aspects of the Energies of Space.)

25. Pettersson, Hans: Cosmic Spherules and Meteoritic Dust. Sci. Am., vol. 202, no. 2, Feb. 1960, pp. 123-132.

26. Biggs, F. Behn, Jr.: Study of Atmospheric Entry and Impact of High Velocity Meteorites. Quarterly Status Rep. 18, Apr. 1-June 30, 1960, Astrophys. Observatory, Smithsonian Inst., Aug. 31, 1960.

27. Whipple, Fred L., and Hughes, Robert F.: On the Velocities and Orbits of Meteors, Fireballs, and Meteorites. Meteors, T. R. Kaiser, ed., Pergamon Press Ltd., 1955, pp. 149-156.

28. Rinehart, John S.: Meteorites and Ballistics. Tech. Rep. 8, Phys. Div., AF Office Sci. Res., ARDC, Apr. 21, 1958.

29. Hawkins, Gerald S.: A Radio Echo Survey of Sporadic Meteor Radiants. Roy. Astronautical Soc. Monthly Notices, vol. 116, no. 1, 1956, pp. 92-104.

30. Weiss, A. A.: The Distribution of the Orbits of Sporadic Meteors. Australian Jour. Phys., vol. 10, no. 1, Mar. 1957, pp. 77-102.

31. Bain, W. C.: The Azimuth Distribution of Oblique Reflections from Meteor Trails and Its Relation to Meteor Radiant Distributions. Jour. Atmospheric and Terrestrial Phys., vol. 17, nos. 1/2, 1960, pp. 188-204.

32. Vogan, E. L., and Campbell, L. L.: Meteor Signal Rates Observed in Forward Scatter. Canadian Jour. Phys., vol. 35, no. 10, Oct. 1957, pp. 1176-1189.

33. Meeks, M. L., and James, J. C.: Meteor Radiant Distributions and the Radio-Echo Rates Observed by Forward Scatter. Jour. Atmospheric and Terrestrial Phys., vol. 16, nos. 3/4, 1959, pp. 228-235.

34. Forsyth, P. A., Vogan, E. L., Hansen, D. R., and Hines, C. O.: The Principles of Janet - A Meteor-Burst Communication System. Proc. I.R.E., vol. 45, no. 12, Dec. 1957, pp. 1642-1657.

35. Olivier, Charles P.: Catalog of Hourly Meteor Rates. Smithsonian Contributions to Astrophys., vol. 4, no. 1, 1960, pp. 1-14.

36. Olivier, Charles P.: Tables of Hourly Rates Based on American Meteor Society Data. Interim Reps. 28 and 29, Radio Meteor Res. Program, Harvard Univ. Meteor Dept., Harvard College Observatory, May 1958.

37. Manring, Edward R.: Micrometeorite Measurements from 1958 Alpha (Explorer I) and Gamma (Explorer III) Satellites. Geophys. Res. Directorate, Air Force Cambridge Res. Center, 1958.

38. Dubin, Maurice: Meteoritic Dust Measured from Explorer I (1958 Alpha). Geophys. Res. Directorate, Air Force Cambridge Res. Center, 1958.

39. Krassovsky, V. I.: Results of Scientific Investigations Made by Soviet Sputniks and Cosmic Rockets. Astronautica Acta, vol. 6, no. 1, 1960, pp. 45-46.

40. LaGow, H. E., and Alexander, W. M.: Recent Direct Measurements by Satellites of Cosmic Dust in the Vicinity of the Earth. NASA TN D-488, 1960.

41. Anon.: The Environment of a Satellite. (Pioneer I and 1959 Alpha Vanguard II.) NASA, Sept. 15, 1959.

42. Cohen, Herbert A.: Measurements of Flux of Small Extraterrestrial Particles. GRD Res. Notes No. 28, Geophys. Res. Directorate, USAF, Jan. 1960.

43. Kells, M. C., and Keough, D. D.: Impact of High Speed Particles with Solids and Gases. AFCRC TR-59-219, Stanford Res. Inst., Dec. 15, 1958.

44. Komissarov, O. D., et al.: Investigation of Micrometeorites with the Aid of Rockets and Satellites. ARS Jour. Supplement, Oct. 1959, pp. 742-744.

45. Nazarova, T. N.: Results of a Study of Impacting of Meteoric Matter by Means of Instruments Mounted on Space Rockets. Iskusstvennyy Sputnik Zemli, vol. 5, 1960, pp. 38-40.

46. Nazarova, T. N.: Study of Meteoric Particles Through Instruments on the Third Soviet Artificial Satellite. Iskusstvennyy Sputnik Zemli, vol. 4, 1960, pp. 165-170.

47. Dubin, Maurice: IGY Micrometeorite Measurements. Space Research, H. K. Kallmann Bijl, ed., North-Holland Publ. Co. (Amsterdam), 1960.

48. Singer, S. F.: Distribution of Dust in Cislunar Space - Possible Existence of a Terrestrial Dust Belt. Paper presented at meeting Am. Assoc. for Advancement of Sci., New York City, Dec. 27, 1960.

49. Summers, James L.: Investigation of High-Speed Impact - Regions of Impact and Impact at Oblique Angles. NASA TN D-94, 1959.

50. Atkins, W. W.: Hypervelocity Penetration Studies. Proc. Third Symposium on Hypervelocity Impact, vol. I, Feb. 1959, pp. 199-214.

51. Bioletti, Carlton, and Cunningham, Bernard E.: A High-Velocity Gun Employing a Shock-Compressed Light Gas. NASA TN D-307, 1960.

52. Atkins, W. W.: Hypervelocity Penetration Studies. Proc. Fourth Symposium on Hypervelocity Impact, APGC-TR-60-39(1), Sept. 1960.

53. Kinard, William H., and Collins, Rufus D., Jr.: A Technique for Obtaining Hypervelocity Impact Data by Using the Relative Velocities of Two Projectiles. NASA TN D-724, 1961.

54. Anon.: Study of Hypervelocity Impact of Particles on Material. MD 59-114, North Am. Aviation, Inc., June 1960.

55. Gehring, J. William, Jr., and Richards, L. G.: Further Studies of Micro-Particle Cratering in a Variety of Target Materials. Proc. Fourth Symposium on Hypervelocity Impact, APGC-TR-60-39(111), Sept. 1960.

56. Eichelberger, R. J.: Experimental Results in Hypervelocity Impact. Ballistic Res. Labs., Aberdeen Proving Ground, Md.

57. Kineke, John H., Jr., and Holloway, Lee S.: Macro-pellet Projection with an Air Cavity High Explosive Charge for Impact Studies. Memo. Rep. 1264, Ballistic Res. Lab., Apr. 1960.

58. Collins, Rufus D., Jr., and Kinard, William H.: The Dependency of Penetration on the Momentum Per Unit Area of the Impacting Projectile and the Resistance of Materials to Penetration. NASA TN D-238, 1960.

59. Hopko, Russel N., and Kinard, William H.: A Hypervelocity Impact System Using the Relative Velocity of Two Projectile Accelerators. Proc. Fourth Symposium on Hypervelocity Impact, APGC-TR-60-39(11), Sept. 1960.

60. Kinard, William H., and Collins, Rufus D., Jr.: An Investigation of High-Velocity Impact Cratering into Nonmetallic Targets and Correlation of Penetration Data for Metallic and Nonmetallic Targets. NASA TN D-726, 1961.

61. Bjork, R. L.: Effects of a Meteoroid Impact on Steel and Aluminum in Space. Rep. P-1662, The Rand Corp., Dec. 16, 1958.

62. Bjork, R. L.: Meteoroids Versus Space Vehicles. Rep. P-1963, The Rand Corp., Apr. 4, 1960. (See also Paper 1200-60, ARS, May 1960.)

63. Huth, J. H., Thompson, J. S., and Van Valkenburg, M. E.: Some New Data on High-Speed Impact Phenomena. Jour. Appl. Mech., vol. 24, no. 1, Mar. 1957, pp. 65-68.

64. Clay, Wallace G., and Partridge, William S.: Wax Modelling Studies of High-Speed Impact. Tech. Rep. OSR-5, Armed Services Tech. Info. Agency, June 1956.

65. Kinard, William H., Lambert, C. H., Jr., Schryer, David R., and Casey, Francis W., Jr.: Effect of Target Thickness on Cratering and Penetration of Projectiles Impacting at Velocities to 13,000 Feet per Second. NASA MEMO 10-18-58L, 1958.

66. Maiden, C. J., Charest, J., and Tardif, H. P.: An Investigation of Spalling and Crater Formation by Hypervelocity Projectiles. Proc. Fourth Symposium on Hypervelocity Impact, APGC-TR-60-39(111), Sept. 1960.

67. Allison, F. E., Becker, K. R., and Vitali, R.: Effects of Target Temperature on Hypervelocity Cratering. Proc. Fourth Symposium on Hypervelocity Impact, APGC-TR-60-39(1), Sept. 1960.

68. Van Valkenburg, M. E., Clay, Wallace G., and Huth, J. H.: Impact Phenomena at High Speeds. Armed Services Tech. Info. Agency, Feb. 15, 1956.

69. O'Keefe, John A.: The Origin of the Tektites. Space Research, N. K. Kallmann Bijl, ed., North-Holland Publ. Co., Amsterdam, 1960.

70. Macvey, John W.: Craters of the Moon. Space Flight, vol. 111, no. 1, Jan. 1961, pp. 13-15.

71. English, Robert E., and Guentert, Donald: Segmenting of Radiators for Meteoroid Protection. (To be publ. in ARS Jour.)

72. Funkhouser, John O.: A Preliminary Investigation of the Effect of Bumpers as a Means of Reducing Projectile Penetration. NASA TN D-802, 1961.

73. Weatherston, Roger C., and Smith, William E.: A Method for Heat Rejection from Space Powerplants. ARS Jour., vol. 30, no. 3, Mar. 1960, pp. 268-269.

74. Arley, Niels, and Buch, K. Rander: Probability and Statistics. John Wiley & Sons, Inc., 1950.

75. Evans, Robley D.: The Atomic Nucleus. McGraw-Hill Book Co., Inc., 1955.

76. Anon.: Tables of the Cumulative Binomial Probability Distribution. Vol. 35 of The Annals of Computation Lab., Harvard Univ., Harvard Univ. Press, 1955.

77. Acton, Forman S.: Analysis of Straight-Line Data. John Wiley & Sons, Inc., 1959.

78. Mood, Alexander McFarlane: Introduction to the Theory of Statistics, ch. 13. McGraw-Hill Book Co., Inc., 1950.

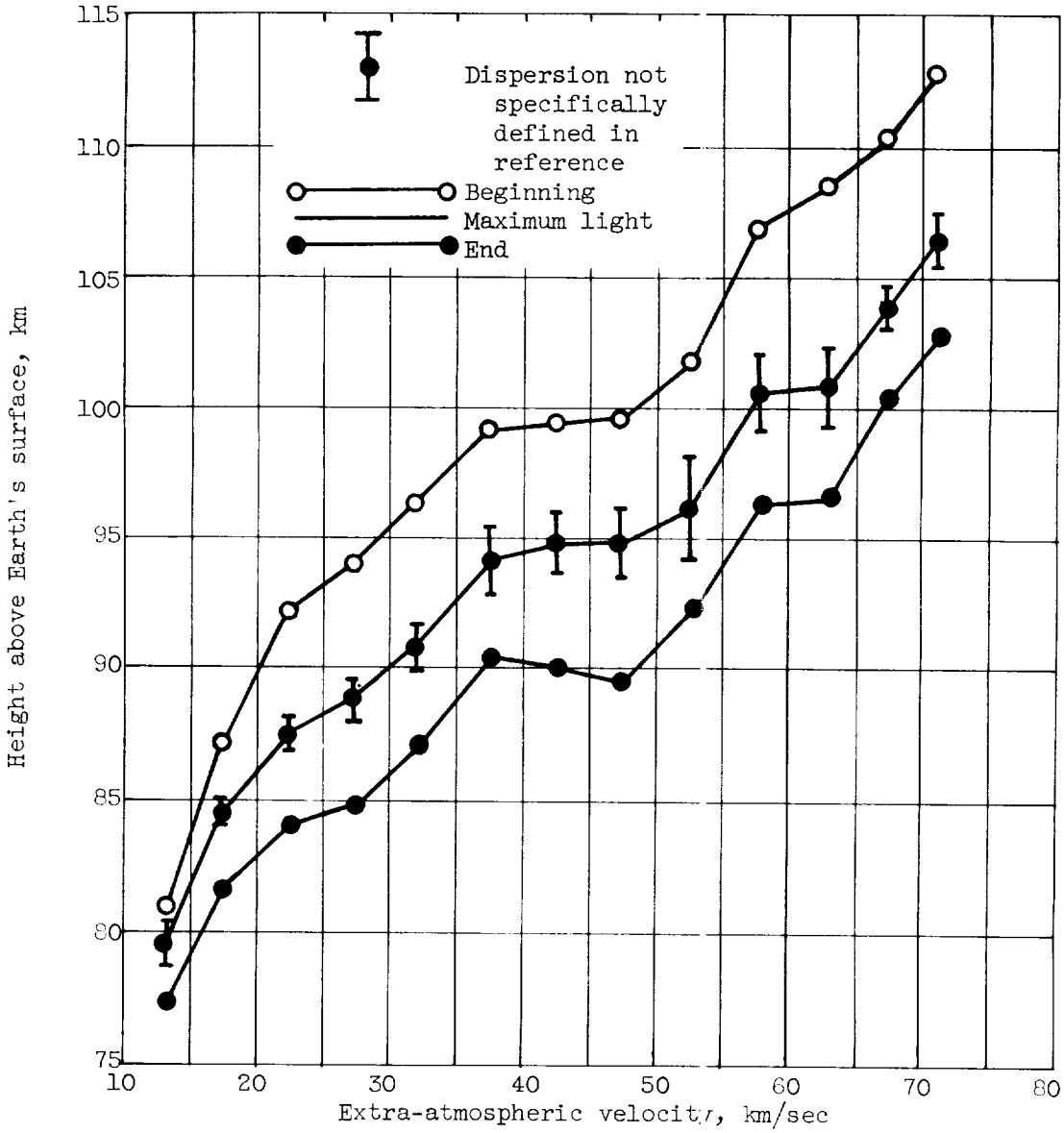


(a) Mean heights of beginning, maximum light, and end for sporadic meteors of various velocities.

Figure 1. - Statistics of meteors in Earth's atmosphere (taken from ref. 16).

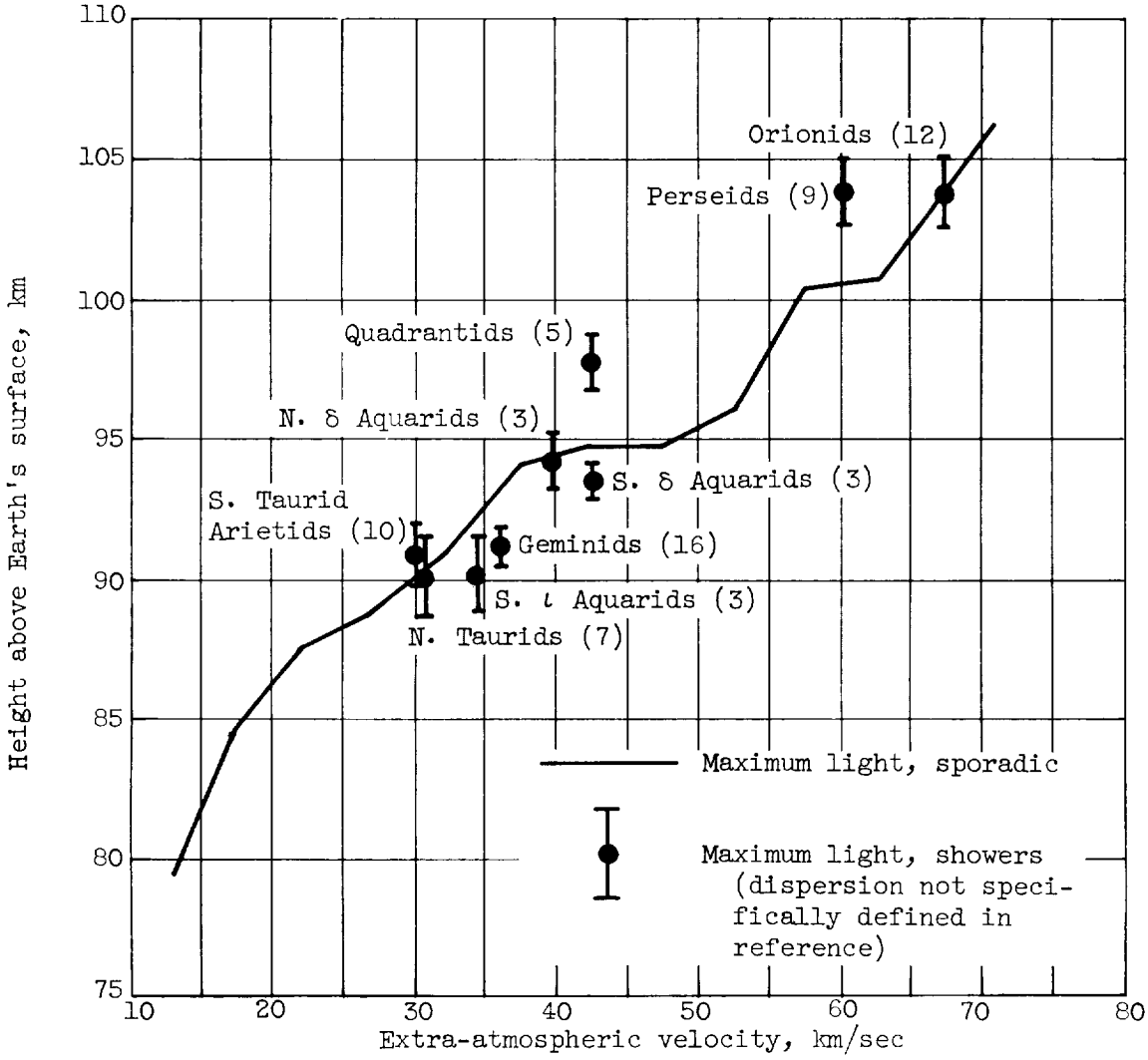


(b) Heights of maximum light for shower meteors.

Figure 1. - Concluded. Statistics of meteors in Earth's atmosphere (taken from ref. 16).

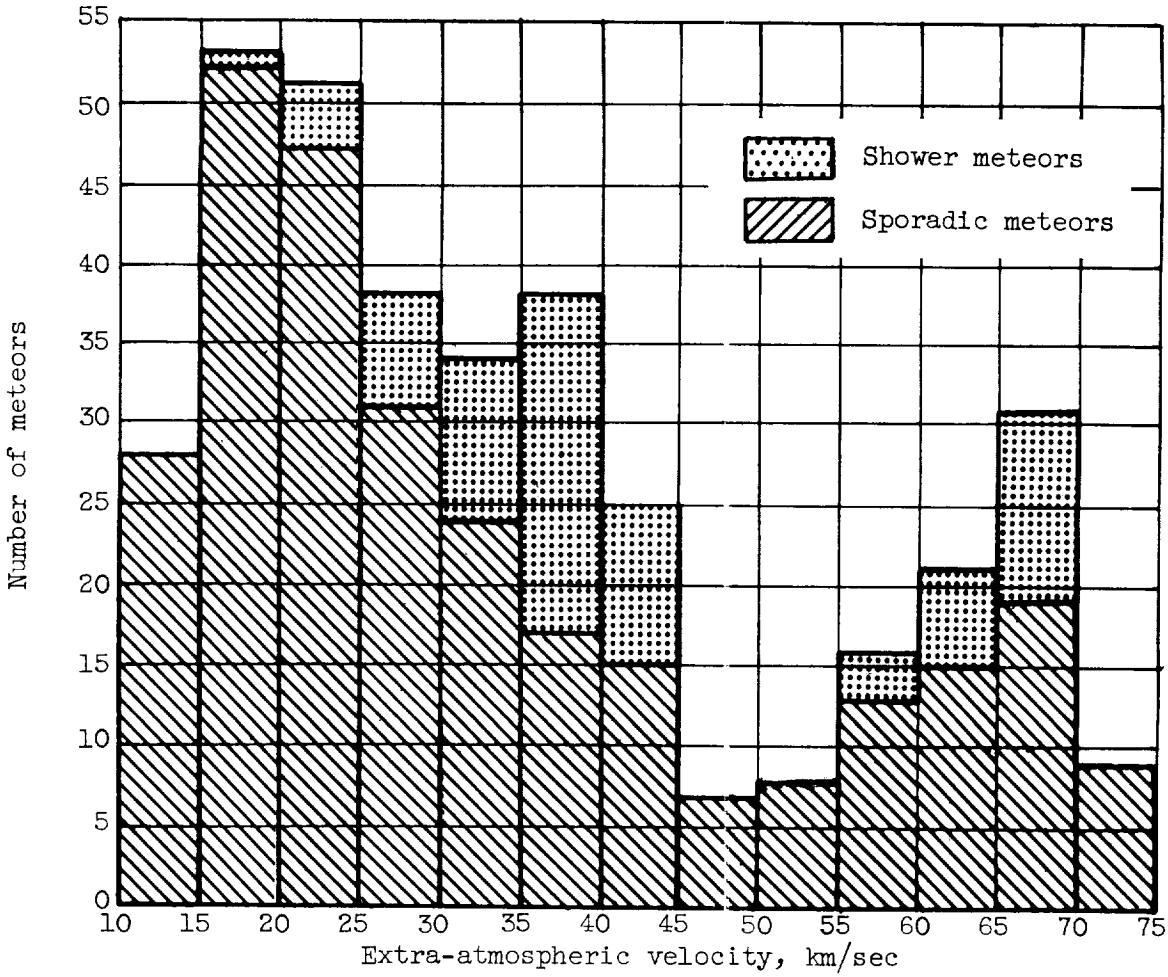


Figure 2. - Distribution of corrected velocities (extra atmospheric) for 285 sporadic and 74 shower meteors (taken from ref. 16).

E-1261

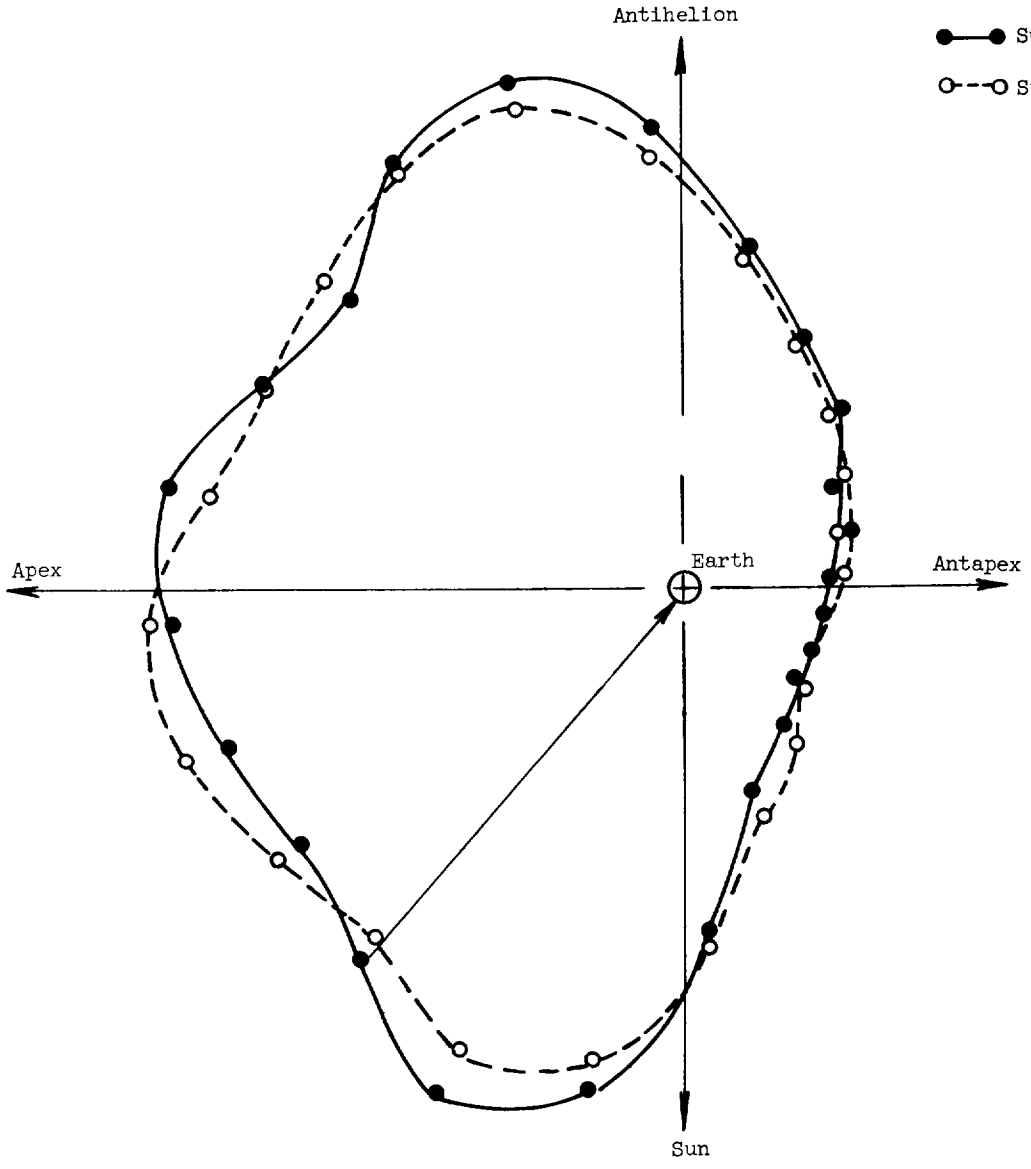


Figure 3. - Polar diagram drawn in the plane of Earth's orbit which shows the apparent number of meteor radients detected per unit angle, per unit time (taken from ref. 29).

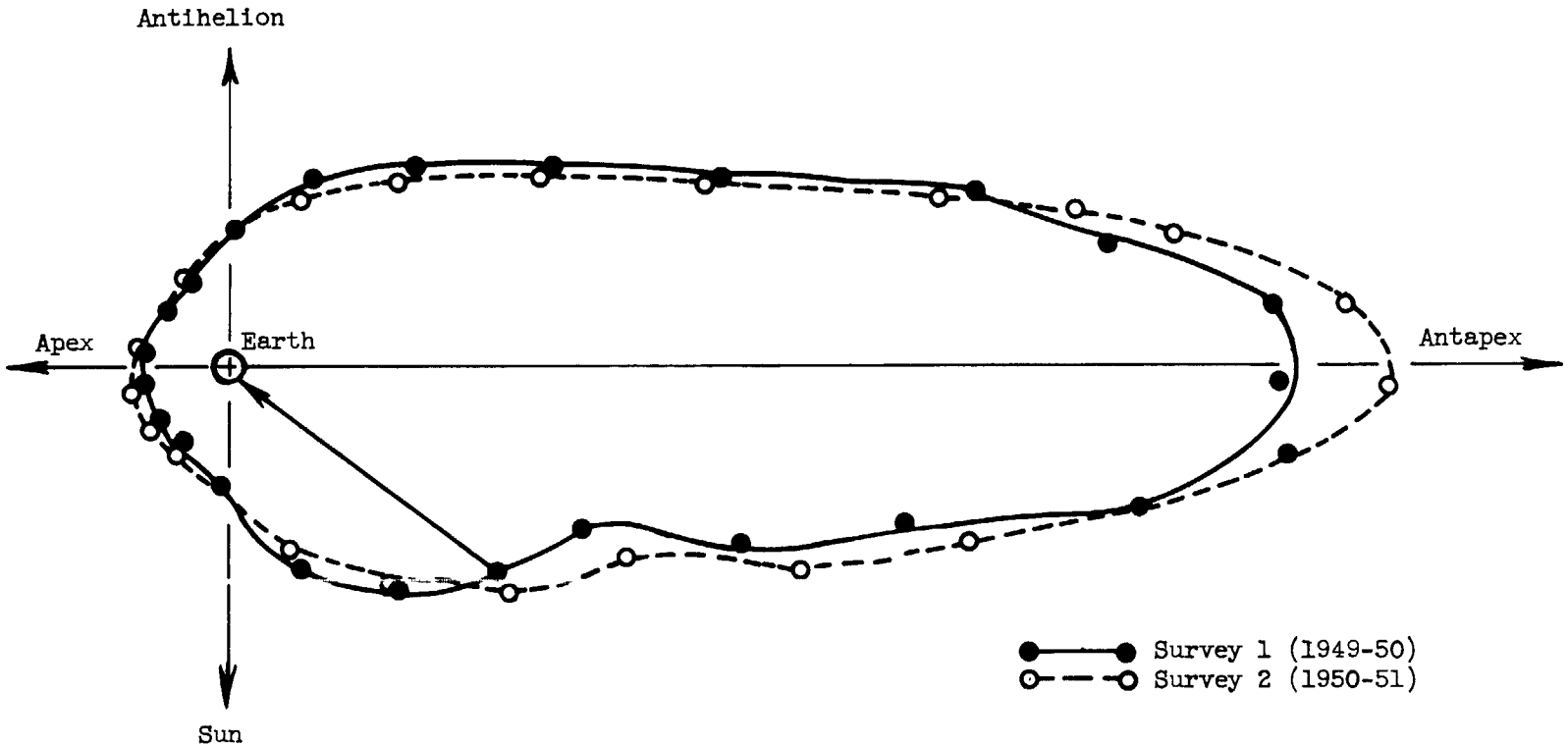


Figure 4. - Polar diagram drawn in the plane of Earth's orbit which shows the number of meteors per unit angle which cross Earth's orbit per unit time (taken from ref. 29).

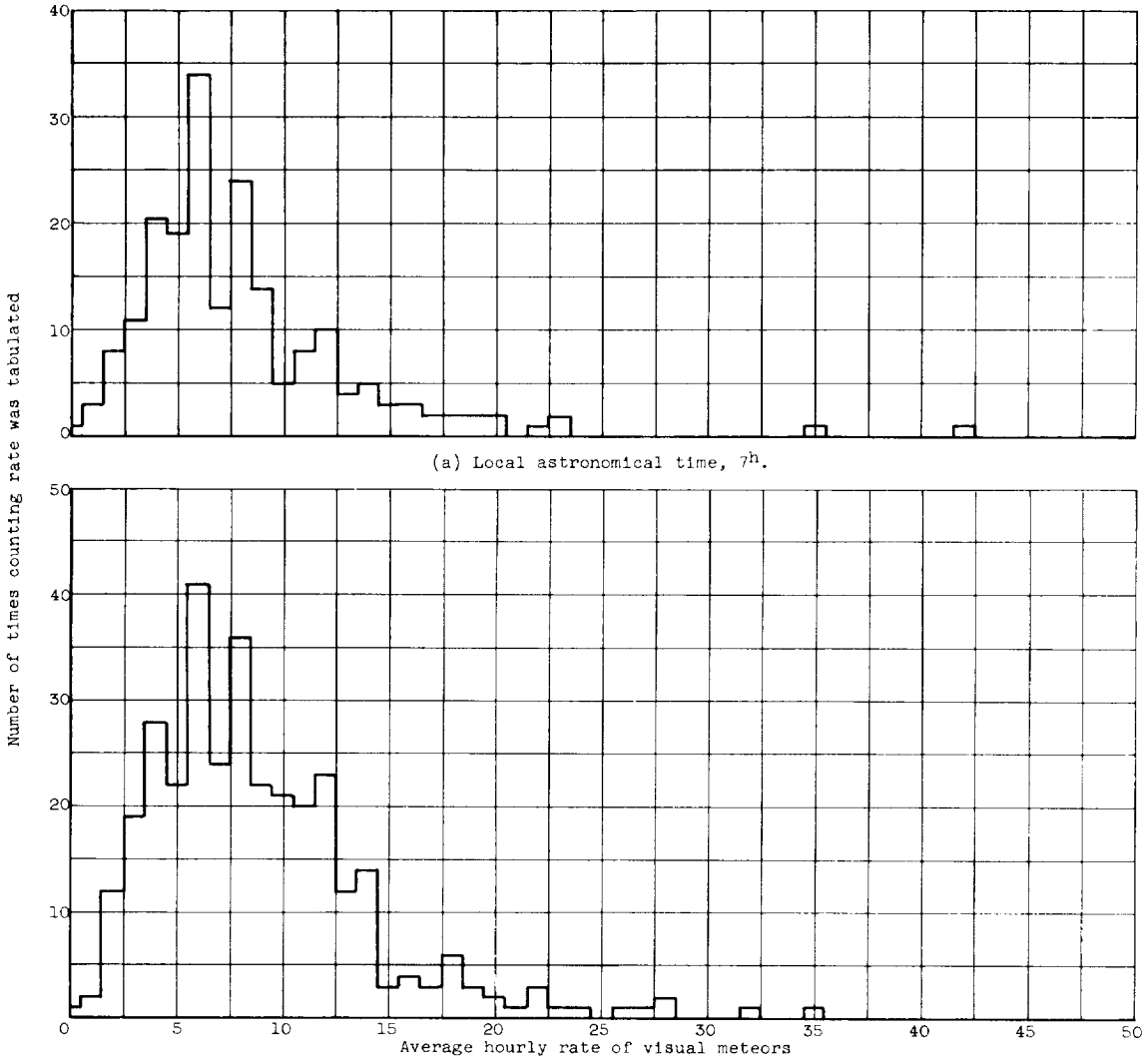


(a) Local astronomical time, $7^h$.

(b) Local astronomical time, $8^h$.

Figure 5. - Frequency distribution of visual meteor sightings. Data obtained from reference 35.

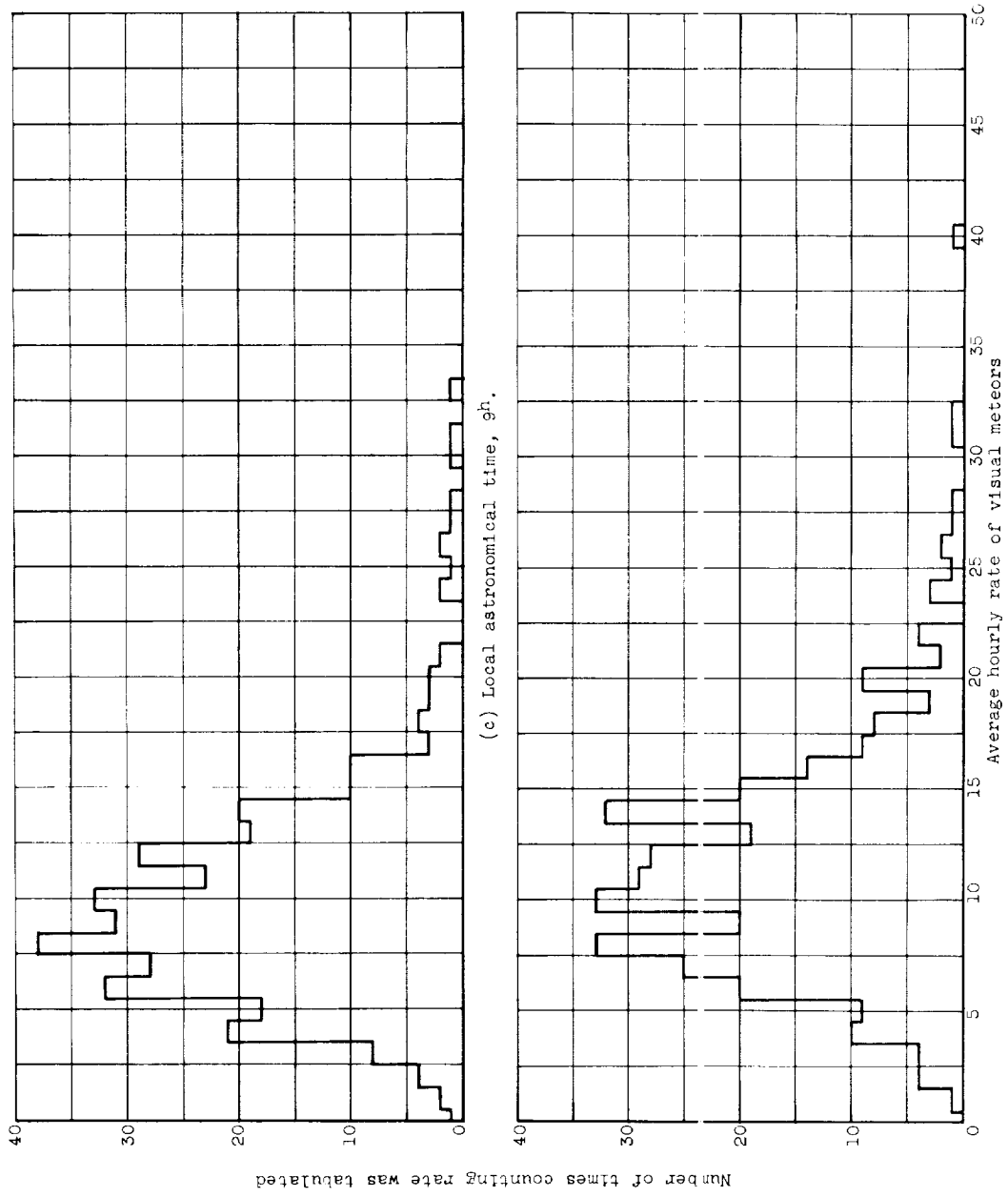


Figure 5. - Continued. Frequency distribution of visual meteor sightings. Data obtained from reference 35.

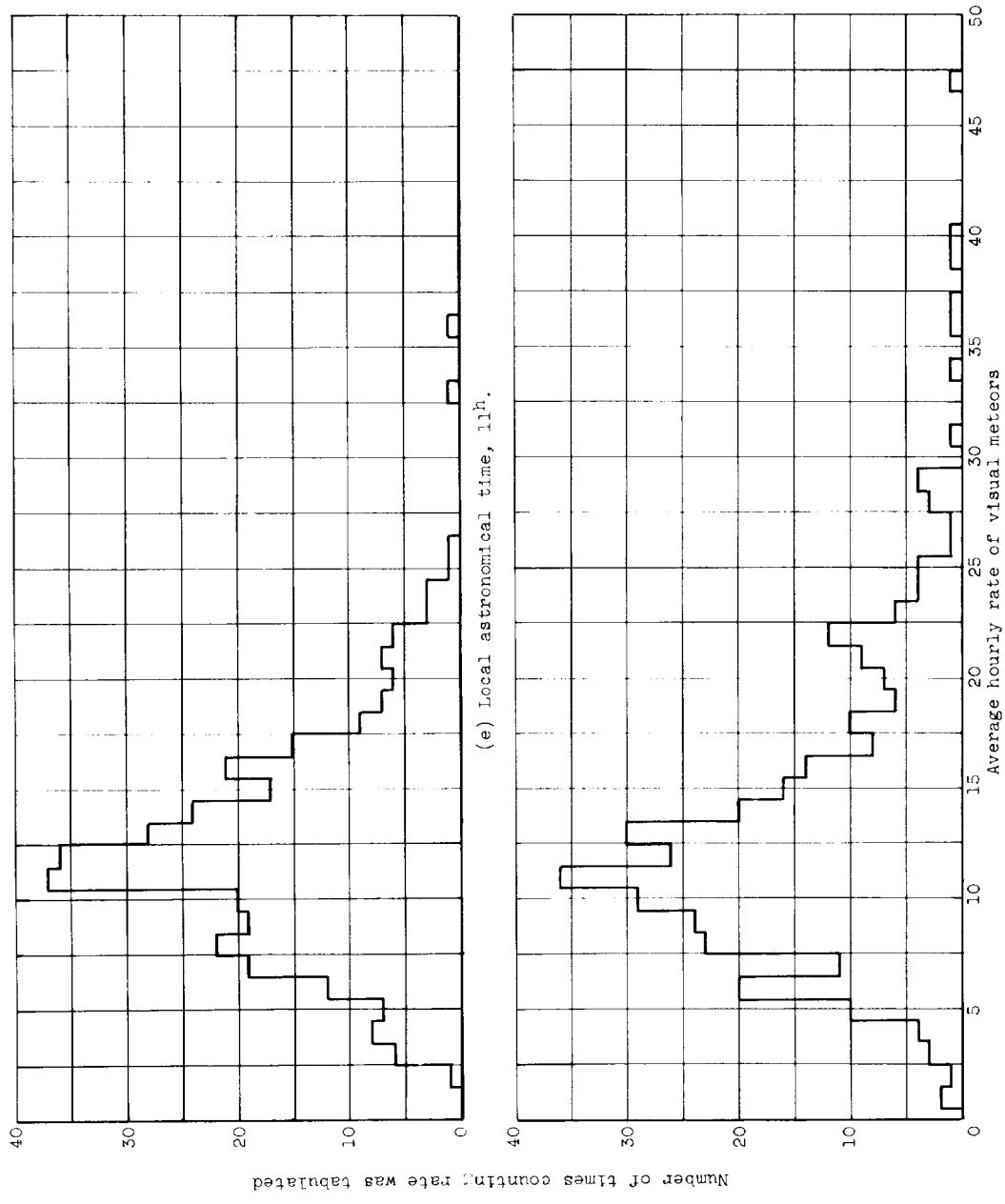


Figure 5. - Continued. Frequency distribution of visual meteor sightings. Data obtained from reference 35.

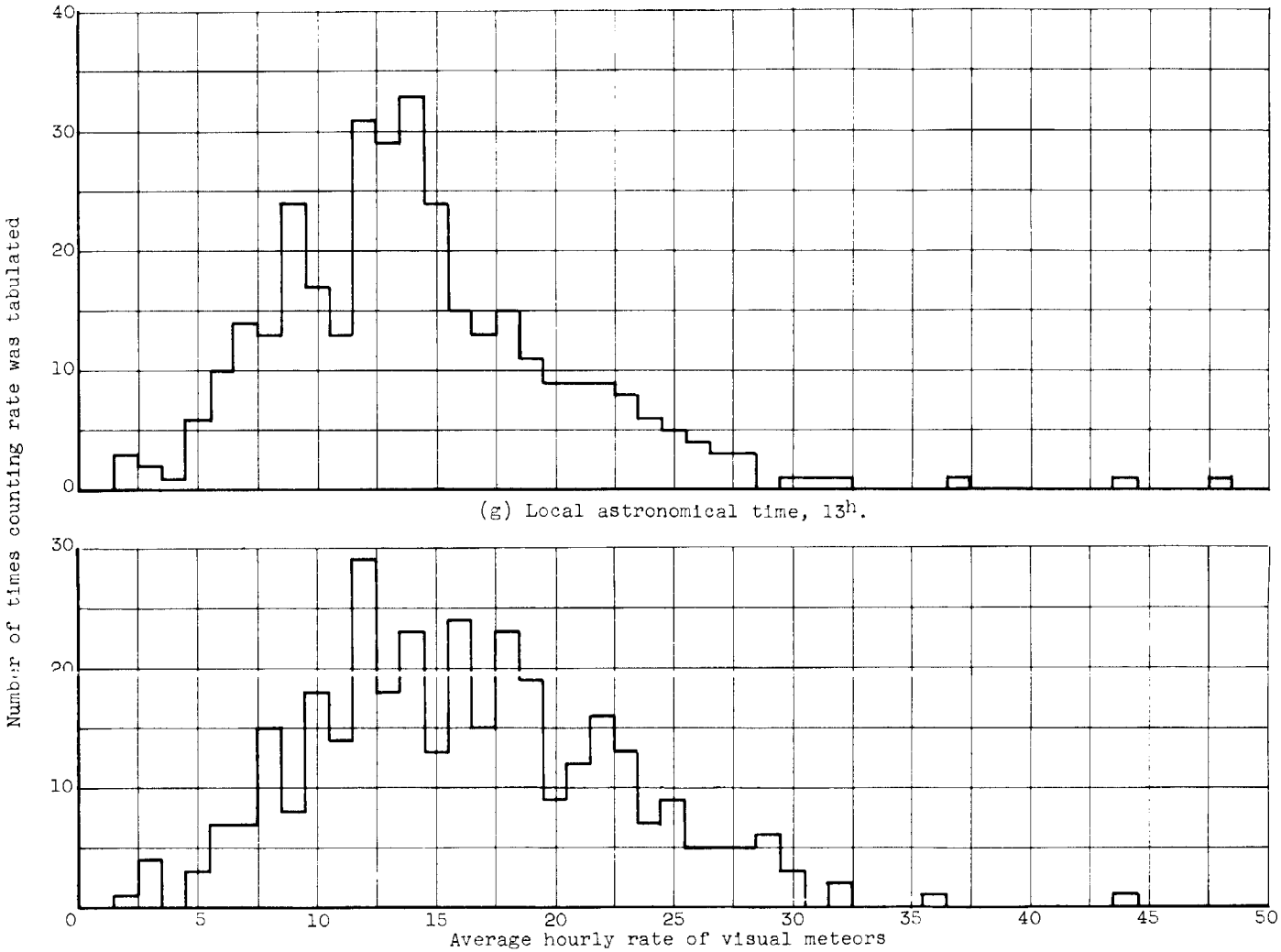


(g) Local astronomical time, $13^h$.

(h) Local astronomical time, $14^h$.

Figure 5. - Continued. Frequency distribution of visual meteor sightings. Data obtained from reference 35.

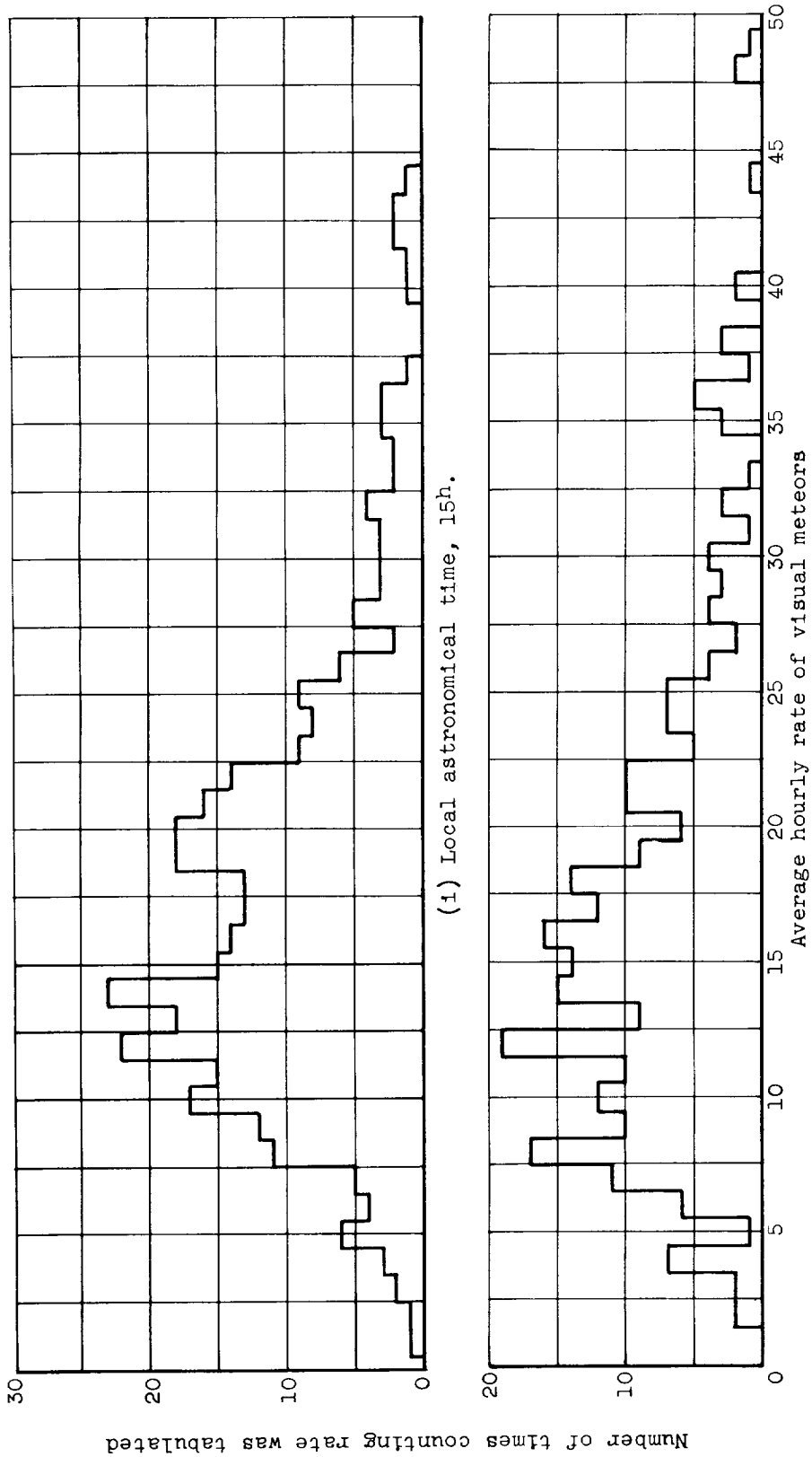


Figure 5. - Concluded. Frequency distribution of visual meteor sightings. Data obtained from reference 35.

Figure 6. - Hourly variation of visual meteors.

| Data point | Reference | Satellite | Estimated particle mass, g | Rate, number/$m^2$-hr |
|---|---|---|---|---|
| 1 | *37 | 1958 Gamma | $\sim 1.4 \times 10^{-9}$ | <9 |
| 2 | 38 | 1958 Alpha | $8 \times 10^{-10}$ | 60 |
| 3a | 39 | Sputnik III | $\sim 2 \times 10^{-8}$ | ~27,000 15 May 1958 |
| 3a | 39 | | $\sim 2 \times 10^{-8}$ | ~18 16-17 May 1958 |
| 3a | 39 | | $\sim 2 \times 10^{-8}$ | <0.36 19-26 May 1958 |
| 3b | 39 | First cosmic rocket | $\sim 10^{-9}$ | <0.7 |
| 3c | 39 | Second cosmic rocket | $\sim 10^{-8}$ | ~0.7 |
| 4 | 40 | 1959 Eta | $\sim 3.3 \times 10^{-9}$ | 2.9 |
| 5a | 41 | Pioneer I | $\sim 10^{-10}$ | 14.4 |
| 5b | 41 | 1959 Alpha I | $\sim 10^{-9}$ | 75.5 |

*Wire-wound card data included; assumed: particle density, 2.7 g/cc; viewing loss, 0.33.

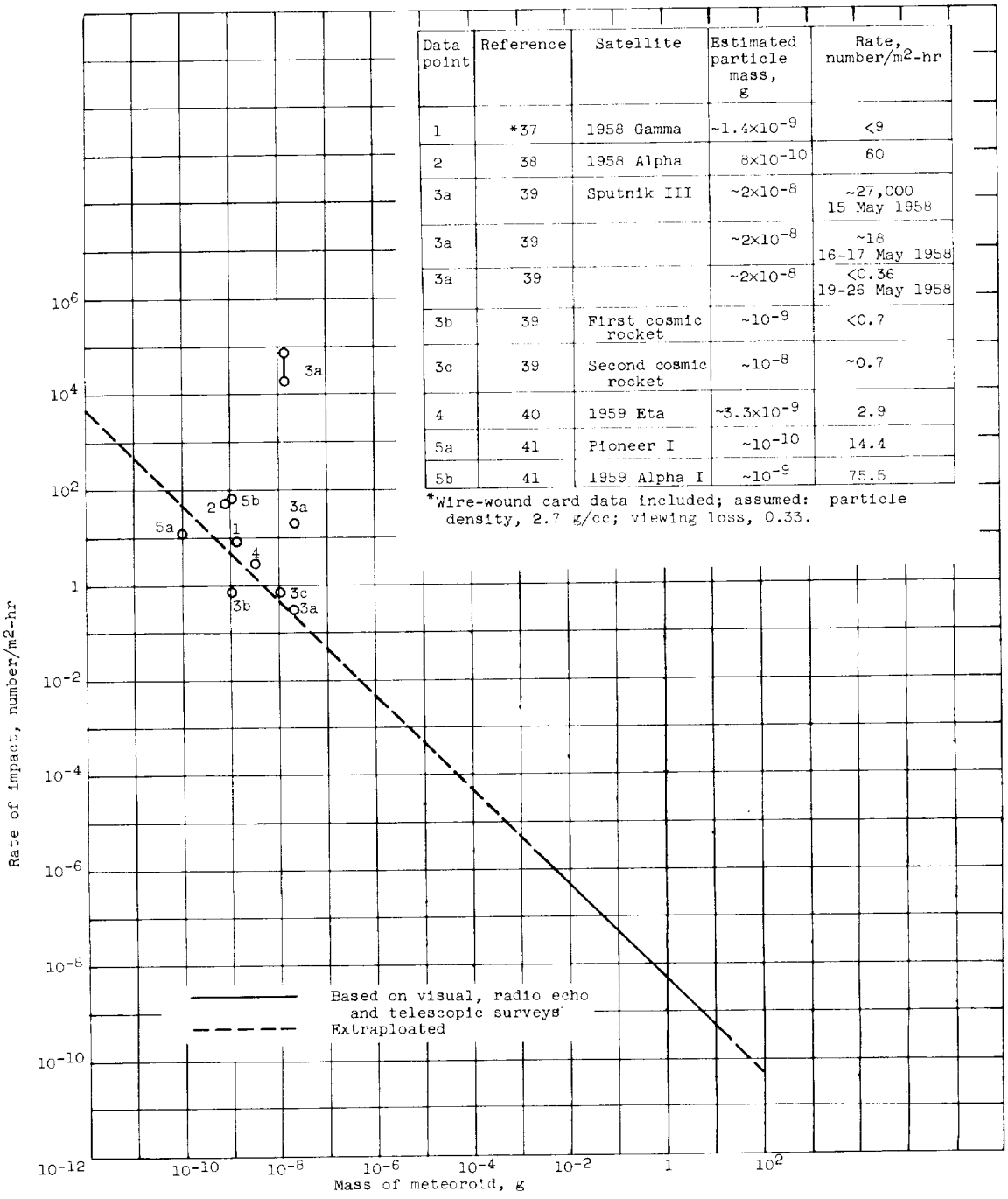


Figure 7. - Comparison of micrometeoroid influx rates.

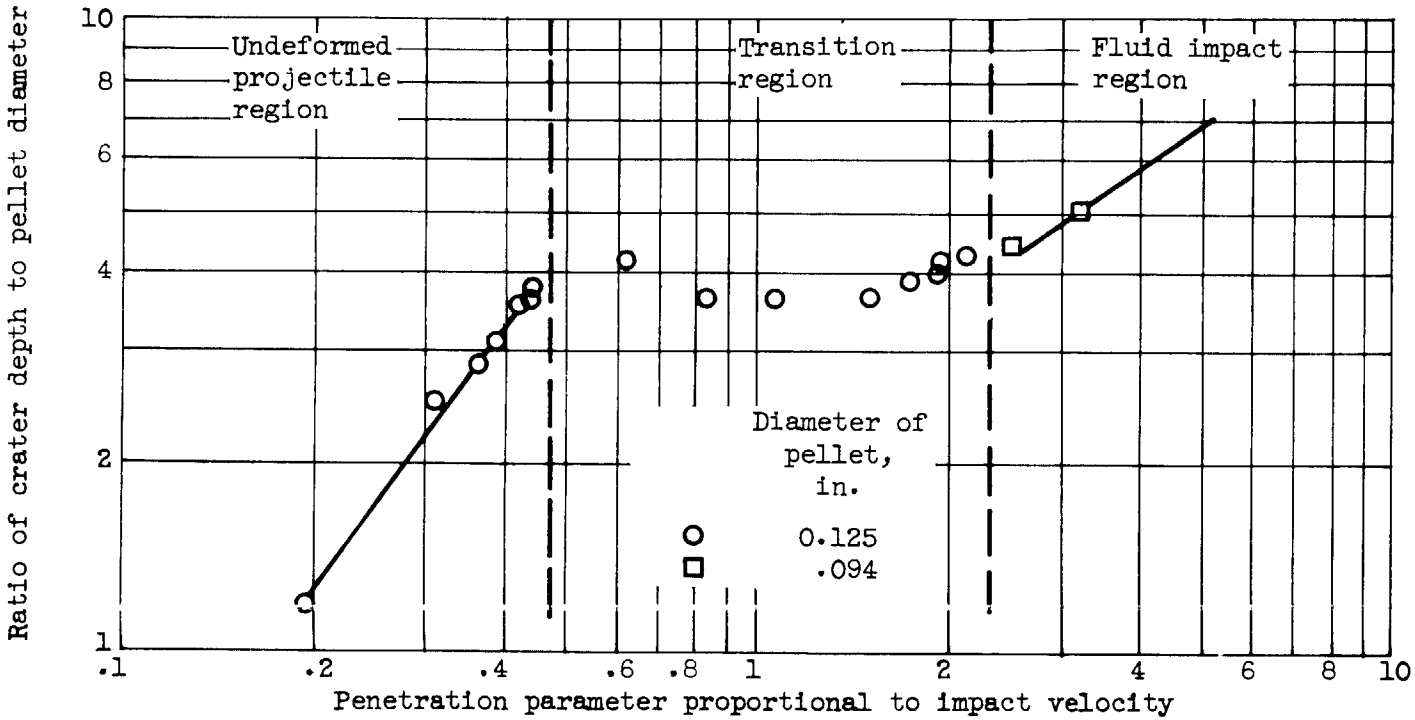


Figure 8. - Basic regions of impact for tungsten-carbide spheres impacting lead targets (taken from ref. 49).

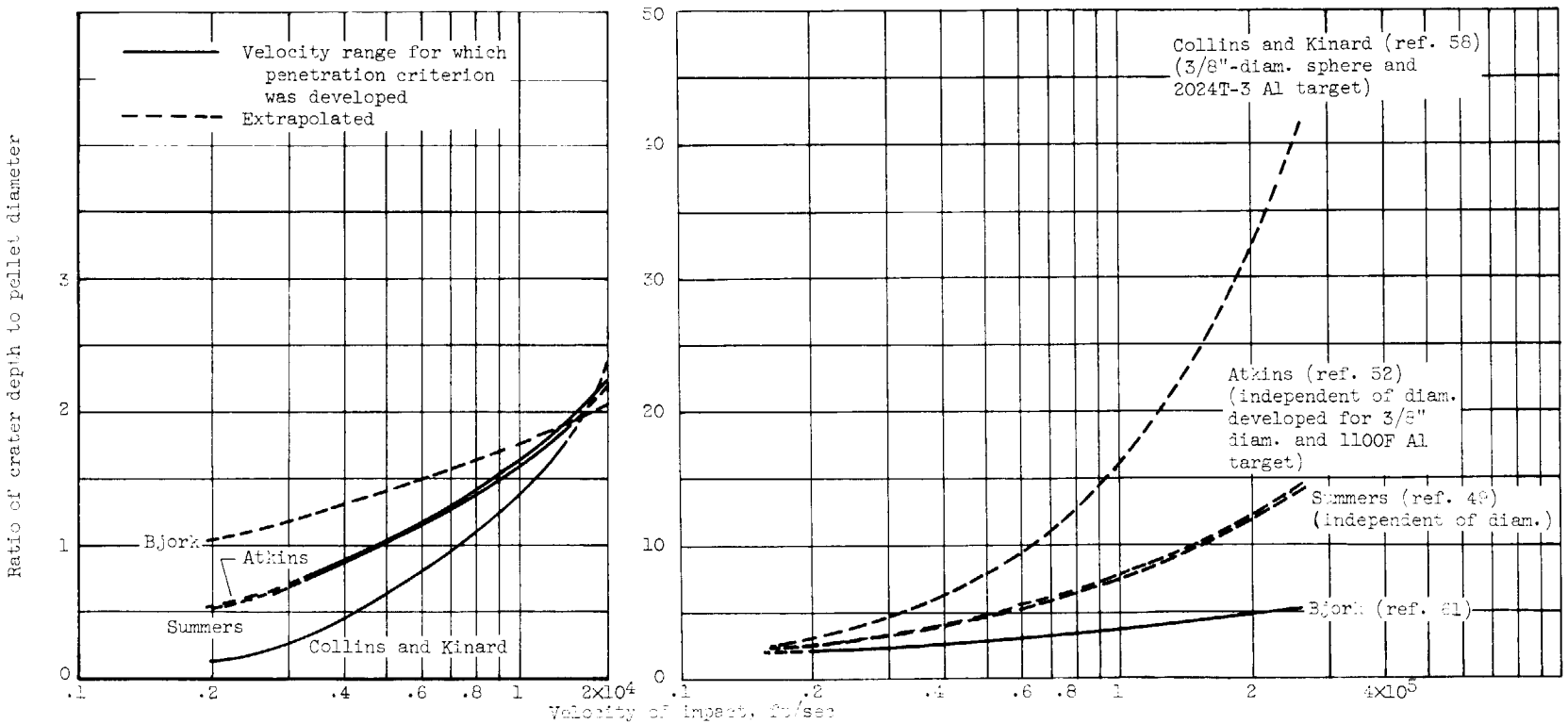


(a) Penetration of aluminum spheres into semi-infinite aluminum targets.

Figure 9. - Predicted depths of penetration.

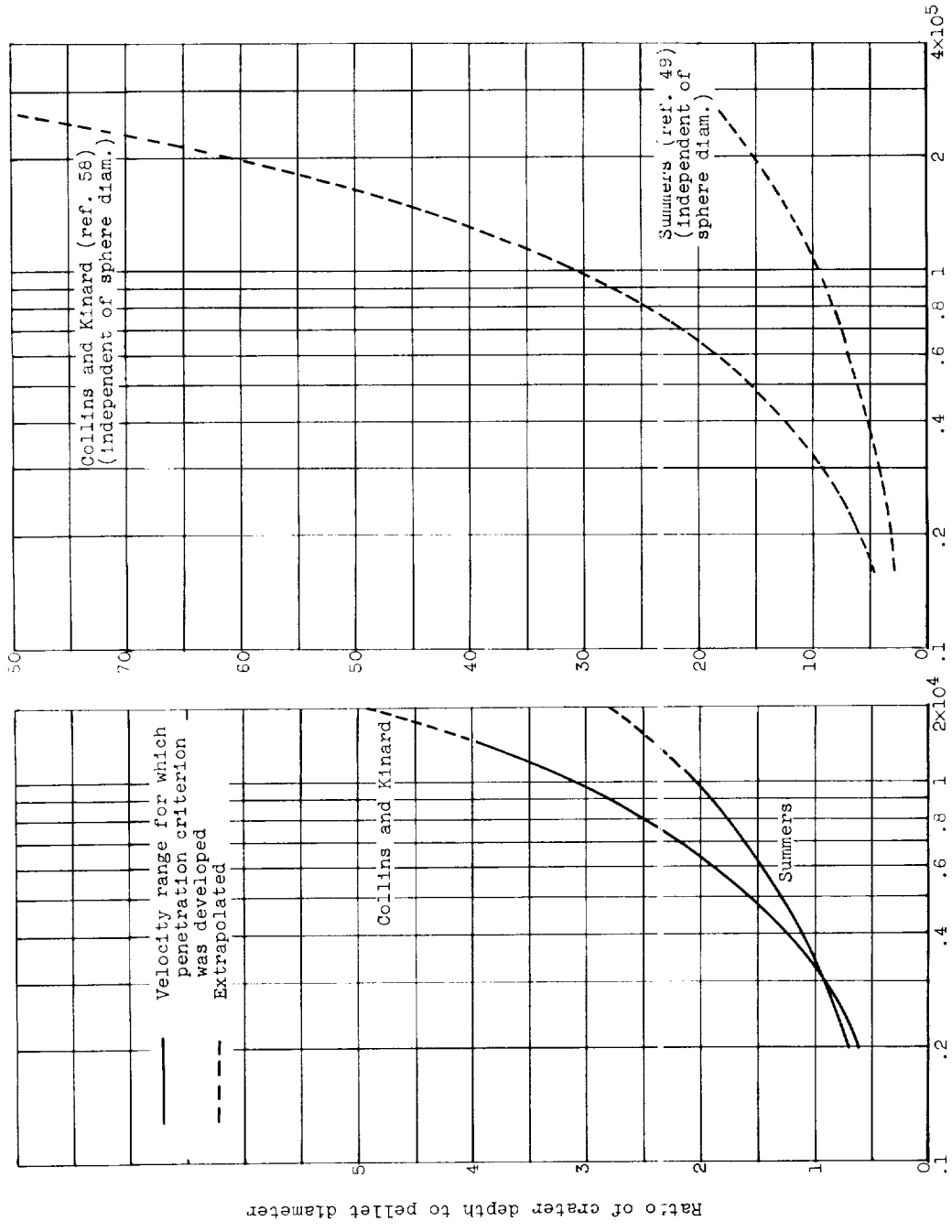


(b) Penetration of copper spheres into semi-infinite copper targets.

Figure 9. - Concluded. Predicted depths of penetration.

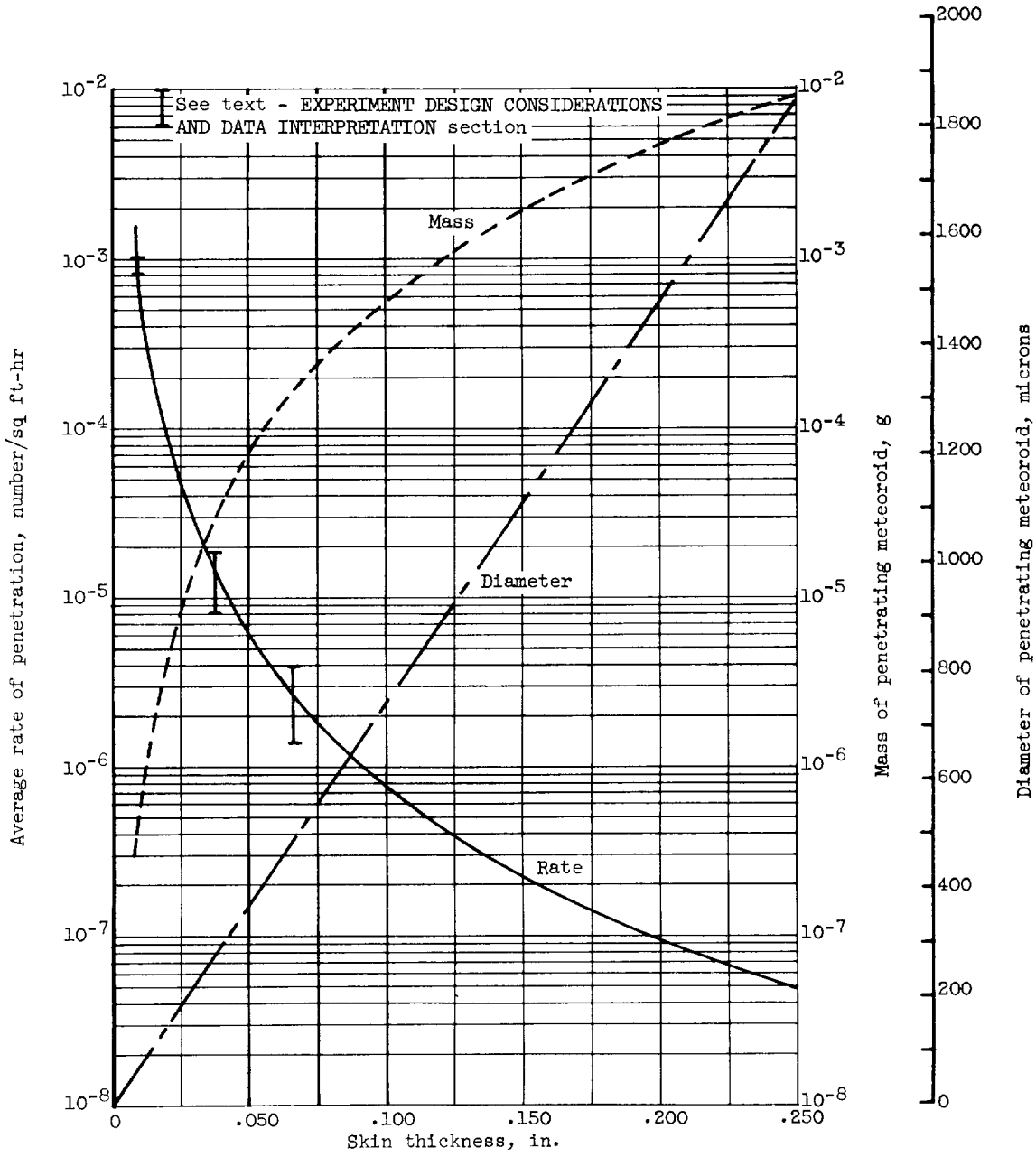


(a) Stainless steel.

Figure 10. - Estimated skin penetration rates by micrometeoroids. Assumptions (see text for details): meteoroid velocity, 15 kilometers per second; meteoroid density, 2.7 grams per cubic centimeter; Summer's modified penetration criteria; Whipple's estimated number flux.

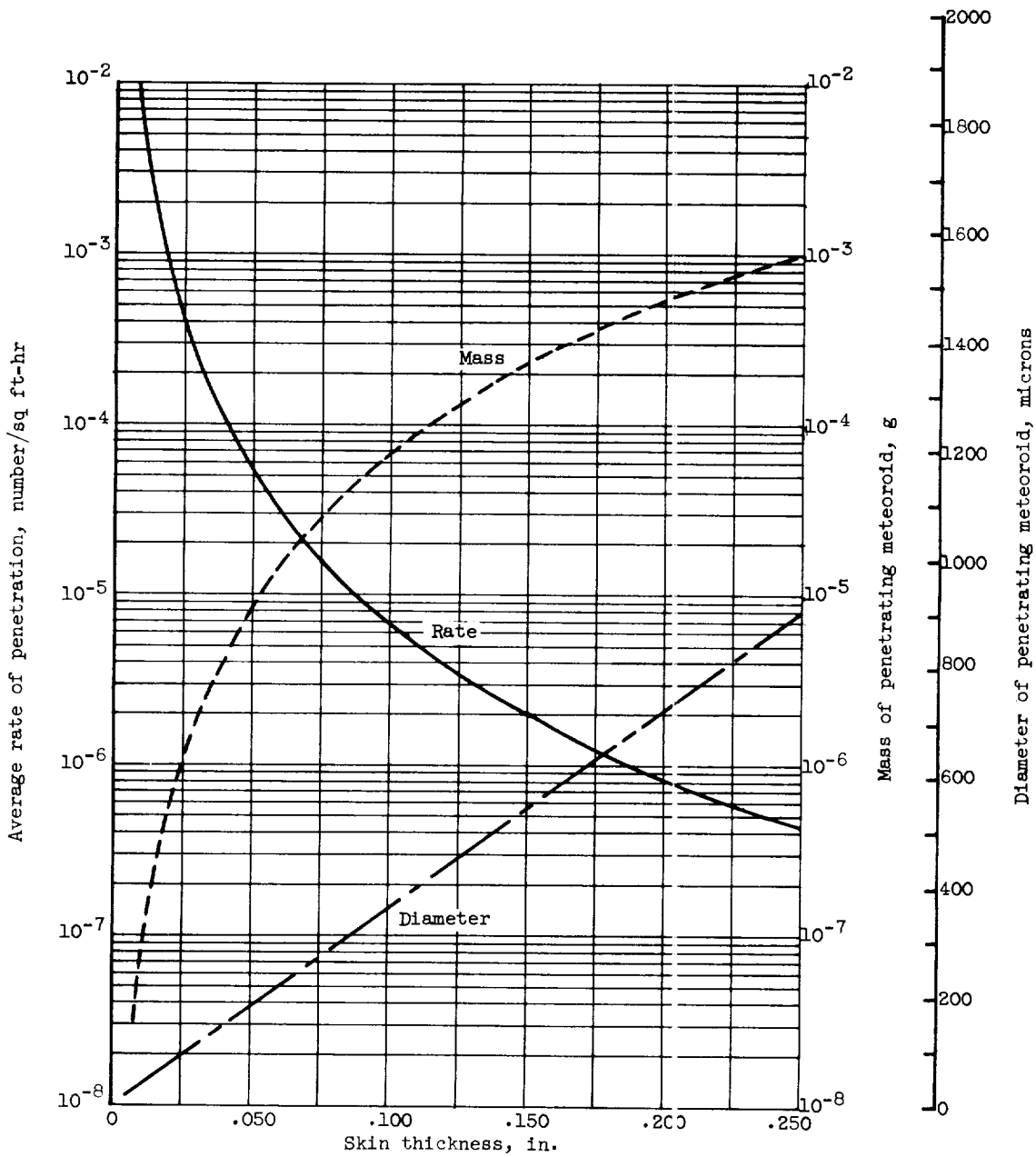


(b) Aluminum.

Figure 10. - Continued. Estimated skin penetration rates by micrometeoroids. Assumptions (see text for details): meteoroid velocity, 15 kilometers per second; meteoroid density, 2.7 grams per cubic centimeter; Summer's modified penetration criteria; Whipple's estimated number flux.

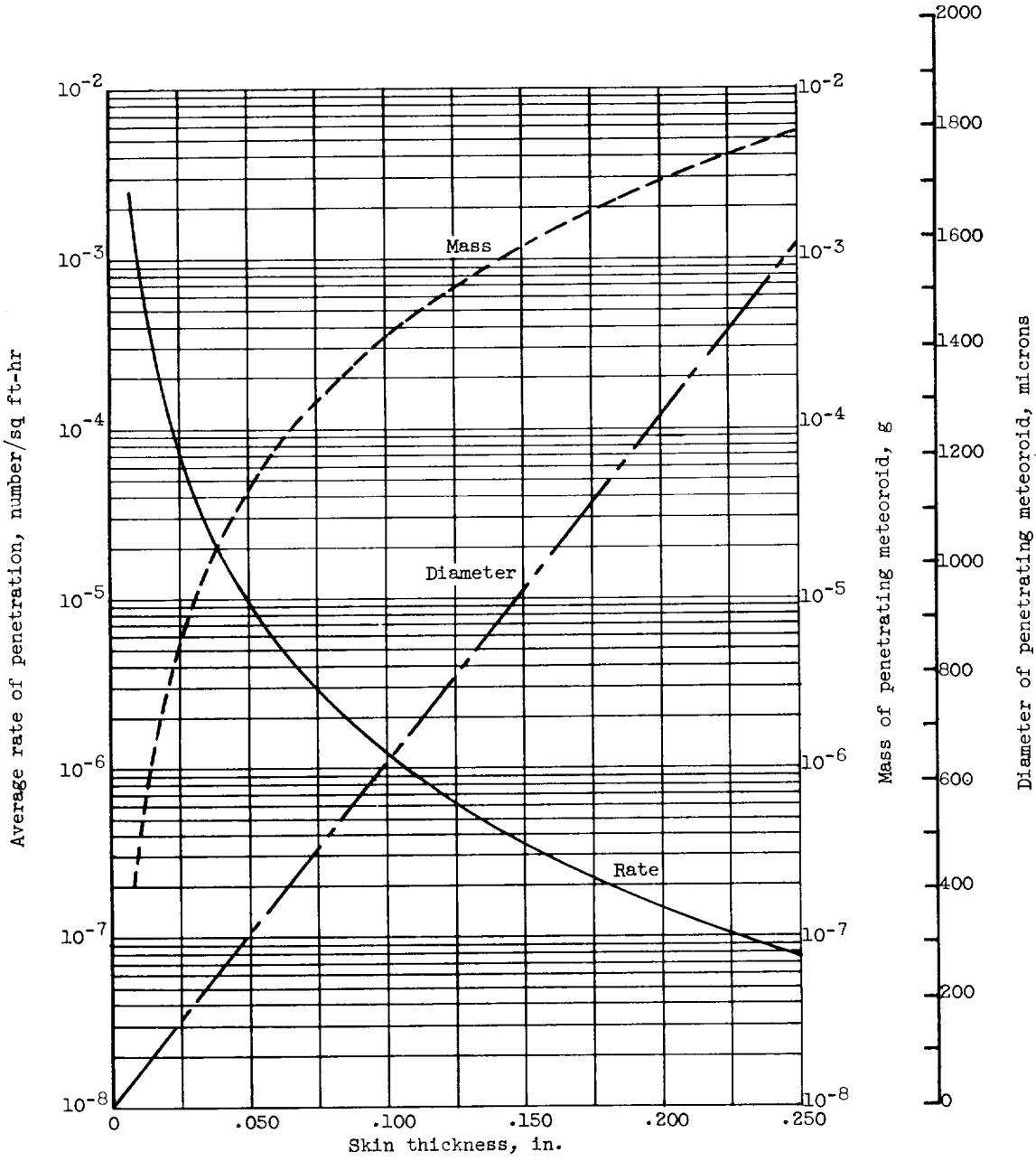


(c) Copper.

Figure 10. - Continued. Estimated skin penetration rates by micrometeoroids. Assumptions (see text for details): meteoroid velocity, 15 kilometers per second; meteoroid density, 2.7 grams per cubic centimeter; Summer's modified penetration criteria; Whipple's estimated number flux.

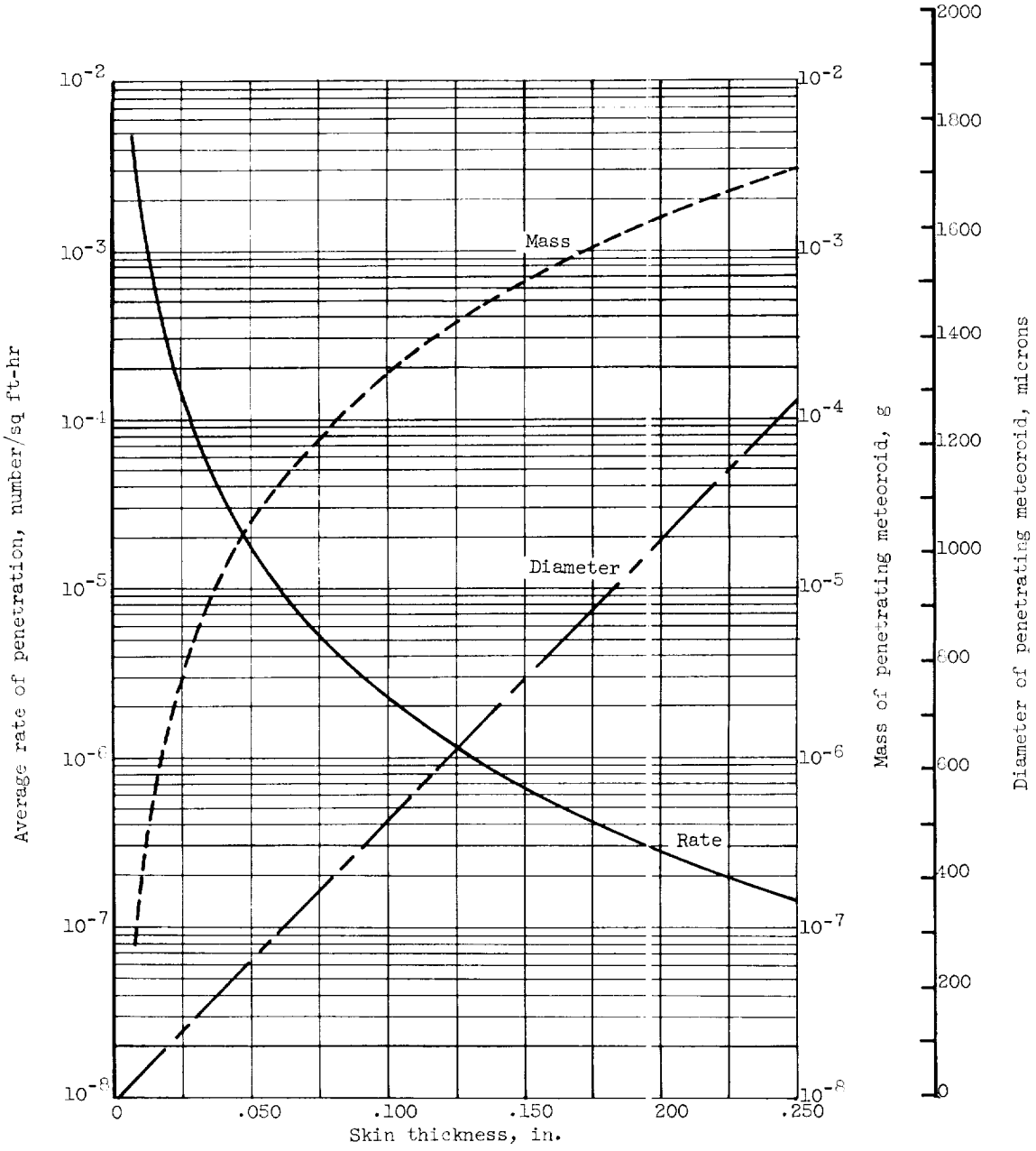


(d) Beryllium or titanium.

Figure 10. - Concluded. Estimated skin penetration rates by micrometeoroids. Assumptions (see text for details): meteoroid velocity, 15 kilometers per second; meteoroid density, 2.7 grams per cubic centimeter; Summer's modified penetration criteria; Whipple's estimated number flux.

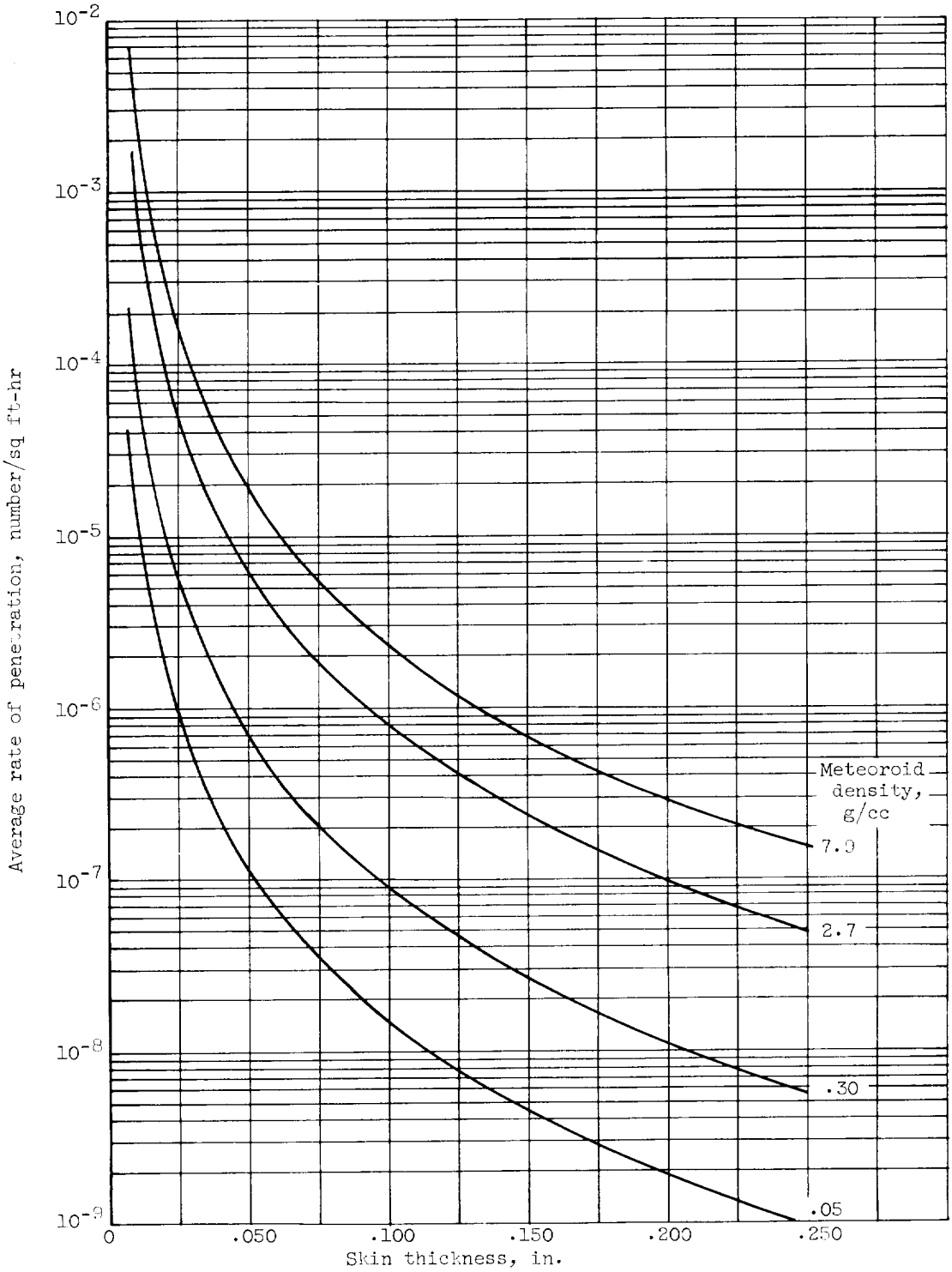


Figure 11. - Effect of meteoroid density on estimated penetration rate (stainless-steel skin). Assumptions (see text for details): meteoroid velocity, 15 kilometers per second; Summer's modified penetration criteria; Whipple's estimated number flux.

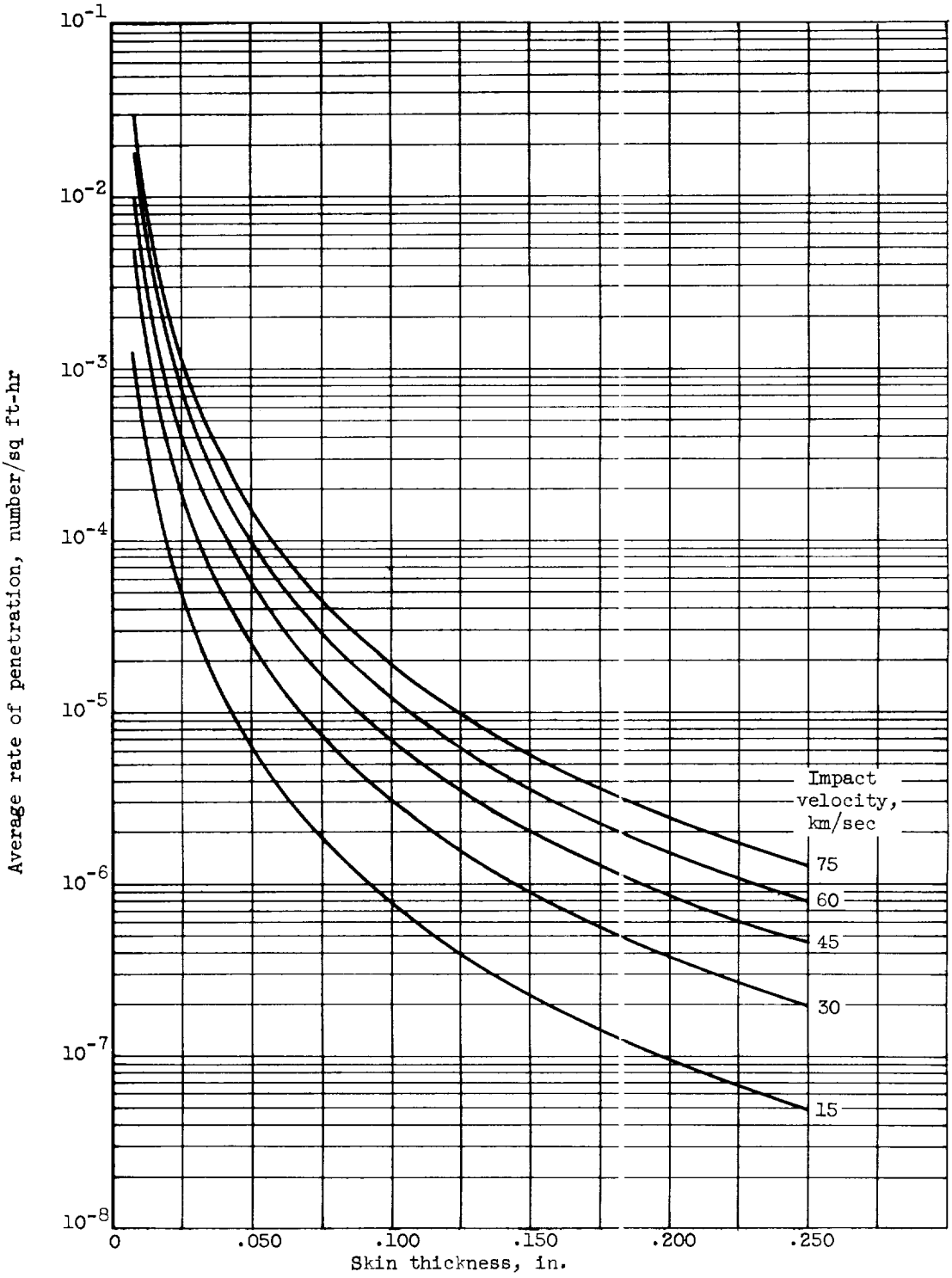


Figure 12. - Effect of micrometeoroid velocity on estimated penetration rate (stainless-steel skin). Assumptions (see text for details): meteoroid density, 2.7 grams per cubic centimeter; Summer's modified penetration criteria; Whipple's estimated number flux.

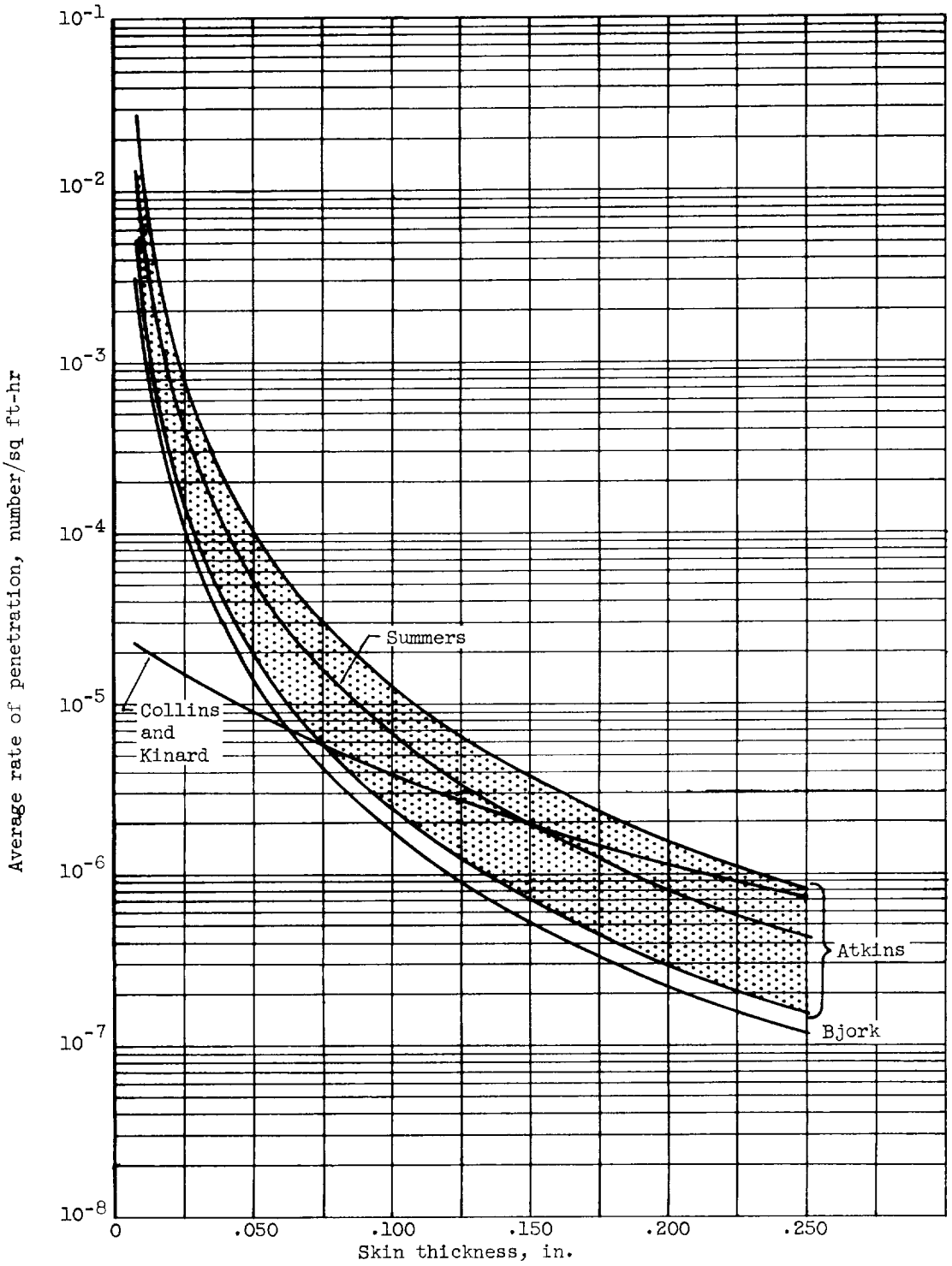


Figure 13. - Effect of penetration criteria on estimated penetration rate (aluminum skin). Assumptions (see text for details): meteoroid velocity, 15 kilometers per second; meteoroid density, 2.7 grams per cubic centimeter; Whipple's estimated number flux.

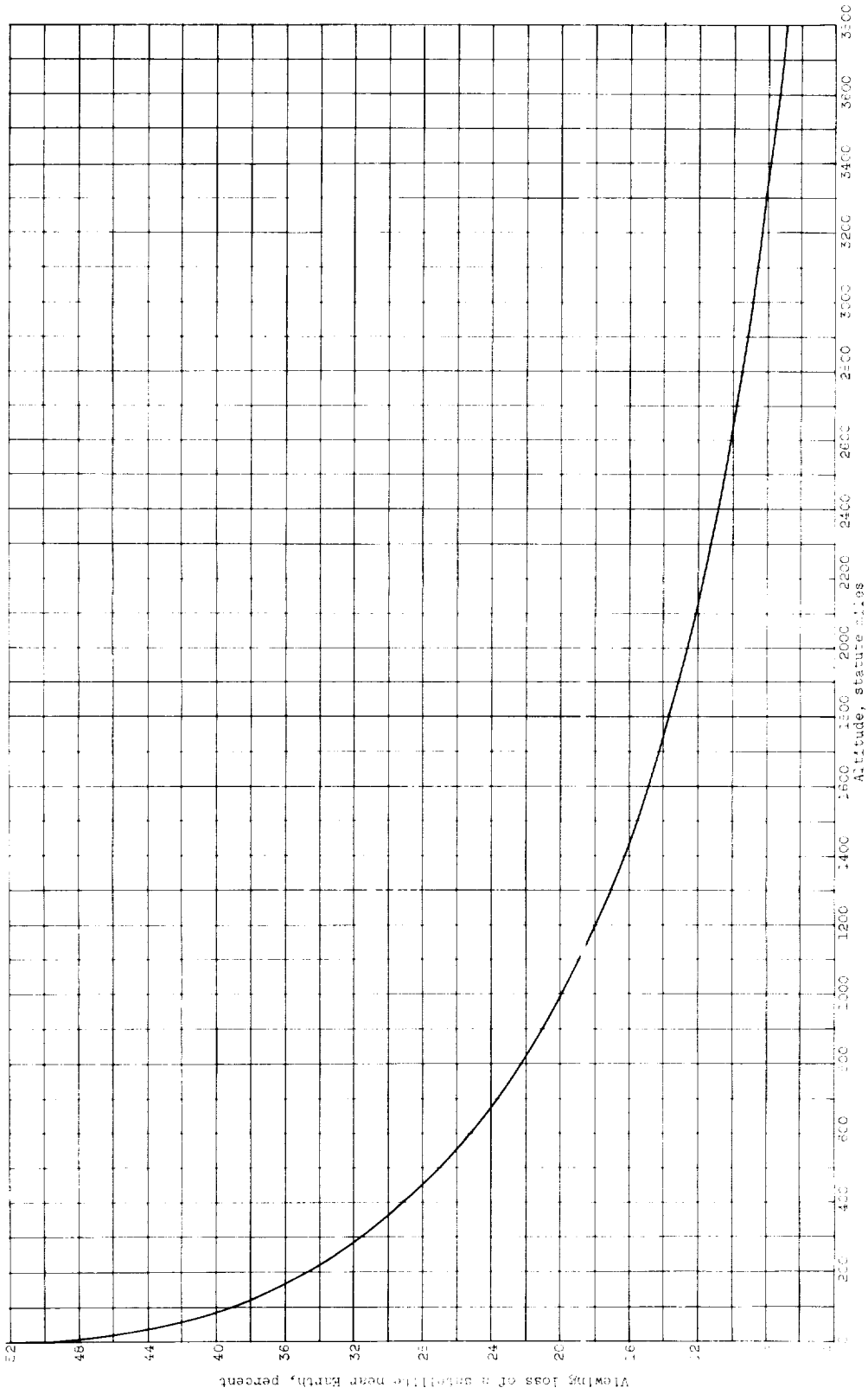


Figure 14. - Viewing loss for near-Earth satellites.

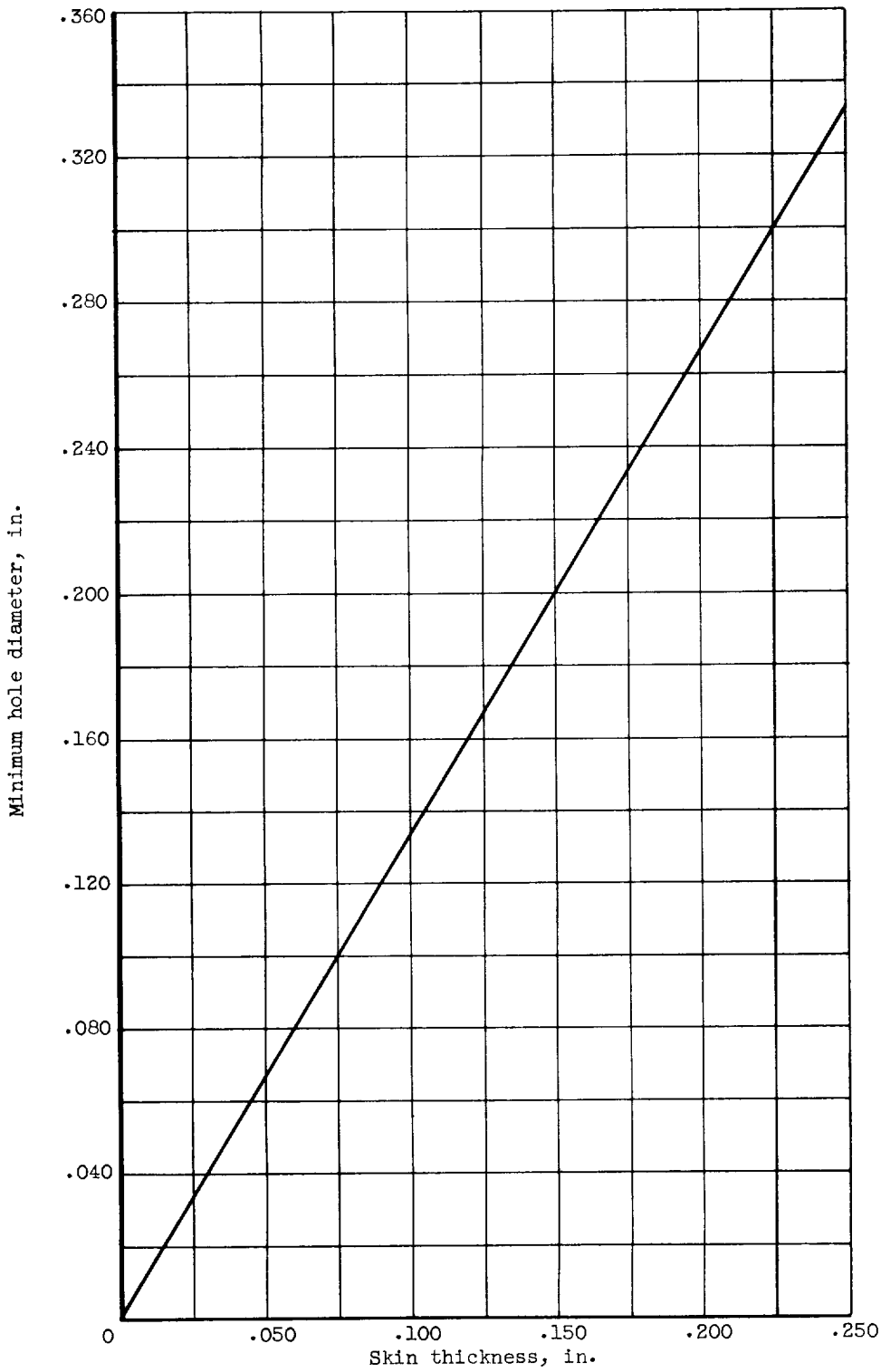


Figure 15. - Estimated minimum hole diameter formed in thin skins.

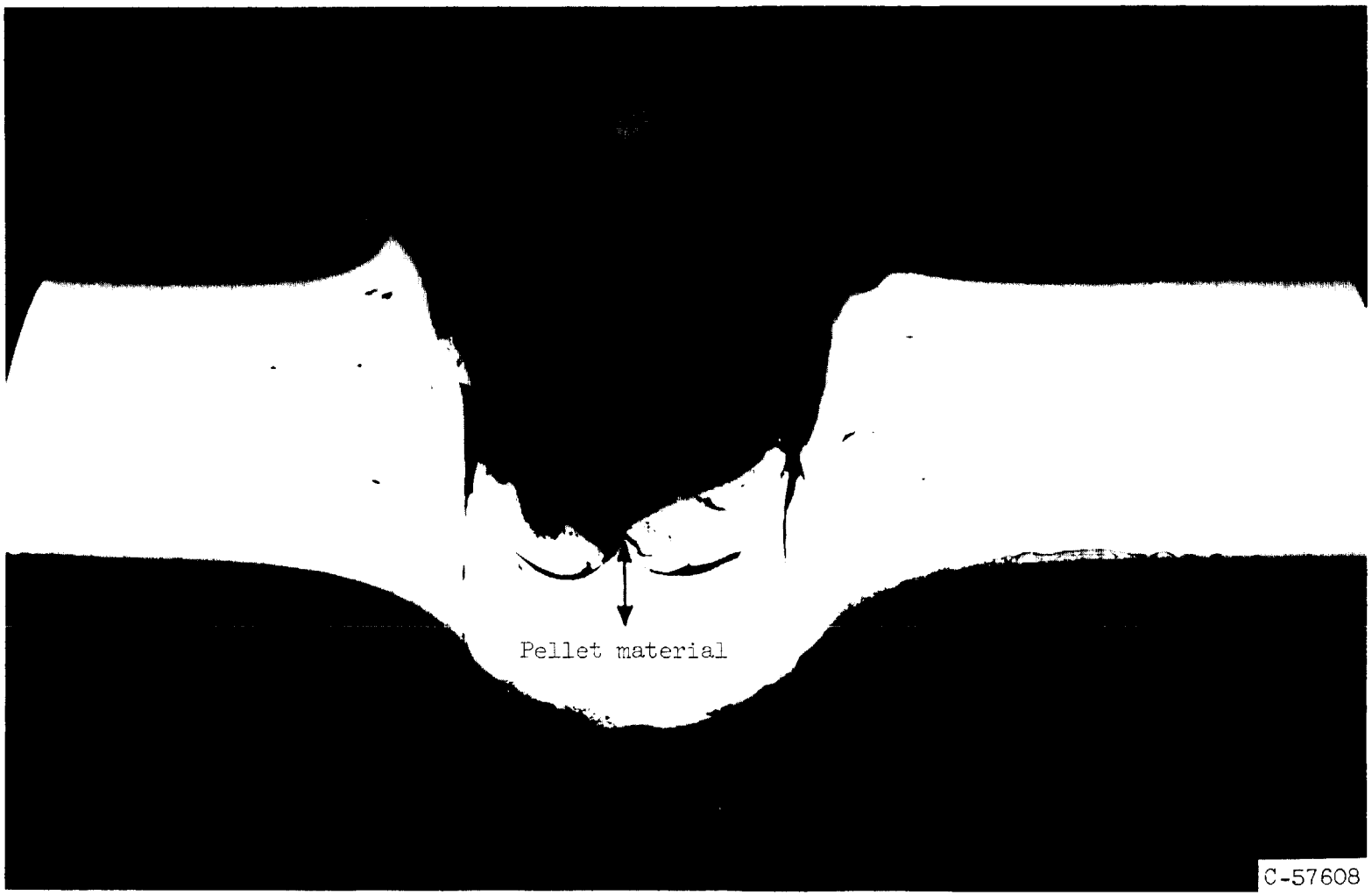


(a) Prior to etching.

Figure 16. - Microphotograph of a partial penetration.

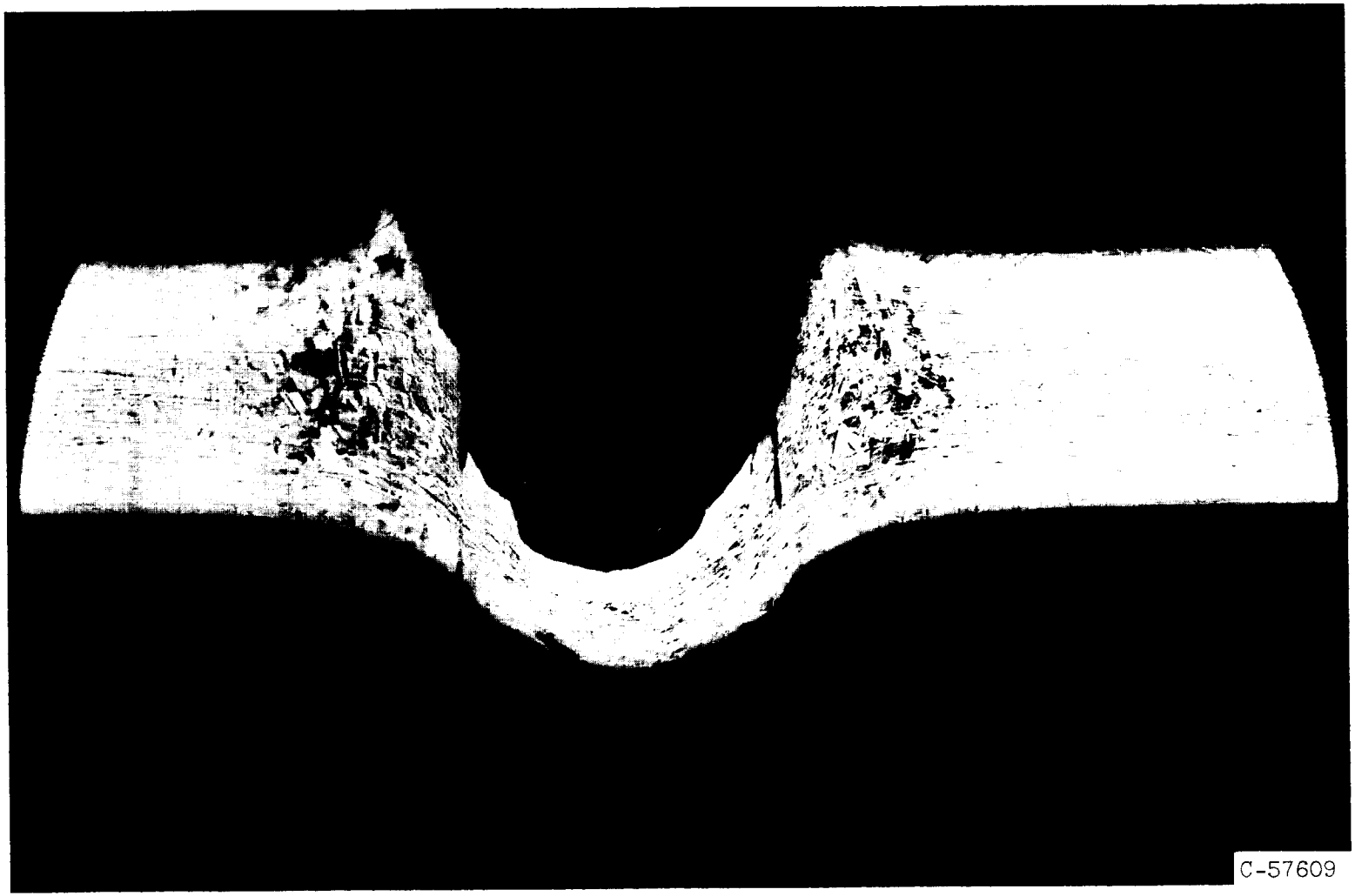


(b) Etched.

Figure 16. - Concluded. Microphotograph of a partial penetration.

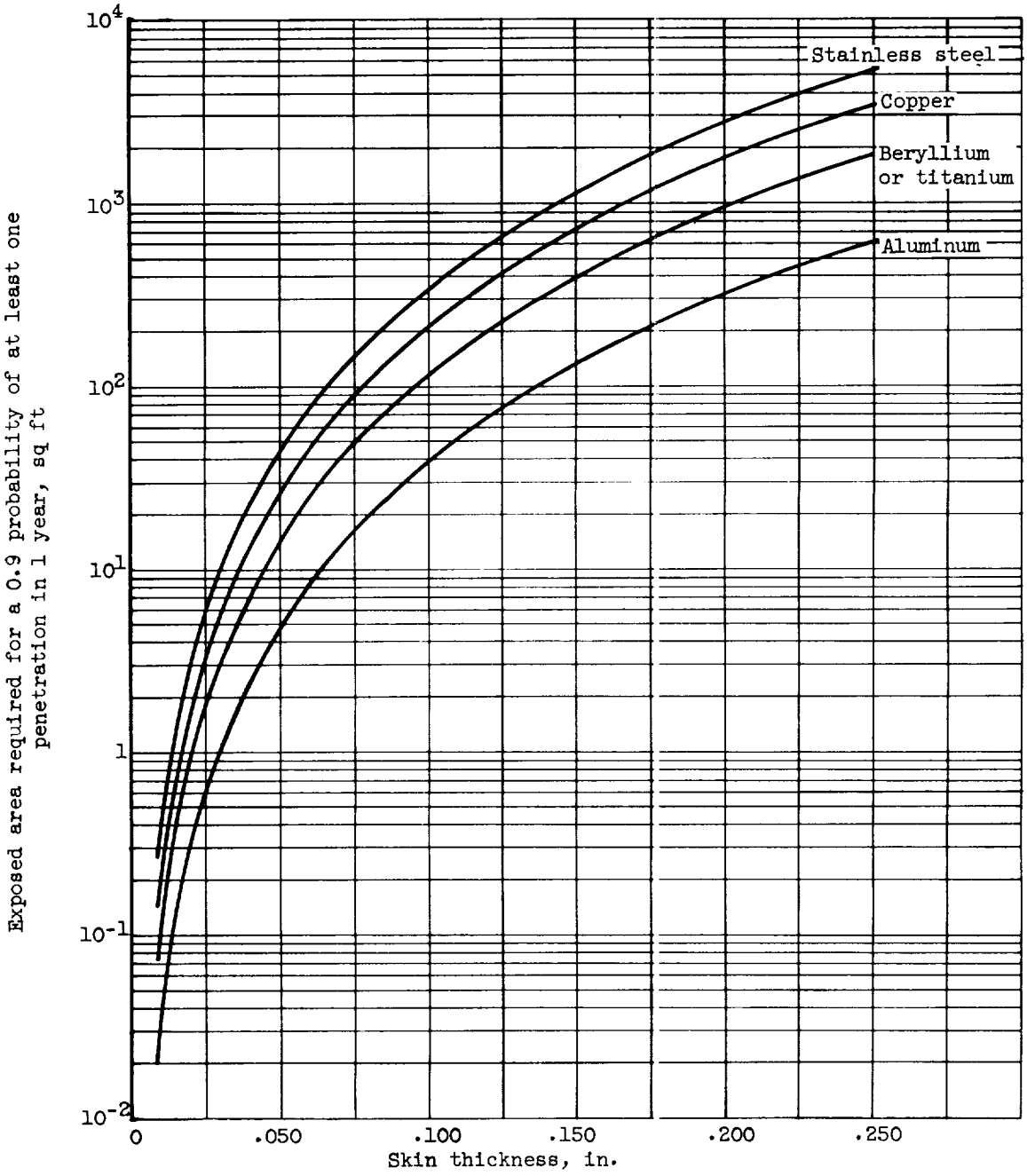


Figure 17. - Estimated area for 0.9 probability of at least one penetration (1-year exposure).

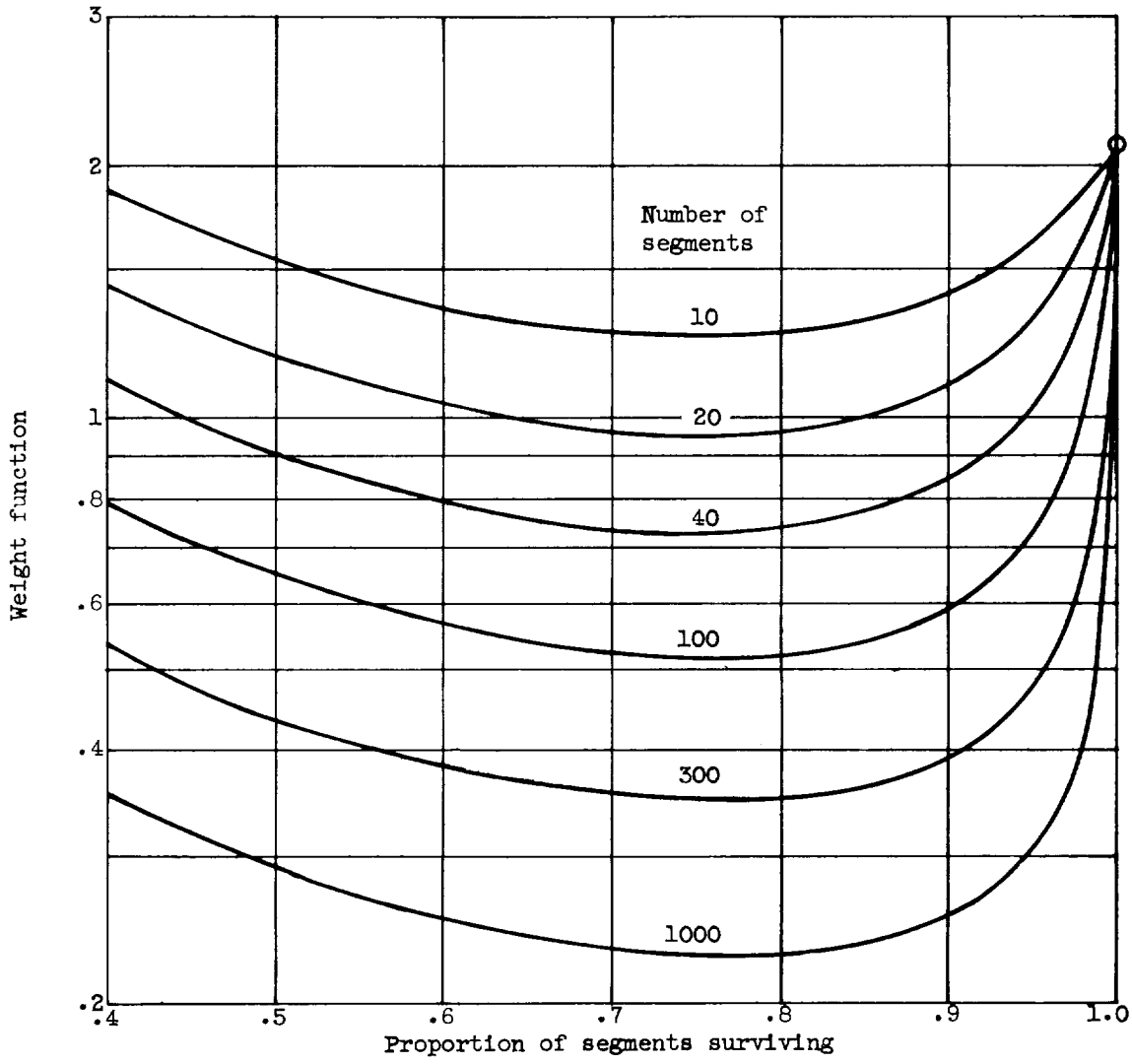


Figure 18. - Weight of vulnerable surface for survival probability of 0.9. (Data taken from ref. 71.)

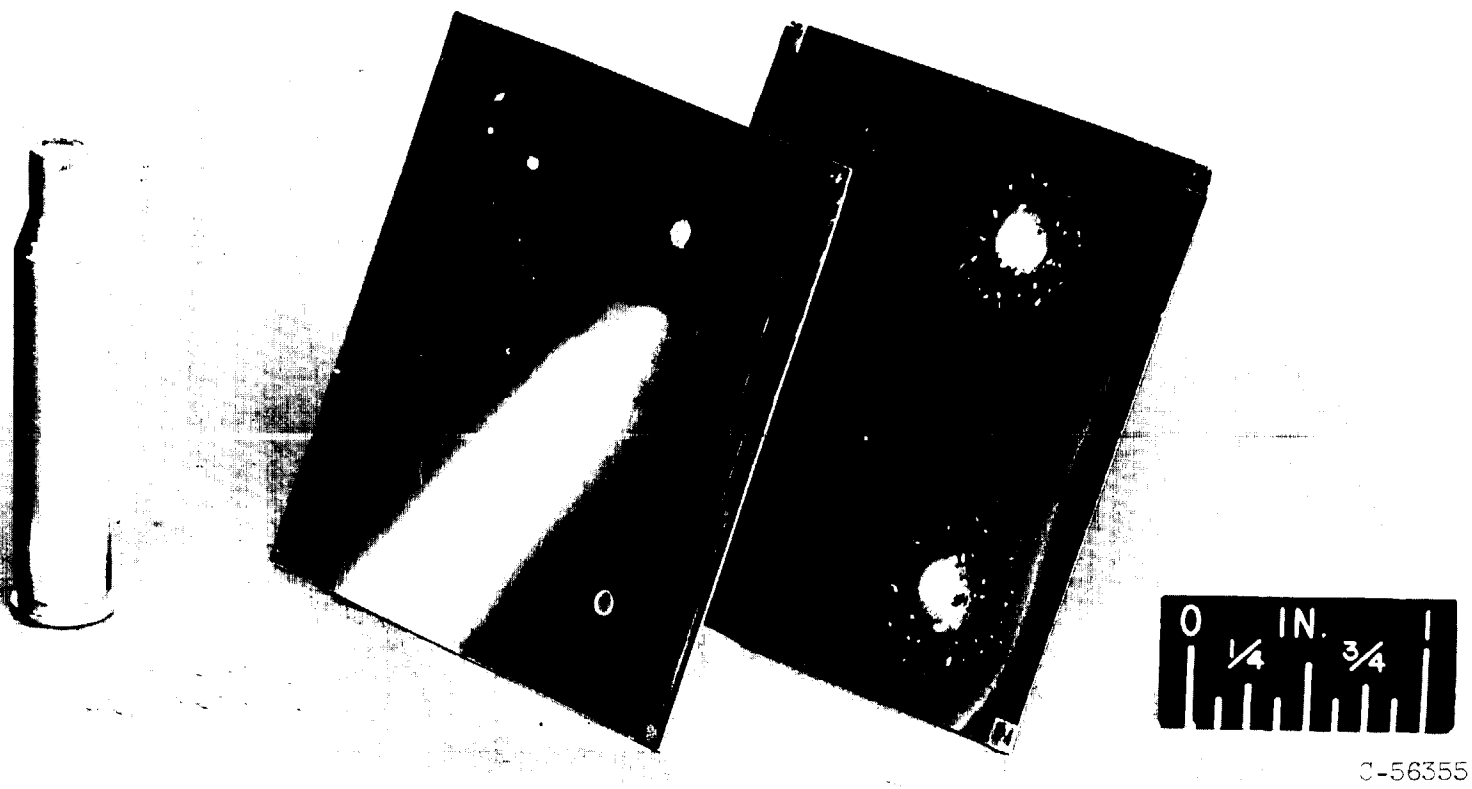


Figure 19. - Bumper effect on 7500 feet per second glass beads.

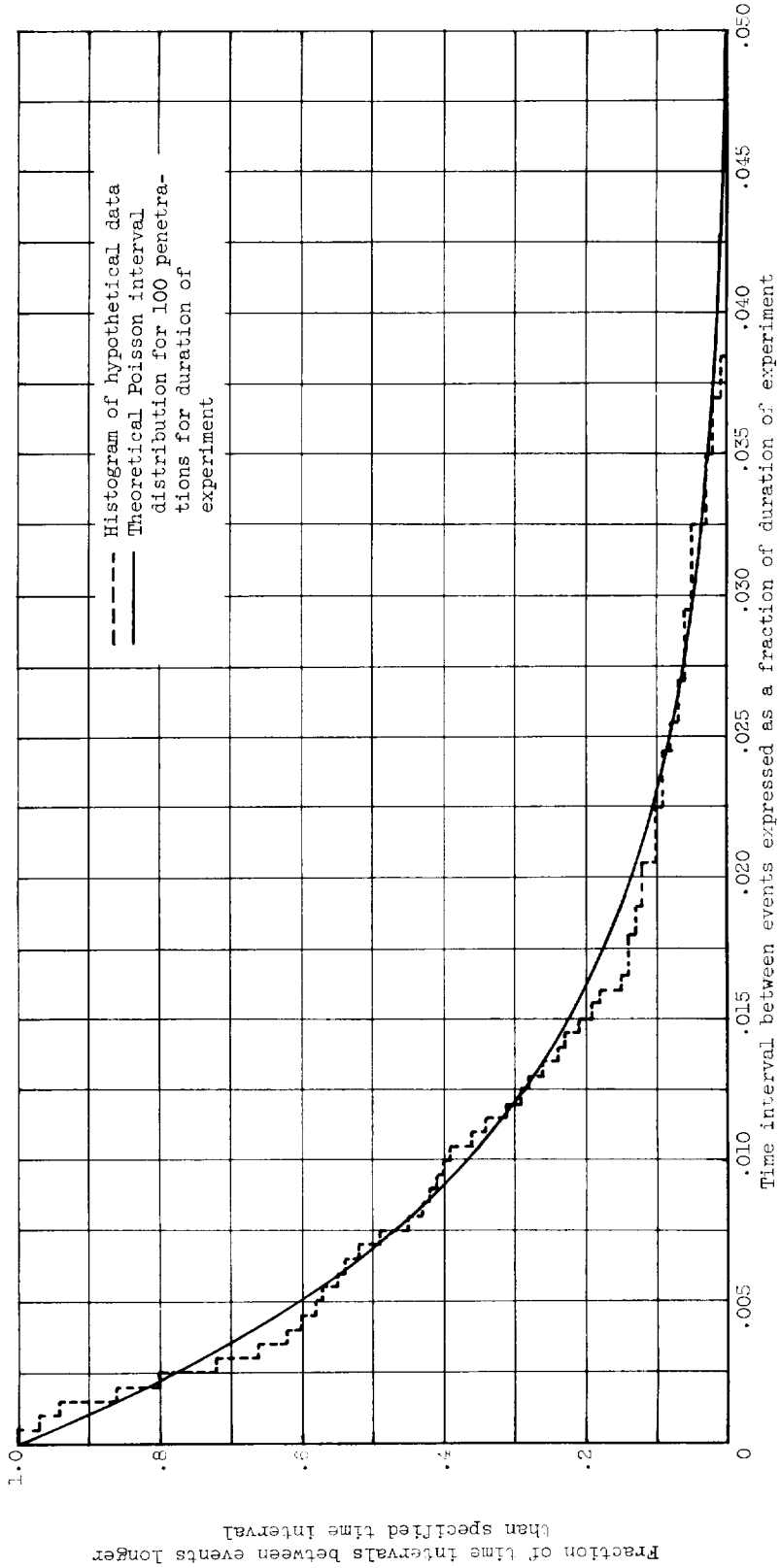


(a) Poisson interval distribution.

Figure 20. - Illustrative example showing comparison of hypothetical data and theoretical distribution.

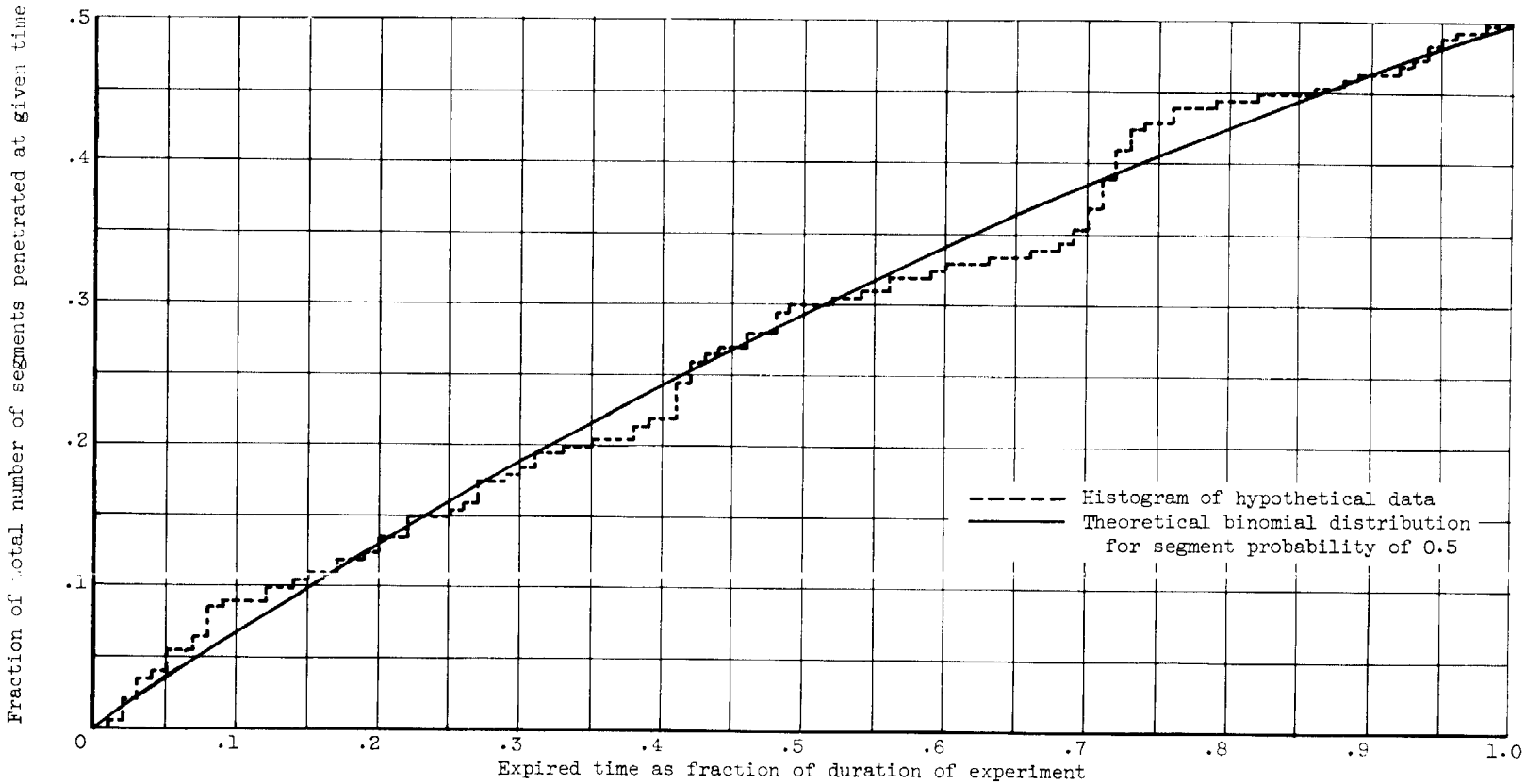


(b) Binomial distribution.

Figure 20. - Concluded. Illustrative example showing comparison of hypothetical data and theoretical distribution.

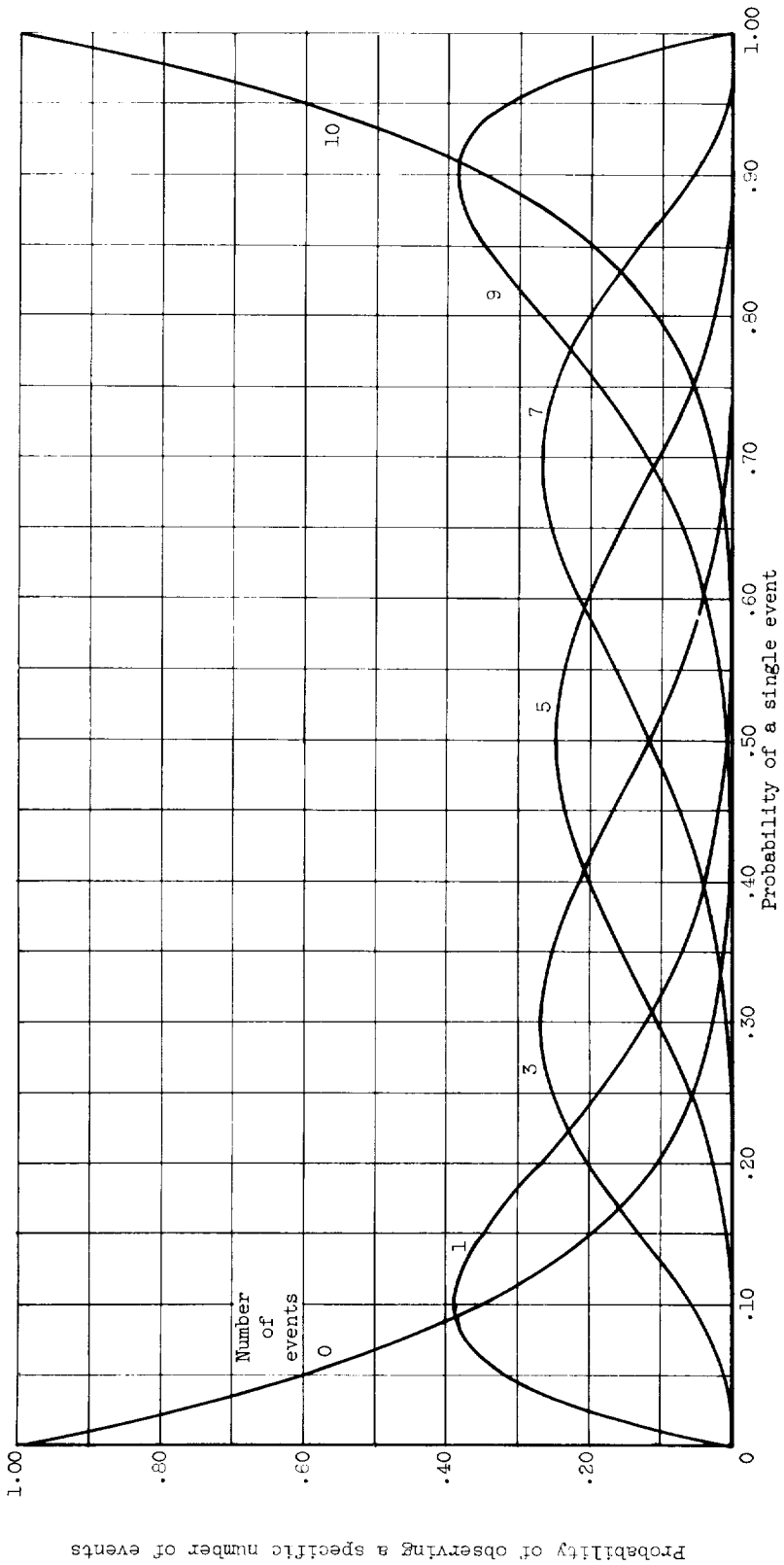


(a) Number of segments, 10.

Figure 21. - Likelihood variation of segment probability for recorded events. (Data obtained from ref. 76.)

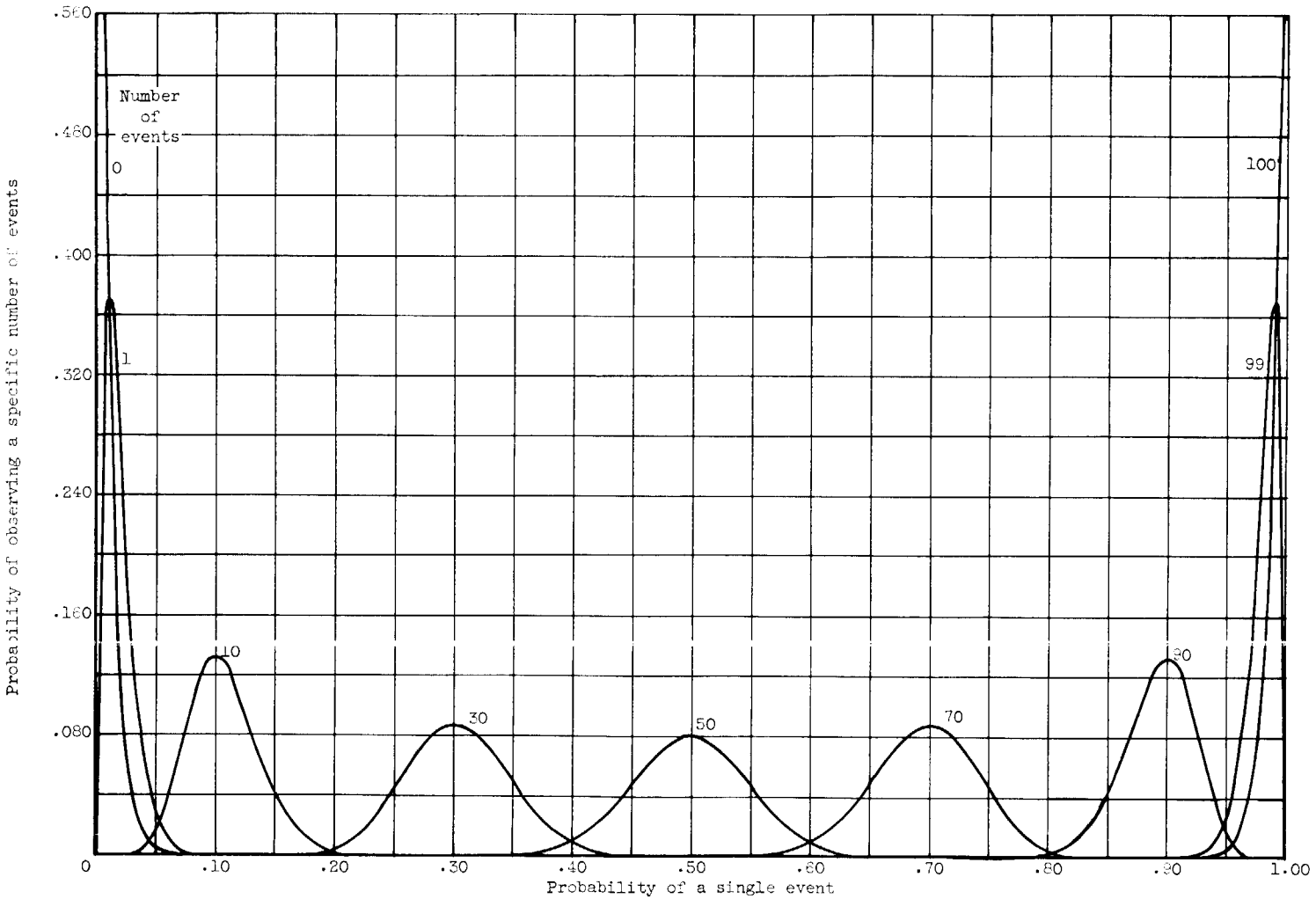


(b) Number of segments, 100.

Figure 21. - Continued. Likelihood variation of segment probability for recorded events. (Data obtained from ref. 76.)

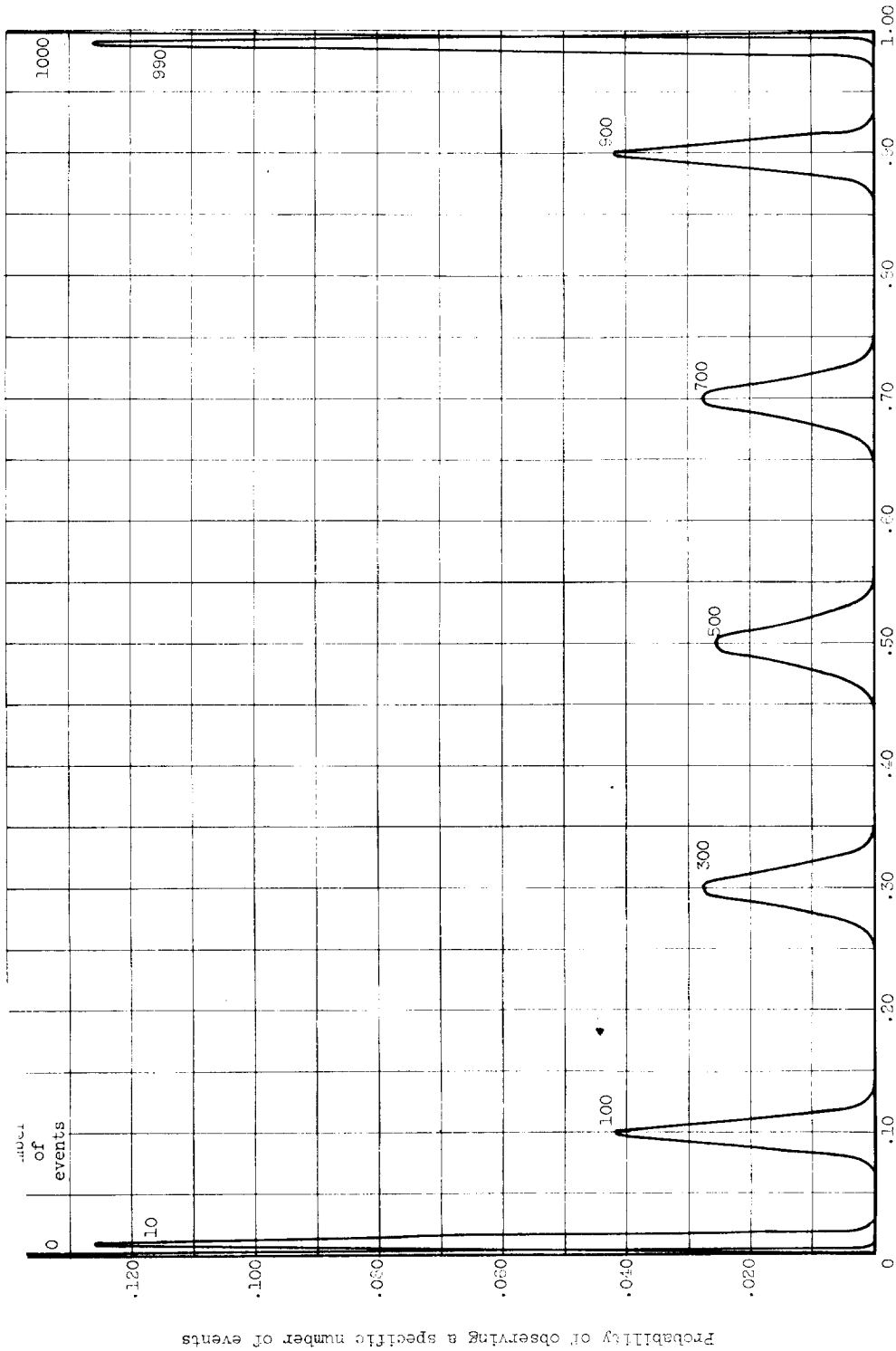


(c) Number of segments, 1000.

Figure 21. - Concluded. Likelihood variation of segment probability for recorded events. (Data obtained from ref. 76.)

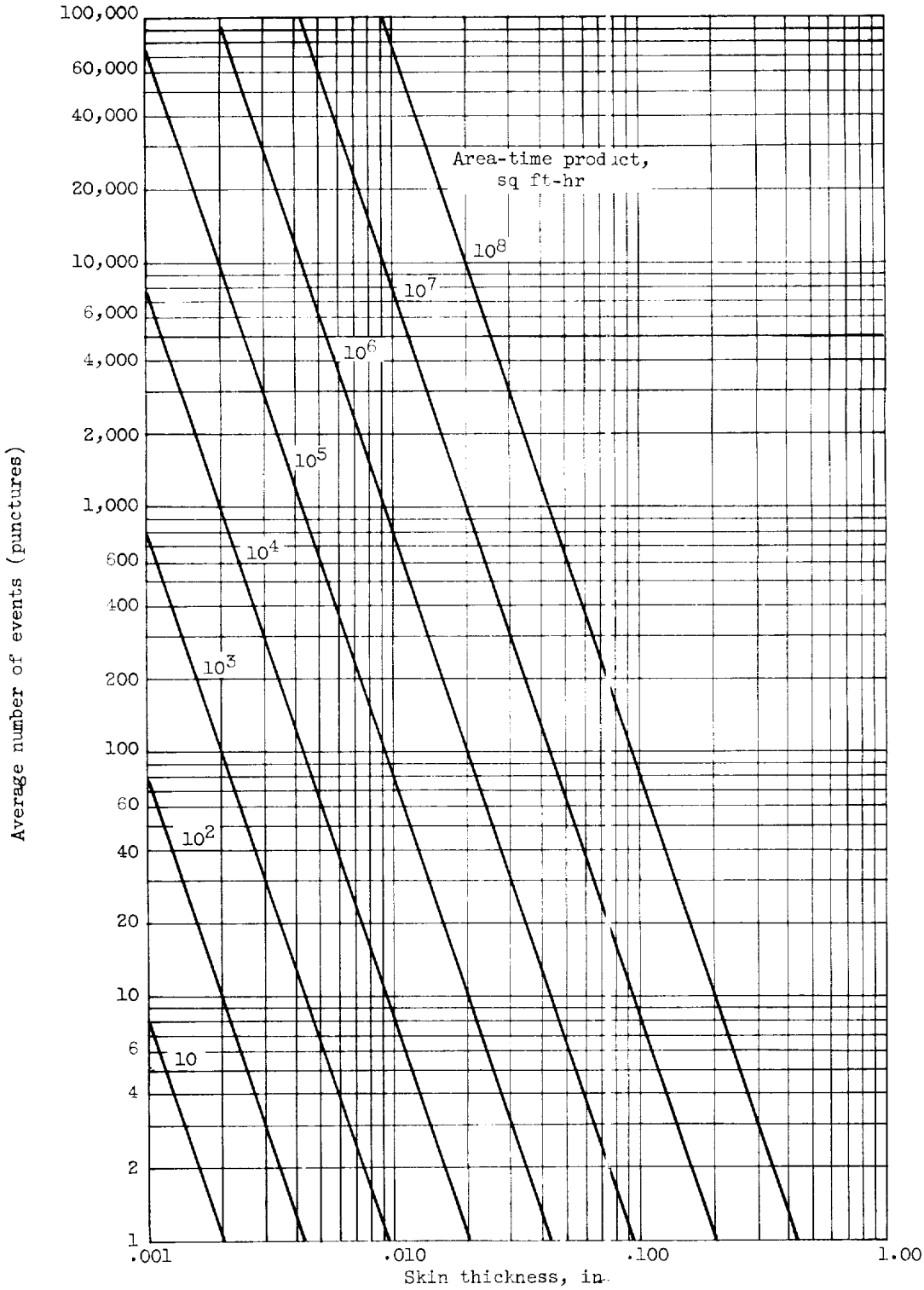


Figure 22. - Required area-time product as a function of skin thickness and average number of events (stainless steel).

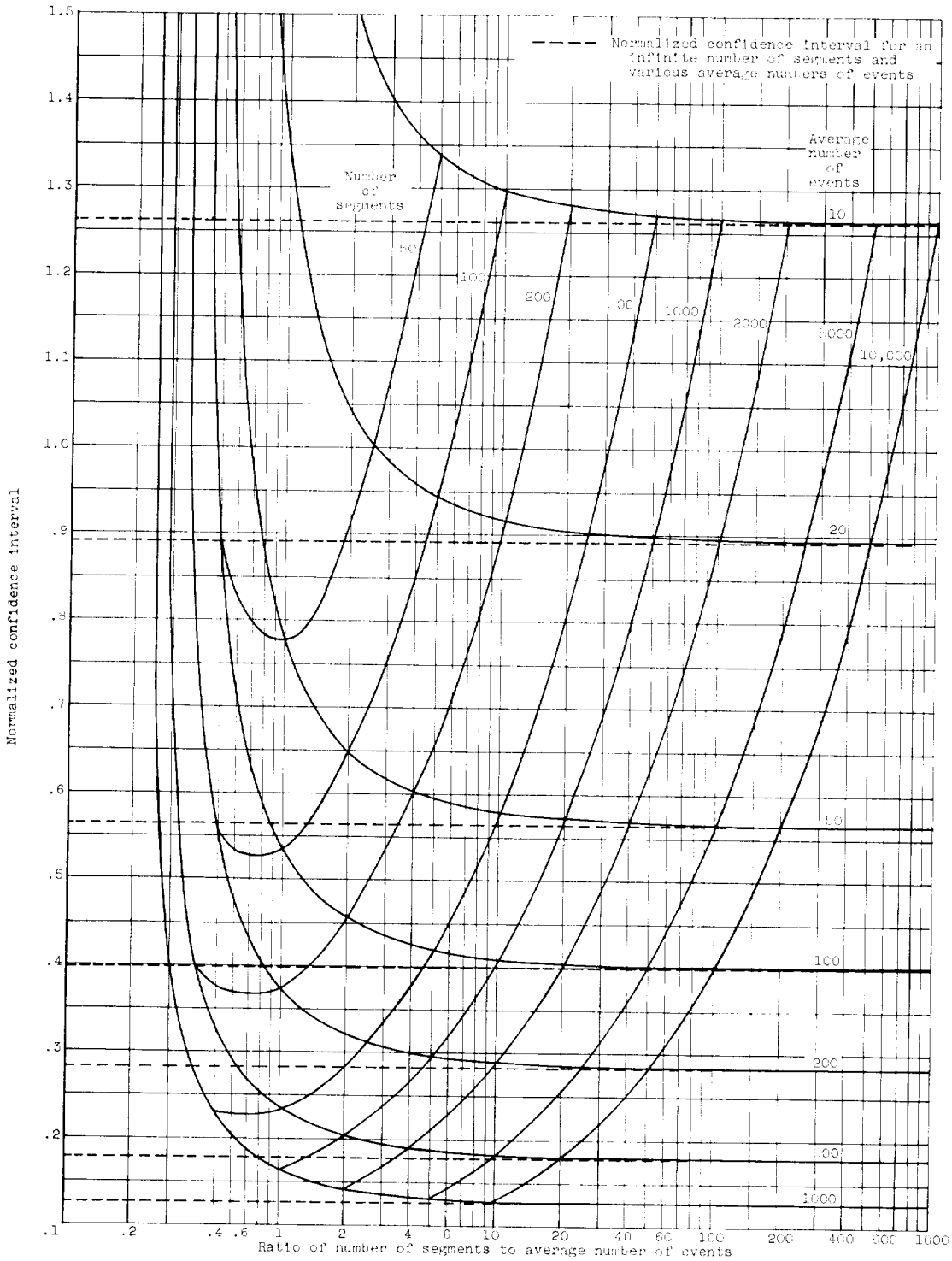


Figure 23. - Variation of confidence interval with average number of events and number of segments (95% confidence level).